# Molecular Characterization of the Plastid-localized ABC Protein TAP1 in *Arabidopsis thaliana*

by

Jan Johansen Hempel

Thesis submitted in fulfillment of
the requirements for degree of
PHILOSOPHIAE DOCTOR
(PhD)


Faculty of Science and Technology

Department of Mathematics and Natural Sciences

2018

University of Stavanger
NO-4036 Stavanger
NORWAY
www.uis.no



ISBN: 978-82-7644-750-7
ISSN: 1890-1387
PhD Thesis UiS no.375

# Acknowledgements

I wish to thank the University of Stavanger for giving me the honor of admission to the doctoral program. Likewise, my gratitude goes to my former employer, Rogaland County Council, which funded much of my work, and supported me during many years working full-time as a senior adviser.

My deepest gratefulness goes to my supervisor Prof. Simon Geir Møller, and my co-supervisor Dr. Jodi Maple-Grødem at Centre for Organelle Research (CORE), a centre based at the University of Stavanger (UiS). Prof. Møller has since 2011 been affiliated with St. John's University (SJU) in New York, the last years also as a Senior Vice Provost. My deepest thankfulness for welcoming me to CORE, UiS, and for giving me the opportunity to study at SJU, to do essential lab work for my PhD thesis, and to guide and discuss theoretical and practical issues. Your facilitations, guidance, your professional knowledge and insights cannot be overestimated. Thank you, Simon, I will always be humble and in very deep gratitude to you!

My thankfulness also goes to Prof. Ales Ventura and Prof. Chris Bazinet at SJU, for admission and offering me a study place at the Department of Biological Sciences, SJU. Likewise, I will thank other colleagues in New York, Drs. Indranil Basak, Ketan Patil, Rashed Abdullah and Sung Su Lee, for their invaluable practical support and advice. I am forever grateful to you!

Dr. Jodi Maple-Grødem has followed me all my years as a PhD student at UiS. She has worked like a mentor and given me excellent tutoring. Two years ago, she formally became my co-supervisor. Her advice and insightful suggestions on the scientific areas are very qualified, and have been a great encouragement to me. In addition, she exhibits very high competence of educational features. As a former principal of a High

School/Junior College, I would have employed her immediately! You have my ultimate and deepest respect and gratitude, Jodi!

In my home, my wife, Kari G. Hempel, has contributed invaluable care, inspiration and support throughout the years. Thank you very much, dear Kari!

Prof. Peter Ruoff and Prof. Cathrine Lillo at CORE, have together with the Head of Department, Gro Johnsen, pricelessly helped and advised me, in addition to suggestions for the practical implementation. Dr. Xiang Ming Xu, Dr. Hong Lin and Senior Engineer Camilla Sletten have made a significant contribution to practical assistance in the laboratory during the early years. Likewise, I will thank Dr. Dugassa Nemie-Feyissa for inspiring discussions and helpful assistance with proteins in the lab.

It would cause too much to mention all colleagues and friends who somehow, with comments or other, have supported me in the work. However, some of the colleagues at CORE have been in a somewhat more professional relationship with regards to advice and comments, and I would like to give them a special thank you: Dr. Amr Ramzy Abass Kataya, Dr. Behzad Heidari Ahootapeh and Dr. Janete Chung.

Finally, I will express my deepest love and recognition to my son Espen†, my daughter Lin and my granddaughters Ida, Amanda, Mie and Julie. I dedicate this thesis to them.

# Table of Contents

# List of Figures

# List of Tables

# Abstract

The two TAP-like genes, *AtTAP1* and *AtTAP2*, belong to the ABC transporter superfamily of *Arabidopsis*. AtTAP2/ALS1 has been shown to be important for aluminum metabolism and tolerance, however, little is known about the function of AtTAP1. This study has investigated expression dynamics of *AtTAP1*, the intracellular localization patterns of AtTAP1, and possible functional roles of AtTAP1 in response to a variety of biotic and abiotic stress factors.

A Yellow Fluorescent Protein (YFP) translational fusion approach showed that AtTAP1 is localized to chloroplasts, with a clear enrichment at the chloroplast membrane and indicating two different patterns of localization: short filaments in close association with the envelope or uniformly distributed with the entire surface of the chloroplast.

Using semi-quantitative RT-PCR in wild-type plants and an *AtTAP1* promoter-beta-glucuronidase (GUS) construct in transgenic plants, *AtTAP1* is demonstrated to have elevated expression in aerial tissues, at lateral root initiation sites and in flowers (sepals). Furthermore, *AtTAP1* expression is increased in response to $Ca^{2+}$ exposure, and to a lesser extent by $Al^{3+}$, which is different from *AtTAP2*, for which lesser expression in response to $Ca^{2+}$ and $Fe^{3+}$ is observed. High $Mg^{2+}$ represses both *AtTAP1* and *AtTAP2* expression, compared to the control. Preliminary observations of auxin stress treatment show an immediate repressed *AtTAP1* expression before restoring during 24 hrs exposure.

Functional analysis, employing an *AtTAP1* loss-of-function *Arabidopsis thaliana* transgenic line, *attap1*, revealed no phenotypic differences as compared to WT plants, in response to $Al^{3+}$, $Fe^{3+}$, $Ca^{2+}$, $Mg^{2+}$, $Cu^{2+}$, methyl viologen (MV), $H_2O_2$, auxin and heat exposure, suggesting that AtTAP1 and AtTAP2 harbor very different functions. Interestingly, *AtTAP1* shows enhanced expression in mechanical wounded leaf tissue indicating a possible involvement in wounding responses in plant defense.

Phylogenetic studies demonstrate essential domains of AtTAP1 and AtNAP14 to be highly conserved, and both proteins to be in closer evolutionary relationship to the homologs of *N. tabacum* and *S. lycopersicum*, than to any of the other species' homolog TAP1 proteins compared.

AtTAP1 and AtTAP2 proteins were detected by Western Blotting. Purification and characterization were not completed, presumably due to toxicity or other inhibited protein production in the host cells. Proteins of AtNAP14 were identified and produced, without further purification and characterization.

# Abbreviations

| | |
|---|---|
| ABA | Abscisic acid |
| ABC | ATP-binding cassette |
| ALS | Aluminum sensitive |
| ATM | Arabidopsis transporters of mitochondria |
| CCMA | Cytochrome C Maturation A |
| cDNA | Complementary DNA |
| cTP | Chloroplast transfer peptides |
| DTT | Dithiothreitol |
| ECL | Electrochemiluminescent |
| EDTA | Ethylenediaminetetraacetic acid |
| Fut | Ferric-iron uptake transporter |
| GFP | Green fluorescent protein |
| GUS | β-Glucuronidase |
| HUGO | Human Genome Organization |
| IAA | Indole acetic acid |
| IPTG | Isopropyl-β-D-1-thiogalactopyranoside |
| $K_m$ | Michaelis constant |
| LB | Luria-Bertoni Broth |
| mAU | milli-absorbance of UV |
| MDR | Multidrug resistance |
| MOPS | 3-Morpholinopropanesulfonic acid |
| MS | Murashige and Skoog |
| MV | Methyl viologen |
| NAP | Non-intrinsic ABC proteins |
| NBD | Nucleotide-binding domains (Also called ABC domains) |
| NBF | Nucleotide-binding folds |
| PAGE | Polyacrylamide gel electrophoresis |
| PBS | Phosphate-buffered saline |
| PCR | Polymerase chain reaction |
| PVDF | Polyvinylidine difluoride |
| qPCR | Quantitative real-time PCR |
| ROS | Reactive oxygen species |
| RT-PCR | Reverse transcription PCR |
| SDS | Sodium dodecyl sulfate |
| Suf | Sulfur protein system |

| | |
|---|---|
| TAE | Tris-acetate-EDTA |
| TAP | Transporter associated with antigen processing |
| TBS | Tris-buffered saline |
| T-DNA | Transfer DNA |
| TGD | Trigalactosyldiacylglycerol |
| TMD | Transmembrane domains |
| $V_{max}$ | Maximal velocity |
| X-gal | 5-bromo-4-chloro-3-indoxyl-β-D-galactopyranoside |
| YFP | Yellow fluorescent protein |

# 1 Introduction

## 1.1 ABC Proteins

### 1.1.1 General Background

The ATP-binding cassette (ABC) protein superfamily constitutes one of the largest protein families found in all living organisms (El-Awady et al. 2016; Henikoff et al. 1997; Kang et al. 2011; Rea 2007; Sánchez-Fernández et al. 2001), and is also referred to as ABC transporters, because the proteins typically function as transporters. The ABC protein system was first discovered and characterized in detail in prokaryotes as early as in the 1970s (Ames and Lever 1970; Ferenci et al. 1977; Kellermann and Szmelcman 1974; Szmelcman et al. 1976), and has received much attention, mainly because ABC proteins are involved in severe inherited human diseases (Dean, Rzhetsky, and Allikmets 2001).

Plant ABC transporters are important for plant growth by transporting molecules, such as plant hormones, metabolites, lipids, contaminants, and defense molecules (Hwang et al. 2016). Knowledge of how plant transporters function is of utmost importance for the world population in the future, as this knowledge can be used to create strategies to improve crops for sustainable food production. Plant membrane transporters that mediate aluminum tolerance have been described, as have transporters responsible for enhancing the concentration of iron and zinc, two essential micronutrients of which over two billion people suffer deficiencies (Schroeder et al. 2013).

ABC proteins appear in all genera of the three kingdoms of life (Higgins 2001) as ancient and powerful transporters exchanging compounds across many different membranes, often against electrochemical gradients by the use of energy released from ATP hydrolysis (Hwang et al. 2016; Wilkens 2015). Significant roles of the ABC transporters in

prokaryotes include pumping essential compounds such as sugars, vitamins and metal ions into the cell (Davidson et al. 2008; Fischer et al. 2010). In eukaryotes transport of molecules to the outside of the plasma membrane, or into membrane bound organelles is of importance, and has been demonstrated, also in connection with cellular detoxification (Kang et al. 2011; Scholz et al. 2011; Shitan et al. 2003).

The highest levels of diversity in ABC transporters are found in terrestrial plants, with *Arabidopsis* encoding 130, rice 133 and moss 125 ABC transporters, whilst mammals like human and mouse, and fruit fly and *C. elegans* encode 49, 53, 56 and 55 ABC transporters, respectively (Hwang et al. 2016). The freshwater algae *Chlamydomonas,* a lower plant, encodes 69 different ABC transporter proteins. From the prokaryotic system the identification of genes for about 70 discrete ABC transporters is reported (Moussatova et al. 2008).

The adaptation of plants to terrestrial life may have been a condition for the evolution of ABC transporters and secondary active transporters, which most biochemical processes are rather slow and therefore convenient to sessile organisms. On the other hand, animals have developed many ion channels or pore-forming membrane proteins. They play important roles for example in the nervous systems, which requires high capacity transporters with short response times (Hwang et al. 2016).

All proteins of the ABC superfamily share a highly-conserved ATPase domain, unequivocally characterized by three short motifs, the Walker A, the Walker B and the ABC transporter signature (Signature, also called the C-loop). In addition, other motifs diagnostic of ABC proteins are present across the different kingdoms (Davidson et al. 2008; Schneider and Hunke 1998).

### 1.1.2 General Structure of ABC Proteins

The ABC membrane-bound transporters are similar in their basic structure having common molecular folds, and four core modules consisting of two conservative nucleotide-binding folds (NBF), also named nucleotide-binding domains (NBD) or ATP binding cassette domains (ABC), and two less conserved transmembrane domains (TMD) (Sánchez-Fernández et al. 2001) (Figure 1.1). The proteins of the ABC transporter family share about 30-40% sequence identity (Higgins 1992). The shared ABC domain provides energy for a large number of fundamental biological processes (Holland and Blight 1999; Saurin, Hofnung, and Dassa 1999; Schneider and Hunke 1998).

The NBF domain comprises approximately 200 amino acids, and can be identified by a specific set of seven highly conserved motifs at the sequence level (ter Beek, Guskov, and Slotboom 2014) . This study focus on four of them, the Walker A, the Walker B, the Signature, and the H-loop. The Signature motif is located between the Walker A and Walker B motifs, and the H-loop is situated downstream of the other three, to the C-terminal end (Sánchez-Fernández et al. 2001; Rea 2007). The three other highly conserved motifs are the A-loop, the D-loop and the Q-loop (ter Beek, Guskov, and Slotboom 2014).

A molecular model architecture of the ABC transporters, with two TMDs embedded in the membrane bilayer and two ABCs located in the cytoplasm, is shown in Figure 1.1(a) and Figure 1.1(b), whilst Figure 1.1(c) shows a diagram of each subunit, TMD and ABC, fused as a dimer (Rees, Johnson, and Lewinson 2009).

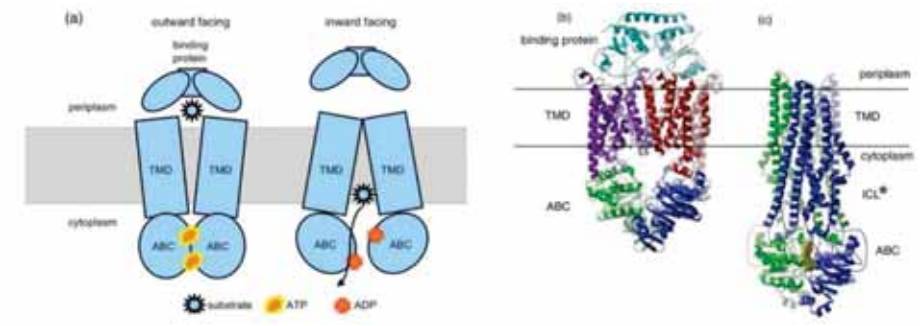


**Figure 1.1 – Molecular architecture of ABC transporters**
Cartoon representation of the modular organization of ABC transporters, composed of two transmembrane domains (TMD) and two ABC (NBD) domains (a). Core transporter of four subunits, two membrane spanning (purple and red) and two ABC subunits (green and blue). The complex also contain the periplasmic binding protein (cyan) (b). Fused TMD and ABC (NBD) of two subunits (green and blue) so that the complete transporter is a dimer. The bound nucleotides in this structure represented by yellow space filling models(c).

*Intracellular loop.

Source: Figure 1.1 copied from (Rees, Johnson, and Lewinson 2009).

The Walker A motif, also known as the Walker loop or P-loop (phosphate-binding loop), is associated with phosphate binding and is crucial for nucleotide-binding (Hanson and Whiteheart 2005). The Walker A motif is an eight amino acid consensus sequence, G-4x-GK-T/S (Walker et al. 1982; Rea 2007). A common feature of ABC proteins is the presence of an ABC Signature motif, containing a ten amino acid consensus sequence, [LIVMFY]S[SG]Gx3[RKA][LIVMYA]x[LIVFM][AG] commonly referred to as LSGGQ (Wilkens 2015), but several exceptions have been reported (Kang et al. 2011; Rea 2007).

The Signature motif sequence (or C motif) is involved in ATP hydrolysis as a gamma (γ) phosphate sensor and/or as a signal across the membrane spanning domains (Davidson et al. 2008). The motif acts as a catalytic subunit and is highly conserved among all eukaryotes, thus indicating a

common catalytic mechanism (Goldberg et al. 1995). The Signature motif occurs only in ABC proteins, and is therefore a distinguishing feature compared to other ATPases (Davies and Coleman 2000).

The Walker B motif has an hhhhDE consensus sequence (Hanson and Whiteheart 2005), where D and E denotes aspartic acid and glutamate residues, respectively, whilst h denotes a hydrophobic amino acid residue (Walker et al, 1982). It is found that the aspartic acid co-ordinates magnesium ions, and the glutamate is essential for ATP hydrolysis (Hanson and Whiteheart 2005).

The H-loop motif, also called the Switch region, usually comprises seven amino acids, always containing an invariant and basic H (histidine) amino acid residue, considered to be polarizing the attacking water molecules during ATP hydrolysis (Garmory and Titball 2004; Kloch et al. 2010; Lewis et al. 2004; Schneider and Hunke 1998). It interacts with the conserved aspartate of the D-loop, the proposed general base, which is the glutamate residue of the Walker B motif, and assists the positioning of the magnesium ion (ter Beek, Guskov, and Slotboom 2014).

### 1.1.3 Chloroplast Transit Peptides

The N-terminal chloroplast transit peptides (cTP) direct chloroplast proteins to the chloroplast stroma where they, during or shortly after entry, are cleaved off by stromal processing peptidase (Robinson and Ellis 1984; Soll and Tien 1998). Information on transit peptides reveal high sequence diversity, and lack consensus or common sequence motifs, which indicate low sequence similarities. It is ascertained that transit peptides contain many small motifs related to critical steps in the chloroplast protein import, but it is unknown how these motifs are organized to produce the transfer peptides with all the different sequences (Lee et al. 2015). Based on data from different approaches, such as dissecting sequence encoded information and biochemical

studies of the transit peptide, accuracy of predicting a chloroplast protein structure by grouping the peptides into multiple sequence subgroups that contain distinctive sequence motifs for chloroplast targeting may be constructive (Lee et al. 2008).

### *1.1.4 ABC Subfamilies*

There are different nomenclature subfamily systems for ABC proteins (Verrier et al. 2008). "*The Arabidopsis thaliana system"* uses phylogenetic and domain organizational information to define 12 or 13 subfamilies. The subfamilies can be divided in three groups: Whole (full-size) molecules, half-molecules (half-size) and soluble molecules (Sánchez-Fernández et al. 2001; Verrier et al. 2008). An alternative system of nomenclature is HUGO (Human Genome Organization), which unifies plant and animal ABC naming systems. This system divides the proteins in nine subfamily groups denoted ABCA – ABCI (Hwang et al. 2016; Kang et al. 2011; Verrier et al. 2008). Those subfamilies, which refer to plants in general, and *Arabidopsis* in particular, can be characterized as the following:

ABCA proteins are half-size type proteins except for one (ABCA1) that appears to be orthologous to a mammalian full-size transporter. All the other 11 proteins in this *Arabidopsis* subfamily are of the half-size type, which have only been identified in plants and prokaryotes (Kovalchuk and Driessen 2010; Peelman et al. 2003).

ABCB proteins include full-size as well as half-size molecules. The *Arabidopsis* genome encodes for about 30 ABCB proteins, compared to 11 in the human genome. Interestingly proteomic data indicates the subcellular localization of AtTAP1 (AtABCB26) to the chloroplast (Ferro et al. 2010), and AtTAP2 (AtABCB27) in the vacuolar membrane (Jaquinod et al. 2007). A phylogenetic tree indicating the relationships of *Arabidopsis* and rice proteins in ABC subfamily B is shown in Figure 1.2 (Verrier et al. 2008).

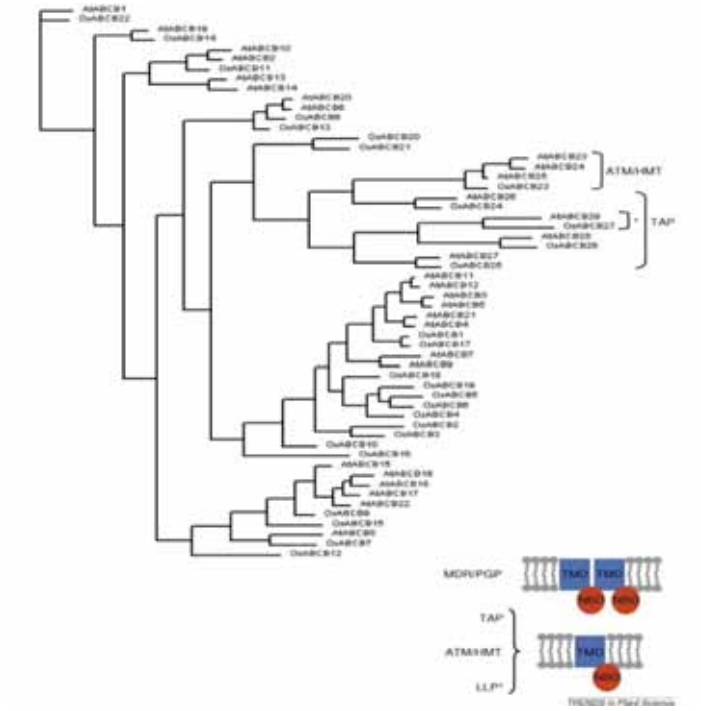


**Figure 1.2 – Phylogenetic relationships of *Arabidopsis* and rice proteins in ABC subfamily B**
Protein sequences aligned with ClustalW and edited using Bioedit to excise an NBD domain aligned across all proteins in each subfamily. A phylogenic analysis was then undertaken using Paup4* to produce un-rooted trees, which were displayed with PhyloDraw. ABC subfamily B comprises the full-length PGP/MDR (P-glycoprotein multidrug resistance) transporters and the three half-size subgroups: HMT/ATM (heavy metal tolerance/ABC transporters of the mitochondrion) transporters, TAP (transporter associated with antigen processing) and LLP (prokaryotic lipid A-like exporters, putative). The asterisk indicates the proteins assigned to the LLP subgroup. The cartoons depict the domain organization of the respective subfamilies and subgroups: TMD, transmembrane domain; NBD, nucleotide-binding domain. The lipid bilayer represented in grey.

Source: Figure 1.2 copied from (Verrier et al. 2008).

ABCC proteins of *Arabidopsis* are all full-size molecules mostly localized to the vacuolar membrane (Nagy et al. 2009; Rea 2007).

ABCD proteins constitute a small group with only one half-size and one full-size member in *Arabidopsis,* the latter of which has been localized to peroxisomes (Hayashi et al. 2002).

ABCE and ABCF subfamily consist of three and four members, respectively, in *Arabidopsis.* They lack a transmembrane domain and probably function in other processes, as orthologs of other organisms participate in ribosome recycling and translational control (Kang et al. 2011; Pisarev et al. 2010).

ABCG proteins belong to the largest ABC subfamily. *Arabidopsis* contains 43 ABCG proteins, both full-sized and half-sized molecules (Hwang et al. 2016; Verrier et al. 2008). The full-sized proteins have only been identified in plants, and localize to the plasma membrane (Choi et al. 2011; Kang et al. 2011).

ABCH proteins are phylogenetically unrelated to subfamily ABCG and have not been identified in plants (Kretzschmar et al. 2011; Verrier et al. 2008).

ABCI proteins bear similarities to components of prokaryotic multi-subunit transporters. In *Arabidopsis,* there are 16 ABCI proteins identified. Some of them are chloroplast localized, such as AtNAP14 and some of the other AtNAPs, and all are assigned to a heterogeneous group designated as non-intrinsic ABC proteins (NAP) (Hwang et al. 2016; Lane et al. 2016; Sánchez-Fernández et al. 2001).

## *1.1.5 Plant ABC Proteins*

### 1.1.5.1 The TAP Proteins

The half-molecule ABC transporters can be divided in five subfamilies of which the transporter associated with antigen processing (TAP)

proteins, (TAP1 and TAP2), belong to one (Kang et al. 2011; Sánchez-Fernández et al. 2001). In the HUGO subfamily system, TAP1 and TAP2 belong to one of three subgroups in the ABCB subfamily, and are assigned ABCB26 and ABCB27, respectively. The other two groups of ABCB proteins are MDR, multidrug resistance, and ATM, transporters of the mitochondria (Lane et al. 2016).

Mammalian transporters of the TAP-type participate in peptide secretion and translocations across membranes of the endoplasmic reticulum (ER). They take part in mechanisms responsible for the presentation of major histocompatibility complex class I antigenic molecules on the surface of the cell. Here heterodimers of TAP1-TAP2 actively transport peptide degradation products from the cytosol into the lumen to associate with molecules of the complex (Abele and Tampe 2004; Reits et al. 2000).

The two TAP genes of *Arabidopsis* (Garcia et al. 2004; Sánchez-Fernández et al. 2001) are both transcriptionally active, and encode forward-orientation, half-molecule proteins that localize to membranes of small intracellular compartments. According to proteomic analysis TAP1 is indicated to localize to chloroplasts (Ferro et al. 2010; Kang et al. 2011), while TAP2 is detected in tonoplast membranes of vacuoles isolated from *Arabidopsis* cell cultures (Jaquinod et al. 2007).

ABC transporters in plants are associated with heavy metal and metalloid detoxifications (Briat 2010; Larsen et al. 2005; Magalhaes et al. 2007; Meyer et al. 2010; Ryan et al. 2011; Song et al. 2010). They are also involved in transport of glucosylated compounds and antibiotics across membranes (Dean and Mills 2004; Kang et al. 2010; Zhao et al. 2011), and in polar auxin transport, lipid catabolism, xenobiotic detoxification, disease resistance and stomatal function (Hwang et al. 2016; Rea 2007). The role of ABC proteins and TAP1 in metal tolerance and reduced accumulation in plants in the context of strategies of “safe-food” is a topic of interest to study (Emamverdian et al. 2015; Gayet et al. 2006;

Singh et al. 2011; Singh et al. 2015; Verbruggen, Hermans, and Schat 2009).

The precise functions of the TAP1 and TAP2 genes of *Arabidopsis* or their homologs in other plants are of high interest. They are suspected to have functional capabilities analogous to those inferred for mammalian TAP genes (Rea 2007). There are reasons to think of TAP1 as a catalyst of transmembrane peptide translocations in different activities (Rea 2007), while TAP2 has been demonstrated displaying an active role in root growth in an aluminum toxic environment (Gabrielson et al. 2006; Larsen et al. 2007; Simoes et al. 2012).

#### 1.1.5.2 The NAP14 Protein

The non-intrinsic ABC proteins (NAPs), represent a heterogeneous group of soluble and non-intrinsic membrane ABC proteins. Within the group there is little structural similarity between members, or to ABC protein subfamilies from other organisms (Sánchez-Fernández et al. 2001). NAPs are small proteins of about 290 amino acids, containing only one nucleotide-binding fold or domain (called NBF or NBD). Indeed, they are considered to be similar to peripheral ATP-binding quarter molecule subunits in prokaryotic ABC transporters (Higgins 1992). Four different genes encode the prokaryotic ABC proteins, where each gene encodes either a NBD or TMD, which are subsequently assembled at the membrane to form a transporter complex. This may imply that plant NAP proteins also form a hetero-tetramer complex in order to function as a transporter (Sugiyama et al. 2006).

Several reports are published on NAP members in Arabidopsis. For example AtNAP1 as a proposed atypical SufB homolog protein involved in iron-sulfur cluster assembly in plastids (Xu et al. 2005). AtNAP1 is also involved in the regulation of chlorophyll degradation (Nagane, Tanaka, and Tanaka 2010). AtNAP6, a plastidic SufD homolog protein, can interact with both AtNAP1 and AtNAP7. AtNAP7 is a homolog to

the SufC protein and located in chloroplasts (Rayapuram et al. 2007). All three proteins are required for Fe-S cluster biosynthesis and repair, and they contribute to a plastidic AtNAP1·AtNAP6·AtNAP7 complex (Hjorth et al. 2005; Moller, Kunkel, and Chua 2001; Xu et al. 2005; Xu and Moller 2004). Furthermore, NAP3 and ALS3, two genes previously identified to function in aluminum tolerance, are reported to encode an ABC transporter complex required for the responses to phosphate deficiency in *Arabidopsis* (Belal et al. 2015). Additionally, AtNAP10 is the plant ortholog of the bacterial CCMA (Cythochrome C Maturation A) protein, and the gene encodes a mitochondrial AtCCMA (Rayapuram et al. 2007).

It has been shown that AtNAP14 participates in iron transport across the chloroplast envelope (Lopez-Millan, Duy, and Philippar 2016). Indeed, AtNAP14 shows similarity to FutC, which functions as a non-intrinsic ATPase as part of the FutABC transporter in Cyanobacteria transporting $Fe^{2+/3+}$ (Katoh et al. 2001; Shimoni-Shor et al. 2010). Loss of NAP14 function mutants show dramatically increased iron concentration in shoots compared to wild-type plants, in addition to damage to chloroplast structures and severe defects (Lopez-Millan, Duy, and Philippar 2016; Shimoni-Shor et al. 2010). The role of NAP14 in regulating different plastid functions and Fe-S cluster biogenesis is proposed, as similar to the stroma localized NBD-NAP protein NAP7/SufC (Balk and Schaedler 2014; Xu and Moller 2004).

### 1.1.6 Bacterial ABC Proteins

The prokaryotic ABC transporters are customarily categorized in three groups, distinguished with respect to the source of energy used: (Ion) Channels, Primary transporters and Secondary transporters (Davidson et al. 2008; Saier 2000). The ABC proteins belong to the Primary active transporters, which connect transport against a concentration gradient to the hydrolysis of ATP.

Some bacterial ABC transporters are involved in the export of virulence factors. Under appropriate conditions, many others can become active for viability and virulence. For example, the iron ABC uptake system is recognized as an important effector of virulence (Davidson et al. 2008; Henderson and Payne 1994). Other examples of functions are sugar import, triggering gene expression, and regulation of osmotic strength by activation of ABC transporters (Davidson et al. 2008; Poolman, Spitzer, and Wood 2004). In addition to the importance in transport, several physiological processes involve the ABC system through regulatory domains in the transporter themselves.

### 1.1.7 Mammalian ABC Proteins

Initially, the eukaryotic ABC transporters were thought only to function as exporters, but several recent studies have shown that some eukaryotic ABC transporters function as importers, translocating substrates from the lumen to the cytosol. This includes the mammalian ABC transporter ABCA4, which is found in retinal photoreceptor cells and associated with Stargardt macular degeneration, a disorder that causes progressive vision loss (Coleman, Quazi, and Molday 2013; Quazi, Lenevich, and Molday 2012). Among the protein subfamilies, no ABCG-full size or ABCI transporters are detected in mouse and human (Almen et al. 2009; Hwang et al. 2016; Mutch et al. 2004; Vasiliou, Vasiliou, and Nebert 2009). Interestingly, there is evidence of a relationship between many mammalian ABC exporters to bacterial ABC half-transporters that dimerize for function (van Veen 2016).

Of the seven subfamilies in the human genome (ABCA – ABCG), ABCE1 (which is the single member in this family which is an organic anion-binding protein) and ABCF do not have transmembrane domains, making transporter function unlikely. They are involved in protein synthesis regulation with no diseases associated with either ABCE or ABCF human genes to date (Vasiliou, Vasiliou, and Nebert 2009).

Many ABC proteins, like ABCA4, are involved in severe inherited diseases, and multidrug resistance in human cancer cell lines, over expressions of certain ABC transporters in tumors has been described (Henderson et al. 2011). Genetic variation in 49 human ABC proteins (Hwang et al. 2016) is associated with a variety of human inherited disorders. These are for example cystic fibrosis, neurological disease, Tangier disease, retinal degeneration, adrenoleukodystrophy, cholesterol and bile defects, anemia, cancer, and drug response phenotypes (Dean, Rzhetsky, and Allikmets 2001; Dizdarevic and Peters 2011; Vasiliou, Vasiliou, and Nebert 2009; Wilkens 2015).

The mammalian ABCA subfamily consists of 12 members, all full-length transporters. From disease-associated phenotypes, analysis of knockout mice, and biochemical and cell based studies, the ABCA proteins are suggested to play an important role in phospholipid translocations and cellular homeostasis (Coleman, Quazi, and Molday 2013). Mutations in these genes, and deficiencies in the proteins, is associated with many diseases, affecting organs, tissues and regulatory processes (Coleman, Quazi, and Molday 2013).

The ABCB transporters are involved in transporting a broad spectrum of drugs. Mutation and characterization studies have for example revealed involvement in phospholipid translocation, biliary excretion and liver disease (Coleman, Quazi, and Molday 2013). The human ABCB9 protein, which is phylogenetic closely related to TAP1 and TAP2, is found to be associated with the leukemia (GeneCards, Human Gene Database, ABCB9 Gene) (Zhang et al. 2000).

In the ABCC subfamily we find members that have a ubiquitous expression profile, and confer resistance to a broad-spectrum of antitumor drugs, glutathione-conjugates and sulfate-conjugates. Work in mice has revealed a role for an ABCC protein in the erythrocyte membrane (Coleman, Quazi, and Molday 2013).

The human ABCD subfamily contains four genes that encode half-transporters of which mutants are known to cause ALD (adrenoleukodystrophy) disease and Zellweger syndrome (Vasiliou, Vasiliou, and Nebert 2009).

Four of five members of the ABCG family are cholesterol transporters. The remaining, ABCG2, is highly expressed in epithelial cells of the placenta, kidney and intestine, where it is suggested to play a role in different regulating processes of xenobiotics. ABCG2 is also shown to promote enhanced exposure in human gastric carcinoma cells and breast cancer cells (Coleman, Quazi, and Molday 2013; Woehlecke et al. 2003).

## 1.2 Stress Factors and Characterization of TAP1

Exposure of mutants and wild-type organisms to different exogenous stress factors is of interest to identify and characterize genes and proteins. From these experiments we can get information, for example, on biochemical processes that involve plant development, growth and diseases, in addition to secondary stresses like nutrition (excess or deficiency) and oxidative stresses.

In this study, wildtype, *A. thaliana* (Col-0) and a knockout mutant, *attap1* (SAIL_8_B04), are inspected after exogenous treatments to reveal any differences in phenotypic expression. Several exogenous stress factors were used for this purpose, including metals such as aluminum, iron, calcium, magnesium and copper, and non-metal treatment as the chemicals methyl viologen (MV), hydrogen peroxide and auxin, in addition to heat stress and wounding. The selected factors are described below.

### 1.2.1 Metals as Stress Factors

*Aluminum,* $Al^{3+}$. Aluminum toxicity in acid soils represents a severe worldwide agricultural problem that limits productivity through

inhibition of root growth and elongation, and by that shoot development as well as water and nutrient uptake (Larsen et al. 2007; Larsen et al. 2005; Gabrielson et al. 2006; Kochian, Hoekenga, and Pineros 2004). Tolerance of aluminum in plants is due to two principal mechanisms, internal detoxification and its extrusion from root cells (Simoes et al. 2012). Experiments using acid nutrient medium of various concentrations of $AlCl_3$, revealed significant inhibition of root growth in *AtTAP2* mutants compared to wild-type (Larsen et al. 2007). Furthermore, data demonstrates that high auxin levels may weaken AtTAP2-dependent aluminum detoxification, and negatively regulate tolerance to aluminum through *AtTAP2* expression alterations and distribution of aluminum within plants (Zhu et al. 2013). Given that AtTAP1 and AtTAP2 are from the same TAP subfamily, it is possible that they are involved in the same biological processes.

*Iron, $Fe^{3+}$*. Chloroplasts are the largest deposits for iron, which is the most common redox-active metal, and is essential for photosynthetic electron transport and other metabolic processes, as well as a cause of oxidative damage (Divol et al. 2013; Duy et al. 2011). Mutants harboring gene defects for iron-responsive proteins, phenotypically resemble iron-deficient plants (Pan et al. 2015). Excess iron is highly toxic and arrests primary root growth by decreasing both cell elongation and division (Li et al. 2015).

*Calcium, $Ca^{2+}$*. Calcium is an important regulator of plant growth and development, and calcium participates in processes that involve nearly all aspects of development (Harper, Breton, and Harmon 2004; Hepler 2005). *Arabidopsis* seedlings respond to increased intracellular calcium concentrations by regulating the expression of genes encoding proteins that bring about tolerance, and analysis indicates that promoter motifs are calcium-regulated in plants (Whalley et al. 2011).

*Magnesium, $Mg^{2+}$*. As a most important macronutrient and constituent for chlorophyll biosynthesis, magnesium is involved in plant growth and

development, and plays a significant role in toxicity of heavy metals. For example, cadmium-induced toxicity in Japanese mustard spinach is reported to be alleviated by magnesium, and cadmium accumulation was also 40% reduced (Singh et al. 2015). Similarly, magnesium is able to alleviate aluminum toxicity in a number of plant species by displacing or competing with aluminum from binding sites, for example on the root cell wall and plasma membrane (Chen and Ma 2013).

Little is known about the signaling pathways that are involved in magnesium stress, but studies in recent years may lead to improvements in this area of research. Some magnesium transporters have been identified, but transcriptional levels of these transporters changed little with stress situations, be it deficiency or excess (toxicity), whilst the stress activated many other transporters (Guo et al. 2015). However, plant specific proteins have been shown to modulate susceptibility by preventing growth in response to increased external concentrations of magnesium. Genetic evidence from experiments with mutants of *Arabidopsis* show that some protein kinases are required for growth homeostasis under stress of high Mg concentrations (Mogami et al. 2015). The mutants showed increased susceptibility, and reduced shoot growth in respond to high external Mg concentration (Mogami et al. 2015).

*Copper, $Cu^{2+}$*. The transition metal copper is an important micronutrient for all living organisms in general, and for plant growth and development especially. Copper participates in numerous physiological regulations, and is an important cofactor for many proteins involved in neutralizing processes, lignification of cell wall, ethylene perception, and formation of phenolics in response to pathogens (Burkhead et al. 2009; Chen et al. 2011; Zhang et al. 2014). However, excess copper is toxic, and hypersensitivity in such environments are described in *Arabidopsis* mutants (Chen et al. 2011).

### 1.2.2 Non-Metal Stress Factors

*Methyl viologen (MV).* MV is one of the most commonly used herbicides. It is widely used for weed control (Haley 1979) and causes rapid membrane damage and efficiently induces cell death in green plants. It is unknown how MV is transported into the chloroplast, which is its major target site. However, a number MV-resistant *Arabidopsis* mutants have been reported, together with identification of a MV-mutant containing a gene encoding a putative transporter protein localized to the Golgi apparatus (Li et al. 2013; Han et al. 2014).

*Hydrogen peroxide ($H_2O_2$).* Oxidative stress leading to production of reactive oxygen species (ROS), of which the most important is $H_2O_2$, may be caused directly or indirectly, as results of abiotic stresses (Vranova, Inze, and Van Breusegem 2002). Oxidative damage to proteins, DNA, and lipids is a common feature of the different ROS activities. Treatment of *Arabidopsis* with $H_2O_2$ induces elevation of nutrient ionic levels, such as the concentration of cytosolic calcium, and expression of genes (Desikan et al. 2001; Hu et al. 2007), and tolerance to $H_2O_2$ has been determined on the basis of seed germination, seedling growth and oxidative damage, using various mutants (Al-Quraan, Locy, and Singh 2011).

*Auxin.* The phytohormone auxin (Indole-3 acetic acid, IAA) is involved in a multitude of developmental and physiological processes (Benjamins and Scheres 2008). Auxin is mainly synthesized in leaf primordia and young leaves, and from here is transported to other sites of action. Many ABC transporters might have affinity for auxin, and function in auxin transport (Kang et al. 2011). As mentioned above, data demonstrates that auxin negatively regulates tolerance to aluminum through AtTAP2 expression alterations and distribution of aluminum within plants (Zhu et al. 2013).

*Heat stress.* Heat stress in plants is connected with increased risk of incorrect and incomplete protein folding, and denaturation of

intracellular proteins and membrane complexes (Baniwal et al. 2004; Kosova et al. 2011). *Arabidopsis* is reported to harbor many heat stress genes. Heat stress responses include upregulation of enzyme activities and other profound reactions leading to programmed cell death (Majoul et al. 2004; Zhang et al. 2010). Enhanced expression of heat stress-inducible genes in *Arabidopsis* has been reported (Sato et al. 2014), and plants are found to be more susceptible to a combination of salt and heat stress compared to each of the different stresses applied individually. Such stress combinations result in enhanced expression and accumulation of transcripts, unique to the stress combination (Suzuki et al. 2016).

*Wounding.* When wounding plant tissues, new tissues generates to restore the damage. Regeneration of tissue involves expression of genes related to cell division, hormones and transcription factors (Asahina et al. 2011; Birnbaum and Sanchez Alvarado 2008; Reid and Ross 2011).

Different transgenic lines of *Arabidopsis* respond to mechanical wounding by wound-inducible gene expression as predominantly in particular organs and tissues are reported (Gupta et al. 2012; Bohlmann et al. 1998). Induction of the wounding response is shown for ABC proteins, such as AtABCG11 and AtABCD1. The former respond and is upregulated to wounding, as well as to glucose, salt and ABA treatments (Panikashvili et al. 2007), while the other is involved in basal and wound-induced jasmonic biosynthesis in leaves (Theodoulou et al. 2005). Interestingly, wound-induced resistance has been shown to be preceded by, and dependent upon, a burst of calcium, and that systematic cytosolic calcium elevation is activated upon wounding (Beneloujaephajri et al. 2013; Kiep et al. 2015).

## *1.3 The Objectives of the Thesis*

Studies of plant transporters can provide value to agriculture, by revealing the role of transporters in enabling plants to adapt to environmental stress conditions, which can impact plant production and crop yields. Additionally, it can provide insight into human transporters, and thereby contribute indirectly to developing methods to overcome chemical and drug resistance, and to gain novel insights into the cause of diseases.

The objectives of this study are:

1. To analyze the functional role of AtTAP1, primarily through the characterization of the mutant *attap1* in response to different abiotic treatments, and by comparing expression patterns of *AtTAP1* to *AtTAP2*.
2. To investigate on the evolution and conservation of *AtTAP1* and *AtNAP14*.
3. To analyze the enzymatic function of the proteins AtTAP1, AtTAP2, and AtNAP14.

The results are presented in detail in this thesis, and the main results of *AtTAP1* and AtTAP1 are presented in an article, submitted to *Journal of Plant Research* (Appendix 1).

Intentionally left blank

# 2 Materials and Methods

## 2.1 Materials

### 2.1.1 Buffers, Media and Solutions

Media for cultivating bacteria and plants were autoclaved. All other solutions were filter sterilized (0.2 µm).

Media used: LB (25 g LB Broth (10 g Bactotryptone, 5 g Bactoyeast extract, 10 g NaCl), adding $dH_2O$ to 1000 ml, adjusting pH 7.0), LB-Agar (15 g agar in 1000ml LB medium), MS (4.3 g/l MS salts, 10 g/l sucrose (1%), 112 mg/l vitamin B5, adjusting pH 5.8, 7 g/l plant agar), ½MS (half-strength Murashige and Skoog means 2.15 g/l MS salts).

Final concentrations of antibiotics: Ampicillin (AMP) 100 µg/ml, BASTA (ppt) 10 µg/ml, Chloramphenicol (Cam, Cp) 34 µg/ml, Kanamycin (Kan) 50 µg/ml, Spectinomycin (Spec) 100 µg/ml. Antibiotics were filter sterilized, and added to autoclaved media after cooling to 50 ºC.

### 2.1.2 Enzymes and Commercial Kits

Enzymes and commercial kits, together with the source, are described with methods used. All enzymes and kits were used in accordance with the manufacturer's protocol and instructions.

## 2.1.3 Plant Material

### 2.1.3.1 *Arabidopsis thaliana*

**Col-0 (WT)** was used in all experiments as the wildtype *Arabidopsis* line.

***attap1*, SAIL_8_B04 (N800375/CS800375),** (Arabidopsis Biological Resource Centre, The Ohio State University, www.abrc.osu.edu): Arabidopsis mutant of *AtTAP1* (*At1g70610*) with a T-DNA insert.

### 2.1.3.2 *Nicotiana tabacum*

*Nicotiana tabacum* (tobacco) were used for all tobacco experiments.

## 2.1.4 Bacterial Strains

### 2.1.4.1 *Escherichia coli* (*E. coli*)

**DH5α**: This strain of *E. coli* was developed for laboratory cloning use, and has multiple mutations that enable high-efficiency transformations (Taylor, Walker, and McInnes 1993).

**BL21(DE3)pLysS** (Novagen): DE3 lysogen expresses T7 polymerase upon IPTG induction. The pLysS plasmid produces T7 lysozyme to reduce basal level expression of the gene of interest. It is suitable for production of protein from target genes cloned in pET vectors. The strain is chloramphenicol resistant.

**Rosetta (DE3)pLysS** (Novagen): In Rosetta(DE3)pLysS the rare tRNA genes are present on the same plasmids that carry the T7 lysozyme. This can improve the expression of foreign proteins, relative to BL21(DE3)pLysS. The strain is chloramphenicol resistant.

#### 2.1.4.2 *Agrobacterium tumefaciens*

*A. tumefaciens*, a bacterium commonly found in the soil, has the property of transforming normal plant cells to tumor-forming cells. The bacteria harbors a tumor inducing (Ti) plasmid, which contains a left and right sequence flanking the transfer DNA (T-DNA).

**ABI-1**: This strain was used in transformations to generate stable transgenic Arabidopsis plants. ABI-1 possesses the Ti plasmid, which is kanamycin resistant.

### 2.1.5 Vectors

**pPCR-Script Cam SK(+)** (Stratagene): The pPCR-Script Cam SK(+) cloning vector includes a chloramphenicol-resistance gene, a *lac* promoter for gene expression, T3 and T7 RNA polymerase promoters for *in vitro* production of RNA, and the SK multiple cloning site (MCS), which is modified to include the *SrfI* restriction-endonuclease target sequence. Insertion of a PCR product disrupts the LacZ' fragment, enabling the selection of colonies harboring positive ligation products based on white/blue screening.

**pJET1.2** (Thermo Fisher): pJET1.2 is a positive selection cloning vector, which contains a lethal restriction enzyme gene that is disrupted by ligation of a DNA insert into the cloning site, allowing for efficient recovery of blunt-ended PCR products. As a result, only bacterial cells with recombinant plasmids are able to form colonies. Re-circularized pJET1.2/blunt vector molecules lacking an insert express a lethal restriction enzyme, which kills the host *E. coli* cell after transformation. The vector harbors a β-lactamase gene conferring resistance to ampicillin.

**pWEN18**: harbors YFP (Yellow fluorescent protein) under the control of the 35S promoter (Kost, Spielhofer, and Chua 1998).

**pBA002a**: is a binary plant transformation vector, which was derived from pBA002 by the removal of the 35S promoter sequence (Kost, Spielhofer, and Chua 1998). The pBA200a confers spectinomycin resistance to *E. coli* and *Agrobacterium*, and BASTA resistance to plants after stable transformation.

**pBADG**: The pBADG vector contains a GFP (Green fluorescent protein) and a GUS (β-Glucuronidase) reporter gene. The pBADG vector confers spectinomycin resistance to *E. coli* and *Agrobacterium*, and BASTA resistance to plants after stable transformation.

**pET28a(+)** (Clontech): pET28(a) is a bacterial expression vector with T7lac promoter, which carries an N-terminal His•Tag/thrombin/T7•Tag configuration.

## 2.1.6 Primers

**Table 2.1 – Primers used in this study**
All primers were ordered from Sigma-Aldrich.

| Primer name | Sequence[a] |
|---|---|
| 1g70610-L: | 5'-ATGGCTCAGCAAGTACTCGGCTGCAC-3' |
| 1g70610-R: | 5'-TAAGACGGCATCGTTTTGTCTCTT-3' |
| 1g70610-KpnI-L: | 5'-AATGGTACCATGGCTCAGCAAGTACTCG-3' |
| 1g70610-KpnI-R: | 5'-AATGGTACCTAAGACGGCATCGTTTT-3' |
| TAP1-Promoter-L: | 5'-ATCCATGGAGGTTAACGATTGGGCAGAAG-3' |
| TAP1-Promoter-R: | 5'-ATGGCGCGCCTTATGTTCGGTGGACTAAAG-3' |
| 35S-promoter-L: | 5'-CACAATCCCACTATCCTTCGCAAGACC-3' |
| YFP-R: | 5'-ACACGCTGAACTTGTGGCC-3' |
| NY/2-R: | 5'-TAGCGGCCGCTTACATGATATAGACGTTGTGGC -3' |
| NOS/2: | 5'-GATAATCA TCGCAAGACCGGCAACAGGA-3' |
| LB1: | 5'-GCCTTTTCAGAAATGGATAAATAGCCTTGCTTCC-3' |
| LB3: | 5'-TAGCATCTGAATTTCATAACCAATCTCGATACAC-3' |
| SAIL_8_B04-L: | 5'-AAGGAAAAAGCTTGAAGCGTC-3' |
| SAIL_8_B04-R: | 5'-TGTTTCCCTCATTCGTTTCAC-3' |
| T7 promoter: | 5'-TAATACGACTCACTATAGGG-3' |
| T7-terminator: | 5'-GCTAGTTATTGCTCAGCGGTG-3' |
| TAP1-L: | 5'-GACTTGGCTCAGACTGTCAGCA-3' |
| TAP1-R: | 5'-CCACTTCACCAGGATGCACGGA-3' |
| TAP1a-L: | 5'-CATTTTGTTTACTTGTTTACAGC-3' |
| TAP1-NheI-L: | 5'-ATGCTAGCATGGCTCAGCAAGTA-3' |
| TAP1-BamHI-R: | 5'-ATGGATCCTCATAAGACGGCATCGTTTTGTC-3' |
| SAIL_409_C10-L: | 5'-AGGATCGTTGGGTTATCTTCG-3' |
| SAIL_409_C10-R: | 5'-GTATCAGTTTCAGCTGCCAGG-3' |
| Actin Forward: | 5'-TGCCAATCTACGAGGGTTTC-3' |
| Actin Reverse: | 5'- GAACCACCGATCCAGACACT-3' |
| pJET Forward: | 5'-CGACTCACTATAGGGAGAGCGGC-3' |
| pJET Reverse: | 5'-AAGAACATCGATTTTCCATGGCAG-3' |
| TAP2-NheI-L: | 5'-TAGCTAGCATGGGCAACAAGAAA-3' |
| TAP2-BamHI-R: | 5'-TAGGATCCTCACAAGGTGGTAAC-3' |
| TAP2-Inside-L: | 5'-GCGCTTATAGGAGTTGGTTTCA-3' |
| TAP2-Inside-R: | 5'-CACCGCTTGGTCCTACTAGTGC-3' |
| NAP14-NheI-L: | 5'-ATGCTAGCATGGCAGTGTCGACGTTTTCG-3' |
| NAP14-SacI-R: | 5'-ATGAGCTCCTAAAGTGGTGGACGTTCTGC-3' |
| NAP14-Inside-L: | 5'-ATCCTGACTTGCTTCCCACTG-3' |
| NAP14-KpnI-L: | 5'-ATGGTACCATGGCAGTGTCGACGTTTTCG-3' |
| NAP14-KpnI-R: | 5'-ATGGTACCAAGTGGTGGACGTTCTGCAAC-3' |

[a] Restriction sites incorporated into primers are underlined

## 2.2 Methods

### 2.2.1 Bioinformatics Methods

**Alignments.** Protein sequences were obtained from *ncbi.nlm.nih.gov,* and aligned with BioEdit software, version 7.2.5.0 (Hall 2011).

**Phylogenetic tree.** A phylogenetic tree was built from alignments to indicate evolutionary relationships using the BioEdit programme, Neighbor-Joining/UPGMA method version 3.6.a2.1 application.

**Identities and similarities.** Percentage identity and similarity of proteins were derived using tool programme *EMBOSS Needle* (http:www.ebi.ac.uk/Tools/psa/emboss_needle).

**Chloroplast transit peptides.** Prediction of chloroplast transit peptides (cTP) was executed using ChloroP 1.1 Predicting Server (Emanuelsson, Nielsen, and von Heijne 1999).

### 2.2.2 Plant methods

#### 2.2.2.1 Plant growth and stress treatments

**Arabidopsis.** Sterilized seeds from *Arabidopsis thaliana*, ecotype Columbia, were sown on ½MS media (adjusted pH5.8) with or without 1% glucose, solidified with 0.7% (w/v) plant agar, and placed in refrigerator at 4 ºC for 48 hrs, before growth in a growth cabinet at 21 ºC in a 16/8 hrs light/dark. For further growth of plants, 14-18 days old seedlings were transferred to soil on rockwool cubes, and placed in a cabinet room at 21 ºC, 16/8 hrs light/dark.

For stress treatments, plants were exposed to different solutions of chemicals: $AlCl_3$ (Fisher), $FeCl_3$ (Fisher), $CaCl_2$ (Sigma-Aldrich), $MgCl_2$ (Sigma-Aldrich), $CuSO_4$ (Sigma-Aldrich), $H_2O_2$ (J.T. Baker), Methyl

viologen (MV) (Sigma-Aldrich), or Auxin (IAA) (Sigma-Aldrich), using the concentrations specified in the result section. 14 days old seedlings were treated with each solution by applying 3 ml directly to the surface of the plate. Fresh solution was applied every second day.

To study different effects of metal ions on root length, seeds were grown on ½MS medium containing different metal ions. Seedlings were grown for 16 days in a vertical position, or for 12 days in horizontal position followed by 21 days in a vertical position. Seedlings were photographed, and the root lengths measured with a ruler.

For phenotypic analysis of soil grown plants in response to iron stress, two week old plants were watered regularly with 2.0 mM $FeCl_3$ for six weeks and inspected every fifth day.

For treatment with auxin, seedlings were transferred to wells containing ½MS with 1% sucrose added 50 µM auxin and placed on bench at room temperature and continuous light, for up to 24 hrs. Treated seedlings were harvested after 6, 12 and 24 hrs.

Leaves of plants were wounded by tearing with a needle.

**Tobacco.** Sterilised seeds were grown on plates with ½MS media containing 1% sucrose, solidified with 0.7% (w/v) plant agar, and placed in cabinet at 21 ºC in a 16/8 hrs light/darkness exchange. Seedlings were transferred to Magenta boxes (Sigma-Aldrich) after 2-3 weeks, and grown in the same conditions.

#### 2.2.2.2 Sterilizing Seeds

Seeds treated with 70% Ethanol with 0.05% Triton were gently shaken for 5 min, then the Ethanol/Triton removed, replaced with 100% ethanol, and gently shaken for 5 min. Finally the ethanol was removed before washing three times with $dH_2O$.

#### 2.2.2.3 Plant Transformation

The Floral dip method was used to generate transgenic Arabidopsis plants, stably transformed with 35S-AtTAP1-YFP/pBA002a, pBADG or pBADG/GUS, using Agrobacterium-mediated transformation (Clough and Bent 1998). To select transgenic plants, seeds were sown on ½MS media containing BASTA. Microscopy studies were performed on leaves of first generation transformants. The leaves were analyzed for YFP fluorescence from chlorophyll, using a Nikon A1R confocal laser scanning microscope.

#### 2.2.2.4 Biolistic Transformation of Tobacco

Particle micro-bombardment was used to transiently express protein fusions in epidermal cells of tobacco plants. AtTAP1-pWEN18 and AtNAP14-pWEN18 were transiently expressed in tobacco leaf cells by particle bombardment (Kost, Spielhofer, and Chua 1998). The protocol of Biolistic® PDS-1000/He Particle Delivery System (Bio-Rad) was followed with the following specifications.

Gold particles (microcarriers) (BIO-RAD Lab.): 1 ml 100% ethanol was added to 35 mg of micron gold 0.6 µm in a 1.5 ml Eppendorf tube, vortexed for 2-3 min, centrifuged (5 sec at 11000 rpm), and the pellets washed three times in 100% ethanol. 50 µl was transferred to a prechilled centrifuge tube, centrifuged for 2 sec at 6500 rpm, the ethanol removed, and the pellets washed 4 times with cold sterile water, centrifuging for 2 sec at 6500 rpm between each washing step. Subsequently, the pellets were re-suspended in 50 µl cold sterile water, and the following added in order: 10 µl of plasmid DNA (1 µg/µl), 50 µl 2.5 M $CaCl_2$ and 20 µl 0.1 M spermidine (free-base) while shaking. The mixture were vortexed at 4 °C in a cold room for 20 min before adding 200 µl 100% ethanol, centrifuged for 2 sec at 6500 rpm and the microcarriers pelleted 4 times with 200 µl 100% ethanol by pulse centrifugation for 2 sec at 6500 rpm. The particles were finally re-suspended in 30 µl 100% ethanol, and stored on ice, before pipetting and spreading 5 µl of the gold suspension

onto the center of the macrocarrier (BIO-RAD Lab) for immediate use in biolistic transformation. The biolistic transformation was carried out using a PDS-1000/He$^{TM}$ Biolistic Particle Delivery System (BIO-RAD Lab), which is powered by a burst of helium gas to accelerate the microcarriers into the sample. All transformations were performed using 1300 psi rupture discs (BIO-RAD Lab) under 27-28 (in.) Hg vacuum. Exposed tobacco leaves samples were placed on MS medium for transformation, and stored on the bench (room temperature) for 48 hrs before image acquisition. The tobacco leaf cells were analyzed for YFP fluorescence using a Nikon A1R confocal laser scanning microscope.

#### 2.2.2.5 General Staining Method/GUS Staining

Arabidopsis plants stably expressing GUS reporter constructs, were examined for GUS expression by histochemical staining executed with X-Gluc (Jefferson 1987; Jefferson, Kavanagh, and Bevan 1987). Tubes with different aerial tissues or roots in X-Gluc substrate, were placed in water bath, 37 ºC for 1:00, 2:00, 6:30, 7:15 and 24:00 hrs. Tissues incubated over-night were cleared with 70% ethanol before inspection by microscopy.

### *2.2.3 Bacterial Methods*

#### 2.2.3.1 Chemically Competent DH5α Cells

Cells from a single colony of *E. coli* was inoculated into 5 ml LB medium and grown overnight in shaker, at 250 rpm, 37 ºC. One ml of the overnight culture was then inoculated into 200 ml LB medium, in a sterile 1000 ml Erlenmeyer flask. The culture was grown at 37 ºC shaking at 250 rpm until an $OD_{600}$ of 0.5-0.7, before immediately cooling on ice for 15 min. The bacteria cell culture was aliquoted into two pre-chilled and sterile polypropylene tubes, and centrifuged for 10 min at 4000 rpm at 4 ºC. Supernatants were discarded, and pellets re-suspended

in 10 ml ice-cold 0.1 M $MgCl_2$ solution. The re-suspended cells were centrifuged for 10 min at 4000 rpm at 4 ºC, the supernatants discarded and the pellets re-suspended in 10 ml ice-cold $CaCl_2$, before incubation on ice for 30 min. Subsequently the re-suspended cells were centrifuged for 10 min at 4000 rpm at 4 ºC. The supernatants were discarded and the pellets re-suspended in 2 ml ice-cold MOPS glycerol, before aliquoting 100 µl in Eppendorf tubes and immediately freezing in liquid nitrogen, and then stored in freezer at –80 ºC.

#### 2.2.3.2 Transformation of Chemically Competent *E. coli* Cells

An aliquot of 100 µl competent cells was thawed on ice and mixed with ~1 µg of plasmid DNA. Then incubated on ice for 30 min before the transformation mixture was heat-shocked for 45 sec in a water-bath at 42 ºC and immediately incubated on ice for two min. 500 µl LB medium was added to the transformed cell mixture, before incubation for 45 min at 37 ºC on a shaker, 250 rpm. Thereafter, the transformation mixture was centrifuged at 3000 rpm for two min, and some of the supernatant was discarded. The pelleted cells were re-suspended in the remaining 50-200 µl supernatant. The re-suspended cells were spread on LB-Agar selection plates containing appropriate antibiotics, and incubated over-night at 37 ºC. Transformed *E. coli* cells were visible as colonies.

#### 2.2.3.3 Chemically Competent ABI Cells

Cells from a single colony of *Agrobacterium* were inoculated into 5 ml LB medium containing kanamycin and grown overnight in a shaker, 250 rpm at 28 ºC. The next day 2 ml of the overnight culture was transferred to 50 ml LB medium containing kanamycin in a sterile 250 ml conical flask, and grown in a shaker, 250 rpm at 28 ºC to an $OD_{600}$ of 0.5-1.0. The cells were then chilled on ice for ~10 min before harvesting at 5000 rpm and 4 ºC, for 10 min in a SS-24 rotor (Sorvall). The pelleted cells were gently re-suspended in 1 ml ice-cold 20 mM $CaCl_2$, and dispensed

into 100 µl aliquots in 1.5 ml pre-chilled Eppendorf test tubes. The tubes were immediately frozen in liquid nitrogen and stored at -80 ºC.

#### 2.2.3.4 Transformation of Chemically Competent ABI Cells

Competent *Agrobacterium* was prepared using the freeze-thaw method. For each transformation an aliquot of competent cells was put on ice and ~1 µg of plasmid DNA immediately added. The cells were then thawed by incubating the tube in a 37 °C water bath for 5 min, mixing gently half way through. Subsequently 1 ml of LB media was added, and the cells incubated at 28 °C with gentle shaking (100 rpm) for ~four hours. 150 µl of the cells was then spread on an LB-agar plate containing the appropriate antibiotic, and incubated at 28-30 °C for 2-3 days.

### 2.2.4 Vectors Constructed

***AtTAP1-pPCR-Script Cp$^R$.*** The 2103-nucleotide *AtTAP1 (At1g70610)* cDNA was amplified from cDNA using PWO polymerase, and using primers 1g70610-L/1g70610-R (Table 2.1) and cloned into the vector pPCR-Script Cp$^R$, following the manufacturers instructions. The vector was transformed into DH5α, and bacteria colonies selected on LB-Agar media containing chloramphenicol and X-gal.

***PromoterTAP1--pPCR-Script Cp$^R$.*** The upstream 701-nucleotide promoter region of the *AtTAP1* gene was amplified from DNA using PWO polymerase and the primers TAP1-Promoter-L/TAP1-Promoter-R (Table 2.1), and cloned into the vector pPCR-Script Cp$^R$. The vector was transformed into DH5α, and bacteria colonies selected on LB-Agar media containing chloramphenicol and X-gal.

***PromoterTAP1-pBADG.*** The promoter region of the *AtTAP1* gene was excised from the vector *PromoterTAP1-pPCR-Script Cp$^R$*, using restriction enzymes NcoI and AscI, and ligated into pBADG. The resulting construct, *PromoterTAP1-pBADG*, places the GUS gene

located inside the pBADG plasmid, under the control of the *TAP1 promoter*. The construct was transformed into DH5α and further into ABI-1 bacteria, and cells grown on LB-Agar media containing kanamycin and spectinomycin.

***AtTAP1-pWEN18.*** The *AtTAP1* cDNA was excised from *AtTAP1-pPCR-Script Cp*$^{R}$ using KpnI, and ligated into pWEN18, which was prepared by digestion with KpnI and subsequent dephosphorylation. The vector was transformed into DH5α, and the cells grown on LB-Agar media containing ampicillin.

***35S-AtTAP1-YFP/pBA002a.*** The insert *35S-AtTAP1-YFP* was excised from *AtTAP1-pWEN18* using SpeI and AscI, and cloned into the vector pBA002a. The vector was transformed into DH5α, and the cells grown on LB-Agar media containing spectinomycin.

***AtTAP1-pJET1.2.*** The gene *AtTAP1* was amplified from cDNA using Phusion PCR, and the primers TAP1-NheI-L/TAP1-BamI-R (Table 2.1), and cloned into the vector pJET1.2, using the manufacturers Blunt-End cloning protocol. The vector was transformed into DH5α, and the cells were grown on LB-Agar media containing ampicillin antibiotic.

***AtTAP1-pET28a(+).*** The *AtTAP1* cDNA was excised from *AtTAP1-pJET1.2*, using NheI and BamHI, and cloned into the vector pET28a(+). Thereafter, the vector was transformed into DH5α, and grown on LB-Agar containing kanamycin. *AtTAP1-pET28a(+)* was then transformed into BL21(DE3)pLysS or Rosetta(DE3)pLysS bacteria, and grown in LB media containing kanamycin and chloramphenicol.

***attap1-pJET1.2.*** Genomic DNA from the mutant *attap1* (with a T-DNA insert) was amplified using primers SAIL_8_B04-L/LB3 (Table 2.1), and Blunt-End cloned into vector pJET1.2.

***AtTAP2-pJET1.2.*** The 1935-nucleotide *AtTAP2 (At5g39040)* cDNA was amplified from cDNA using Phusion PCR and primers TAP2-NheI-

L/TAP2-BamI-R (Table 2.1), and cloned into the vector pJET1.2, using the manufacturers Blunt-End cloning protocol. The vector was transformed into DH5α, and the cells grown on LB-Agar media containing ampicillin.

***AtTAP2-pET28a(+).*** *AtTAP2* was excised from *AtTAP2-pJET1.2*, using NheI and BamHI, and cloned into the vector pET28a(+). Thereafter, the vector was transformed into DH5α, and grown on LB-Agar containing kanamycin. *AtTAP2-pET28a(+)* was then transformed into BL21(DE3)pLysS or Rosetta(DE3)pLysS bacteria, and grown in LB media containing kanamycin and chloramphenicol.

***AtNAP14-pJET1.2.*** The 873-nucleotide *AtNAP14 (At5g14100)* cDNA was amplified from cDNA using Phusion PCR and primers TAP1-NheI-L/TAP1-BamI-R (Table 2.1), and cloned into the vector pJET1.2, using the manufacturers Blunt-End cloning protocol. The vector was transformed into DH5α, and the cells grown on LB-Agar media containing ampicillin.

***AtNAP14-pET28a(+).*** The *AtNAP14* gene was excised from *AtNAP14-pJET1.2* using NheI and SacI, and cloned into the vector pET28a(+). Thereafter, the vector was transformed into DH5α, and grown on LB-Agar containing kanamycin. *AtNAP14-pET28a(+)* was then transformed into BL21(DE3)pLysS or Rosetta(DE3)pLysS bacteria, and grown in LB media containing kanamycin and chloramphenicol.

***AtNAP14-pWEN18.*** The *AtNAP14* cDNA was amplified from the *AtNAP14-pET28a(+)* using Phusion PCR and the primers NAP14-KpnI-L/NAP14-KpnI-R (Table 2.1), and ligated into pWEN18, which was prepared by digestion with KpnI and then dephosphorylation. The vector was transformed into DH5α, and the cells grown on LB-Agar media containing ampicillin.

#### 2.2.4.1 Sequencing

All vectors generated in this project were confirmed by sequencing, using appropriate primers. The following companies performed the sequencing: John Innes Genome Lab. (UK), Genewiz (US), or Macrogen Europe (NL).

### 2.2.5 DNA/RNA Methods

#### 2.2.5.1 RNA Isolation

RNA was prepared from leaves of Arabidopsis using the Mammalian Total RNA Isolation Miniprep Kit (Sigma-Aldrich) or RNeasy Plant Mini Kit (Qiagen, Chatsworth, CA, USA) kits. The protocol provided by the manufacturer was followed. Isolated total RNA was quantified using NanoDrop 2000 (Thermo-Fisher).

#### 2.2.5.2 Preparing Genomic DNA

Genomic DNA was prepared from leaves of Arabidopsis WT and *attap1* (Mut) plants, to characterize the *AtTAP1* T-DNA insertion line, *attap1*, using the GenElute™ Plant Genomic DNA Miniprep Kit (Sigma-Aldrich) according to the manufacturer's instructions.

#### 2.2.5.3 Isolation of Plasmids

For isolation of plasmid DNA, the kits GeneElute™ Plasmid Miniprep Kit (Sigma-Aldrich), NucleoSpin® Plasmid (Macherey-Nagel) and FastPlasmid Mini-Prep Kit, 5 Prime (Biocompare) were used, following the protocol provided by the manufacturer.

#### 2.2.5.4 Purification of DNA

For isolation of DNA from agarose gels, the GenElute™ Gel Extraction Kit (Sigma-Aldrich), NucleoSpin® Extract II Kit (Clontech

Laboratories, Inc.) or QIAquick PCR Purification Kit (QIAEX II Agarose Gel Extraction Protocol) (Qiagen, Biocompare) were used, following the protocol provided by the manufacturer.

#### 2.2.5.5 Standard Cloning Methods

**Restriction digestion.** Restriction digestion was carried out using the appropriate restriction enzymes, and the optimal buffer as specified by the manufacturer. All digestion reactions were incubated for up to three hours. All restriction enzymes were purchased from NEB or Fermentas.

**Dephosphorylation.** Dephosphorylation of DNA 5' termini was performed using the CIAP enzyme (Sigma-Aldrich), following the instructions from the manufacturer.

**Ligation.** For blunt end pPCR-Script ligations the instructions from manufacturer (Stratagene) was followed. Other ligations were performed using the T4 DNA ligase, following the instruction from the manufacturer (Invitrogen or Fermentas).

#### 2.2.5.6 RT-PCR

First-strand cDNA synthesis was performed using Total RNA from young leaves of Arabidopsis according to the manual of the kit RevertAid First Strand cDNA Synthesis Kit (Thermo Scientific). One µl of first-strand cDNA synthesis reaction was used as a template in each 20 µl PCR reaction. RT-PCR images were developed by VisiDoc-It$^{TM}$ Imaging System (UVP, Cambridge, UK), and densitometry was executed with ImageJ software and relative band intensities normalized to actin set at 1.0.

#### 2.2.5.7 PCR

For amplifying DNA for blunt ended PCR products PWO polymerase (Roche) and Phusion DNA polymerase (NEB) were used following the

protocol of the manufacturer. Other PCR methods using Taq polymerase (Sigma) and Mastermix TopTaq (Qiagen) were executed following the protocol of the manufacturer.

PCR cycler conditions in general was performed with 95 °C and 5 min preheat, 95 °C and 30 sec denature, 55-60 °C and 30 sec annealing, 72 °C elongation for 60 sec per 1 kbp fragment, and 20-35 cycles.

## 2.2.6 Agarose Gel Electrophoresis

Agarose gel electrophoresis was used to confirm PCR products or restriction digests. Agarose gels were made by melting 1% agarose in 50ml 1xTAE buffer (40 mM Tris base, 20 mM acetic acid, 1 mM EDTA). PCR products were mixed with PCR loading buffer (0.25% Bromophenol Blue, 40% Sucrose, $dH_2O$) and GelRed™ (Bitium) prior to loading. Hyperladder I (Bioline), Hi-Lo DNA marker (Minnesota Molecular Inc.), or GenRuler™ 1kb Plus DNA Ladder (Invitrogen/Thermo Fisher), were loaded next to the samples as DNA size markers. Electrophoresis executed in 1xTAE buffer at 95-100 V, and gels viewed using a UVP BioDoc® Imaging Systems (Analytic Jena).

## 2.2.7 Protein Methods

### 2.2.7.1 Preparation of recombinant fusion proteins

Competent *E. coli* strains BL21(DE3)pLysS or Rosetta(DE)pLysS were transformed with *AtTAP1-pET2a(+)*, *AtTAP2-pET28a(+)* or *AtNAP14-pETa(+),* and plated on LB-Agar plates containing kanamycin and chloramphenicol. Transformation was confirmed by colony PCR. Cells from one positive colony were inoculated into 5 ml LB medium containing 2% glucose, kanamycin and chloramphenicol, before growth for three hours at 37 °C, shaking 250 rpm. 200 µl of the overnight culture

were transferred into 10 ml LB medium containing antibiotics, and further grown at 37 °C, shaking 250 rpm, until $OD_{600}$ of 0.5-0.8. The cultures were induced by a final concentration of 0.5 mM IPTG, and replaced in shaker for four hours. Induced cells were harvested by centrifugation at 6000xg for 10 min at 4 °C, the supernatants discarded, and the pellets resuspended in PBS buffer pH 7.4, containing Halt™ Protease Inhibitor Cocktail (100x) (Thermo Scientific) and 0.5 M EDTA Solution (100x) (Thermo Scientific). The cells were sonicated (Branson Sonifier 450 cell disrupter) at 20% amplitude on ice (30 s pulses at one min intervals). Samples were centrifuged at 17000 rpm for 15-20 min. 20 µl 5x Protein loading buffer/dye (10% SDS, 50% glycerol, 250 mM Tris-Cl pH6.8, 5 mM EDTA, 200 mM DTT, 0.25% bromophenol blue) was added to 80 µl of supernatant (soluble fraction). Pellets (insoluble fraction) were re-suspended in 100 µl 1x Protein loading buffer/dye, and vortexed vigorously. Both samples were denatured by boiling (95 °C) for 10 min, before incubation on ice before protein separation and analysis using SDS-PAGE and Western blotting.

#### 2.2.7.2 SDS-PAGE and Western Blotting

SDS-PAGE (sodium dodecyl sulfate-polyacrylamide gel electrophoresis) was used for protein separation under denaturing conditions to ensure protein migration according to molecular weights. Resolving gels (8% or 12% together with 4% stacking gel) were used. BLUEstain™ 2 Protein ladder (Goldbio.com) and PageRuler Broad Range Unstained Protein Ladder (Thermo Scientific) were used as markers. SDS-PAGE was executed in a BioRAD tank containing 1x SDS running buffer (25 mM Tris, 192 mM Glycin, 0.1% SDS, pH 8.6). Gels were stained in 0.2% Coomassie blue staining solution (1000 ml: 0.2% (w/v) Coomassie brilliant blue R250 (2 g/ltr), 500 ml methanol, 400 ml $dH_2O$, 100 ml acetic acid) over-night at room temperature with agitation on rocker. After removing the staining solution, the stained gels were incubated in de-staining solution (1000 ml: 300 ml methanol, 100 ml

glacial acetic acid, 600 ml $dH_2O$) or $dH_2O$, at room temperature for 2-8 hrs or overnight.

For Western Blotting analysis, proteins were transferred from gels to a PVDF (polyvinylidine difluoride) membrane (ThermoFisher Scientific) for further detection of proteins. Methanol treated PVDF membranes were connected with protein gels in a "sandwich"-like, organized layer with sponge, filter paper, gel, membrane, filter paper, and sponge, in a tank filled with 1x transfer buffer (28.8 g glycine, 6.06 g Tris-base, 400 ml methanol, $dH_2O$ up to 2000 ml) for transfer. Membranes were washed in 1xTBS-T (100 ml 10xTBS (160.1 g NaCl, 48.45 g Trizma HCl, $dH_2O$ up to 2000 ml, adjusting pH to 7.6 with HCl), 900 ml $dH_2O$, 1 ml Tween20), and blocked with 5% milk blocking solution (2.5 g skimmed milk in 50 ml 1xTBS-T), before treatment with primary antibody (Anti-6His Tag mouse, Sigma-Aldrich) and secondary antibody (Gout Anti-Mouse 2. antibody, Sigma-Aldrich).

For detection and developing proteins at membranes, the developer machine ChemiDoc™ XRS+ with Image Lab™ Software (Bio-Rad) was used after preparing the membrane with ECL solution (ThermoFisher Scientific).

#### 2.2.7.3 Ion-Exchange Chromatography – Protein Purification

Induced cell cultures were harvested by centrifugation at 6000xg for 10 min at 4 °C, and supernatants discarded. The cell pellets were suspended in Tris-Cl buffer (25 mM Tris, 150 mM NaCl, pH 8.0) with Mini Tablet of Pierce™ Protease Inhibitor, Product #88665 (Thermo Scientific), and sonicated for one hour on ice (Branson Sonifier 450 cell disrupter) at 20% amplitude, one min pulses at one min intervals. Sonicated cells were centrifuged at 4 °C at 12000 rpm for 30 min. Supernatants with soluble proteins were transferred to new sterile tubes and stored at 4 °C. The PhD student Rashed Abdullah at St. John's University, Queens, NY, USA, performed the practical protein purification, using ion-exchange

chromatography equipment Äkta™ Pure system from GE healthcare Bio-Sciences AB. Tubes with proteins referring to diagram peaks, were analyzed using SDS-PAGE method and compared to detect the desired protein.

#### 2.2.7.4 Agarose Columns and His-Tag Protein Purification

Lysates with soluble and insoluble (pellets) proteins were treated according to the protocol of GoldBio.com (MO, USA), using nickel agarose beads for 6xHis-tag protein purification. For insoluble proteins, 8 M urea was added to the binding/wash buffer (50 mM phosphate buffer pH 8.0, 300 mM NaCl, 10 mM imidazole) , and 6 M urea was added to the elution buffer (50 mM phosphate buffer pH 8.0, 300 mM NaCl, 500 mM imidazole). SDS-PAGE was then performed, loading samples from each of the columns 10 washes: the elute, first wash, second wash, third-sixth wash combined, seventh-tenth wash combined, and the flow-through, in addition to the elute of the control lysate (pET28a(+) without AtNAP14 protein).

Dialysis cassettes (ThermoFisher Scientific, Slide-A-Lyzer Dialysis Cassettes, 7k MWCO, No.66370) were used to refold the purified and eluted AtNAP14 protein, following the protocol from the company, washing with 0.1 M Tris-Base buffer added descending concentrations of urea, changing every 12 hrs for five days (4 M, 2 M, 1 M, 0.5 M, 0.25 M, 0.1 M, 0.05 M, 0.025 M, 0.01 M, 0 M). Control (pET28a(+)) went through the same procedure.

Protein concentration was measured using "Bio-Rad Protein Assay" (Bradford method, Bio-Rad), following the protocol of the manufacturer.

#### 2.2.7.5 ATPase Activity

ATPase activity was measured using ATP (ATP-disodium, Sigma-Aldrich) and the $P_i$ColorLock™ assay from Innova Biosciences on the enzyme/protein AtNAP14. The protocol provided by the manufacturer

was followed. The assay is based on the change in absorbance of the dye malachite green in the presence of phosphomolybdate complexes, due to enzyme catalyzing reactions in which inorganic phosphate ($P_i$) is released from an organic phosphorylated substrate.

# 3 Results

As a prominent half-size ABC transporter, which consists of a single nucleotide-binding domain, I found AtTAP1 interesting as a topic to focus on. AtTAP1, Transporter Associated with Antigen Processing, classified to the ABC subfamily B, constitute together with AtTAP2 the TAP proteins in *Arabidopsis thaliana.*

The study of AtNAP14 as a non-intrinsic ABC transporter (NAP) was primarily to focus on ATPase activity, and to compare it with the TAP proteins. The localization pattern at the subcellular level, and evolutionary aspects, were other interesting aspects for further study.

## *3.1 AtTAP1*

### *3.1.1 AtTAP1 and Homolog Proteins*

AtTAP1 contains essential and highly conserved domains. Four of these conserved domains were examined in homologous ABC proteins of plants and non-plants, to investigate the conservation of key domains. Sequences of homologous proteins from key laboratory and commercial plant species, and from non-plant model organisms were selected for analysis. Six plants, in addition to *Arabidopsis*, were inspected: *Nicotiana tabacum* (tobacco), *Solanum lycopersicum* (tomato), *Oryza sativa* (rice), *Triticum aestivum* (wheat), *Physcomitrella patens* (moss) and, *Chlamydomonas reinhardtii* (green algae) (Table 3.1.). Five non-plant model organisms were inspected: *Homo sapiens* (human), *Danio rerio* (zebrafish), *Drosophila melanogaster* (fruit fly), *Caenorhabditis elegans* (roundworm) and *Saccharomyces cerevisiae* (yeast) (Table 3.2.).

**Table 3.1 – AtTAP1 and related proteins from different plant species**

| Species | Protein name[a] | Amino acid length | Accession code[a] |
|---|---|---|---|
| A. thaliana | AtTAP1 | 700 | NP_177218 |
| N. tabacum | ABCB-26 | 701 | XP_016492080 |
| S. lycopersicum | ABCB-26 | 689 | XP_004252689 |
| O. sativa | ABCB-26 | 688 | XP_015613646 |
| T. aestivum | Unnamed protein | 675 | CDM85589 |
| P. patens | PpABCB-6 | 578 | XP_001781344 |
| C. reinhardtii | Hypothetical protein | 560 | XP_001699295 |

[a]Protein name and accession code obtained from NCBI.

**Table 3.2 – AtTAP1 and related proteins of different non-plant species**

| Species | Protein name[a] | Amino acid length | Accession code[a] |
|---|---|---|---|
| A. thaliana | AtTAP1 | 700 | NP_177218 |
| H. sapiens | ABCB9; TAPL | 766 | NP_062571 |
| D. rerio | ABCB9 | 789 | NP_001119906 |
| D. melanogaster | CG3156 | 692 | NP_569844 |
| C. elegans | Haf-2; HAIF transporter | 773 | NP_495537 |
| S. cerevisiae | MDL2 | 773 | EDN60878 |

[a]Protein name and accession code obtained from NCBI.

Each group of TAP1 proteins was aligned using the BioEdit software. AtTAP2 (644 aa, accession code NP_198720) was also included in the plant group. Figure 3.1 and Figure 3.2 show the alignments. The four highly conserved motifs present are enlarged and aligned (Figure 3.1B and Figure 3.2B).

The ABC superfamily harbors four motifs: (1) the Walker A motif; (2) the Signature motif (ABC transporter signature motif); (3) the Walker B motif and; (4) the H-loop motif (Sánchez-Fernández et al. 2001; Rea 2007). Each of the motifs are highly conserved between the TAP1 proteins, and are situated near the C-terminal of the proteins (Figure 3.1 and Figure 3.2). Each motif is discussed in detail below.

Intentionally left blank

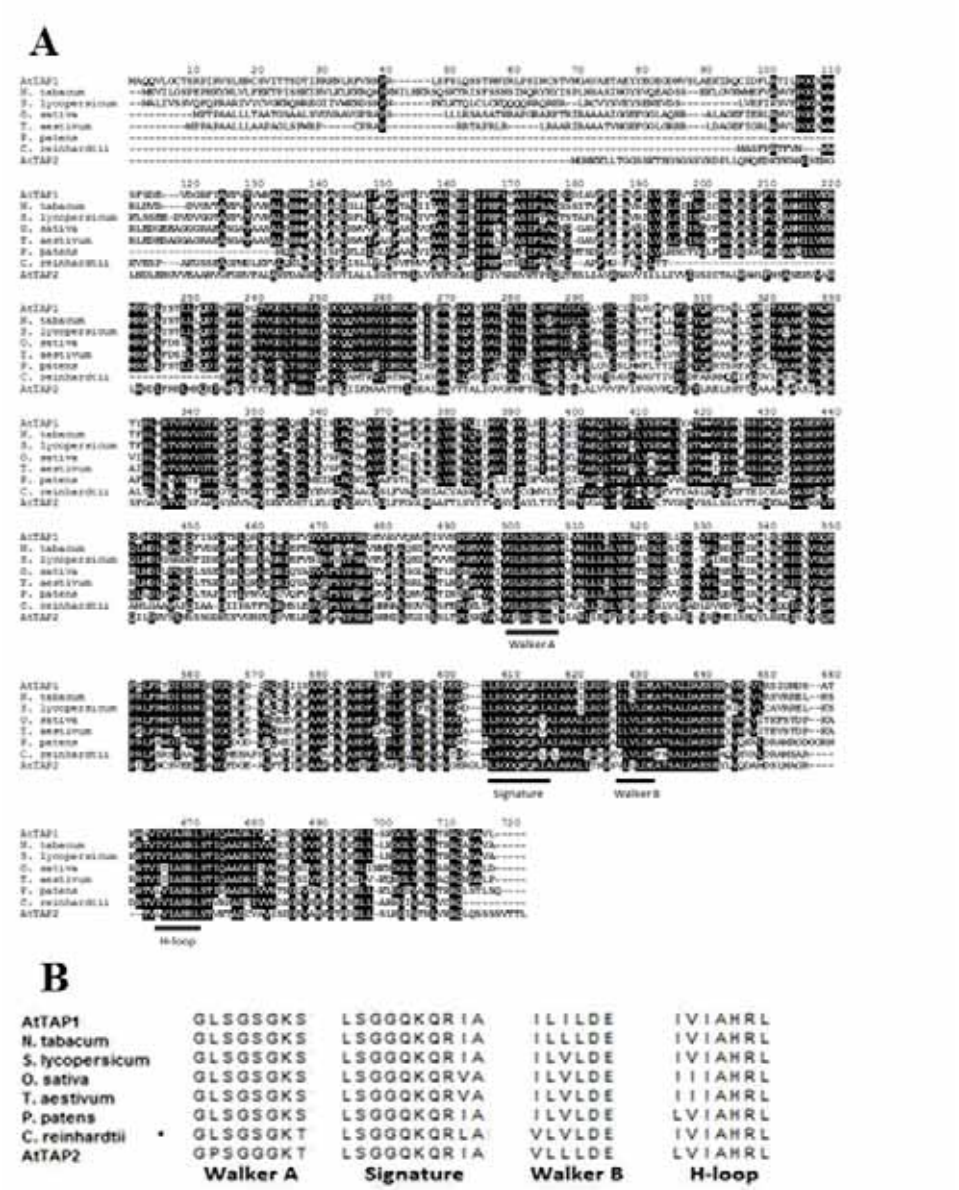


**Figure 3.1 – Alignment of AtTAP1 protein with seven different ABC proteins from other plant species**

(A) Alignment of seven TAP1 proteins and AtTAP2. The motifs are underlined. (B) Enlargement of the four motifs: Walker A, Signature (ABC transporter signature motif), Walker B and the H-loop (region).

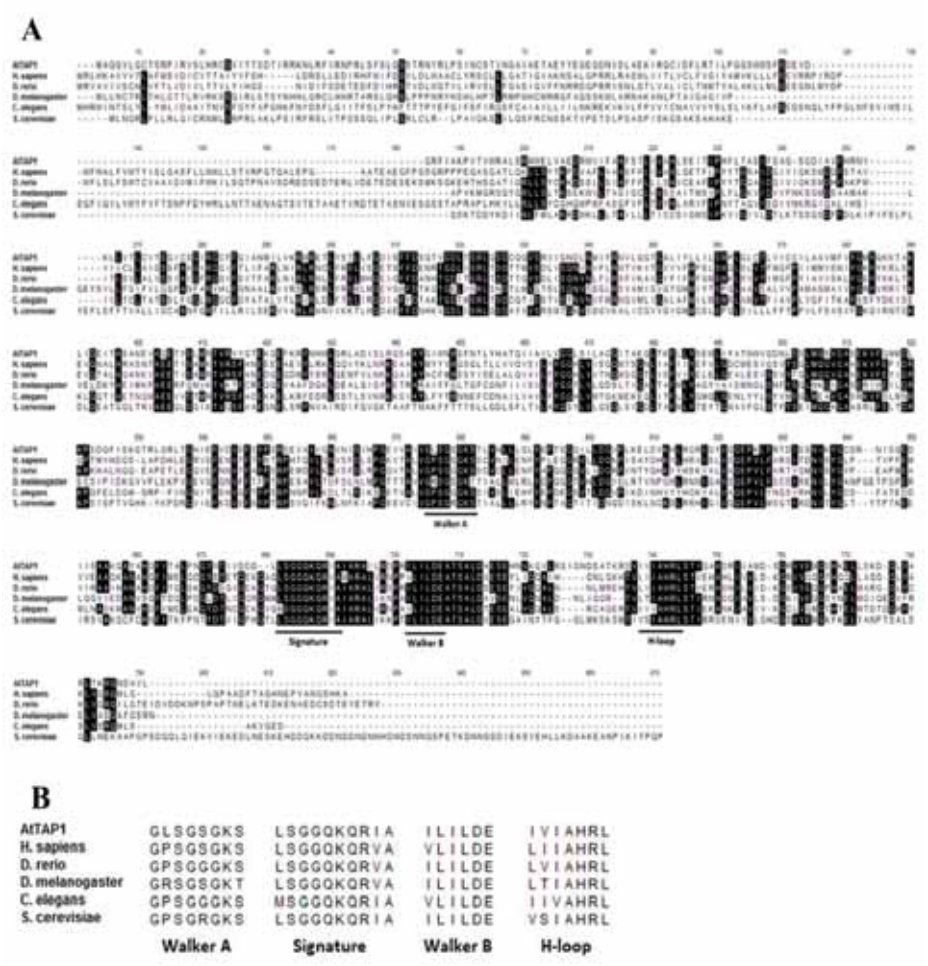


**Figure 3.2 – Alignment of AtTAP1 protein with different ABC proteins from non-plant species**

(A) Alignment of six TAP1 proteins. The motifs are underlined. (B) Enlargement of the four motifs: Walker A, Signature, Walker B and H-loop (region) enlarged.

The Walker A motif is comprised of eight amino acids, and has the pattern G-4x-GK-T/S, where the capital letters denote glycine (G), lysine (K), threonine (T) and serine (S). T/S denotes alternative, and 4x denotes any four amino acids (Walker et al. 1982; Rea 2007). Analysis of the Walker A motif in plant TAP1 proteins reveals that it is perfectly conserved between AtTAP1, and all the higher plant proteins and moss protein (Figure 3.1B). In *C. reinhardtii* there is a difference in the eighth amino acid, where T replaces S, but this does not deviate from the consensus motif. The Walker A motif in non-plant TAP1 is also perfectly conserved with all harboring the G-4x-GK-T/S pattern (Figure 3.2B).

ABC proteins feature an ABC Signature motif, situated between the two Walker boxes (Figure 3.1A and Figure 3.2A). The Signature motif contains a ten amino acid consensus sequence, [LIVMFY]S[SG]Gx3[RKA][LIVMYA]x[LIVFM][AG], commonly denoted LSGGQ, but several exceptions have been reported (Kang et al. 2011; Rea 2007; Wilkens 2015). Analysis of the Signature motif in plant and non-plant TAP1 proteins reveals that the motif is conserved in all the selected proteins (Figure 3.1B and Figure 3.2B). The Signature motif sequence is involved in ATP hydrolysis as a gamma (γ) phosphate sensor, and/or as a signal membrane spanning domain. The motif acts as a catalytic subunit, and is highly conserved among all eukaryotes, indicating a common catalytic mechanism (Goldberg et al. 1995). The LSGGQ Signature motif sequence occurs only in ABC proteins, and for this reason distinguishes ABC proteins from other ATPases (Davies and Coleman 2000). All inspected Signature motifs of the plant proteins differ only in one amino acid, at the ninth position, where the alternatives are the very hydrophobic amino acids L, V or I (Figure 3.1B).

The Walker B motif consensus sequence is reported to be hhhhDE (Hanson and Whiteheart 2005), where D and E denotes aspartic acid and glutamate residues respectively, and h denotes a hydrophobic amino acid (Walker et al. 1982). Analysis of the Walker B motifs of TAP1 proteins reveals perfect conservation, as the differences in the first of the four

amino acids of the non-plants do not break the consensus of the motif (Figure 3.1B and Figure 3.2B).

The H-loop motif, also called the Switch region, usually comprises seven amino acids, always containing an invariant and highly conserved functional feature, the histidine (H), considered to polarize the attacking water molecules during ATP hydrolysis (Garmory and Titball 2004; Kloch et al. 2010; Schneider and Hunke 1998; Lewis et al. 2004). In all inspected plant proteins, four amino acids surrounding the invariant histidine are identical (I, A, R and L).

These data reveal that the key motifs are highly conserved between all TAP1 proteins analyzed, and suggest that all are functional ATPase enzymes.

### 3.1.2 Evolutionary Relationship

Analysis of the alignments shows that the likeness between TAP proteins is more prominent between AtTAP1 and the higher plant proteins, than between AtTAP1 and lower plant and non-plant proteins (Figure 3.1 and Figure 3.2). AtTAP1 is between 60.4% and 68.8% identical, and between 72.8% and 81.4% similar to the analyzed TAP1 proteins of higher plants, whereas AtTAP1 is only 28.5-31.8% identical to non-plant TAP1 proteins (Table 3.3). The level of similarity between AtTAP1 and the non-plant TAP1 proteins is lower (41.9-49.6%), compared to proteins of the higher plants (Table 3.3). AtTAP2 protein shows 31.8% identity and 48.4% similarity to AtTAP1.

A phylogenetic tree was built from the alignments, to indicate the evolutionary relationships and distances of the homologous TAP1 plant proteins (Figure 3.3). AtTAP1 is most closely related to the TAP proteins from *N. tabacum* and *S. lycopersicum.* Furthermore, the phylogenetic tree shows the TAP1 proteins of *N. tabacum* and *S. lycopersicum* to have

closer evolutionary distance to each other than to *O. sativa* and *T. aestivum* (Figure 3.3).

These data reveal that the higher plant TAP1 proteins are highly conserved, indicating that they could have the same function in all species. Additionally, it could support the theory that ABC transporter genes have undergone diversification events during evolution before plants adapted to the land environment (Hwang et al. 2016).

**Table 3.3 – Percentage identity and similarity of AtTAP1 and TAP1 proteins from different plant and non-plant species**

| Species | Protein name | Amino acid length | Identity (%) | Similarity (%) |
|---|---|---|---|---|
| **Higher Plants** | | | | |
| N. tabacum | ABCB-26 | 701 | 68.8 | 81.4 |
| S. lycopersicum | ABCB-26 | 689 | 66.5 | 79.3 |
| O. sativa | ABCB-26 | 688 | 61.4 | 75.4 |
| T. aestivum | Unnamed protein | 675 | 60.4 | 72.8 |
| **Lower Plants** | | | | |
| P. patens | PpABCB-6 | 578 | 49.8 | 66.0 |
| C. reinhardtii | Unnamed protein | 560 | 36.3 | 52.3 |
| **Non-plants** | | | | |
| H. sapiens | ABCB9; TAPL | 766 | 31.8 | 48.9 |
| D. rerio | ABCB9 | 789 | 32.3 | 48.6 |
| D. melanogaster | CG3156 | 692 | 29.9 | 49.6 |
| C. elegans | Haf-2 | 773 | 30.3 | 48.0 |
| S. cerevisiae | MDL2 | 773 | 28.5 | 41.9 |

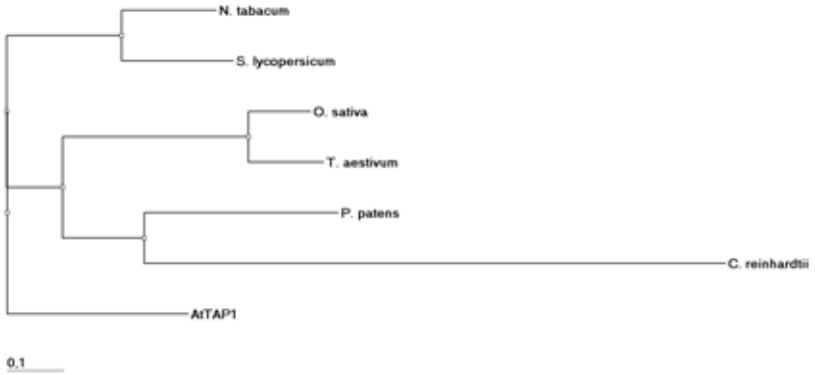


**Figure 3.3 – Phylogenetic tree indicating evolutionary relationships of AtTAP1 to six TAP1 proteins of other plant species**
Branch lengths correspond to sequence differences as indicated by the scale bar.

## 3.1.3 Localization of AtTAP1

### 3.1.3.1 *In silico* Prediction of Subcellular Localization - Chloroplast Transit Peptides and TAP1

Chloroplast transit peptides (cTP) are N-terminal amino acid sequences that direct chloroplast proteins to the chloroplast stroma, and are normally cleaved off, during or shortly after entry, by stromal processing peptidase (Soll and Tien 1998; Robinson and Ellis 1984). Interestingly the TAP1 plant proteins show relatively low levels of identity and similarity in the first 100 amino acids (Figure 3.1). This could indicate that plant proteins harbor a transit peptide, as it is known that sequence similarities between cTPs are low (Lee et al. 2015). To investigate whether each plant protein encodes a cTP, the prediction server ChloroP (Emanuelsson, Nielsen, and von Heijne 1999) was used. This neural network based method indicates the selected TAP1 proteins (and AtTAP2) to have or have not, a predicted N-terminal cTP-containing sequence, and a proposed length of the pre-sequence (Table 3.4).

Three of the proteins, AtTAP1, and TAP1 from *O. sativa* and *T. aestivum*, are predicted to contain a cTP sequence. The other five TAP1 proteins score less than the threshold value 0.500 (Table 3.4) with predictions close to the threshold to predict a cTP. However, given the presence of N-terminal extensions in TAP1 of *N. tabacum* and *S. lycopersicum* (Figure 3.1A), it remains possible that these TAP1 proteins harbor a cTP. *C. reinhardii* and *P.patens* TAP1 proteins, and AtTAP2, do not have extensions in the N-terminal (Figure 3.1A), and are not predicted by ChloroP to harbor a transit peptide. In agreement with this, TAP2 is detected in tonoplast membranes of vacuoles isolated from *Arabidopsis* cell cultures, and not in chloroplasts (Jaquinod et al. 2007). According to the results of the ChloroP 1.1 Prediction Server, the length of the cTP of AtTAP1 is 59 amino acids (Table 3.4).

**Table 3.4 – Predicting chloroplast transit peptides and their cleavage sites of eight TAP proteins**

| Species | Accession code | Length[a] | Score[b] | cTP[c] | cTP-length[d] |
|---|---|---|---|---|---|
| AtTAP1 | NP_177218 | 700 | 0.555 | Y | 59 |
| N. tabacum | XP_016492080 | 701 | 0.466 | - | 79 |
| S. lycopersicum | XP_004252689 | 689 | 0.470 | - | 62 |
| O. sativa | XP_015613646 | 688 | 0.576 | Y | 53 |
| T. aestivum | CDM85589 | 675 | 0.564 | Y | 41 |
| P. patens | XP_001781344 | 578 | 0.449 | - | 59 |
| C. reinhardtii | XP_001699295 | 560 | 0.465 | - | 19 |
| AtTAP2 | NP_198720 | 644 | 0.449 | - | 34 |

[a] Protein sequence length (amino acids). [b]ChloroP prediction score. [c]Y indicates the protein is predicted to harbor a cTP. [d] Predicted chloroplast transit peptide length (Emanuelsson, Nielsen, and von Heijne 1999).

### 3.1.3.2 *In vivo* Subcellular Localization Analysis

Analysis of the AtTAP1 protein sequence revealed prediction of the protein to harbor a cTP. The subcellular localization of *AtTAP1* was subsequently determined using an AtTAP1-YFP fusion protein. *AtTAP1* was cloned into the pWEN18 vector, containing a *YFP* reporter under control of the 35S promoter, and transiently expressed in tobacco leaf cells by particle bombardment (Kost, Spielhofer, and Chua 1998). YFP fluorescence, and auto fluorescence from the chlorophyll, was then detected using a Nikon A1R confocal laser scanning microscope. For all samples the same acquisition settings were employed, and signals of similar intensity compared. (Hanson and Kohler 2001).

The AtTAP1-YFP fusion protein was observed to localize exclusively in the chloroplasts (Figure 3.4). This is in accordance with prediction results of the ChloroP 1.1 Prediction Server (Table 3.4). Two different patterns of AtTAP1-YFP localization were observed: short filaments (Figure 3.4A and Figure 3.4B), or uniformly over the whole surface of the chloroplast (Figure 3.4C). To determine if AtTAP1-YFP was localized throughout the chloroplast, or uniformly with the envelope, serial sections were taken through the chloroplast. Figure 3.4D shows localization of the protein in three section images of an individual chloroplast, and the protein is clearly associated with the chloroplast envelope and not throughout the stroma.

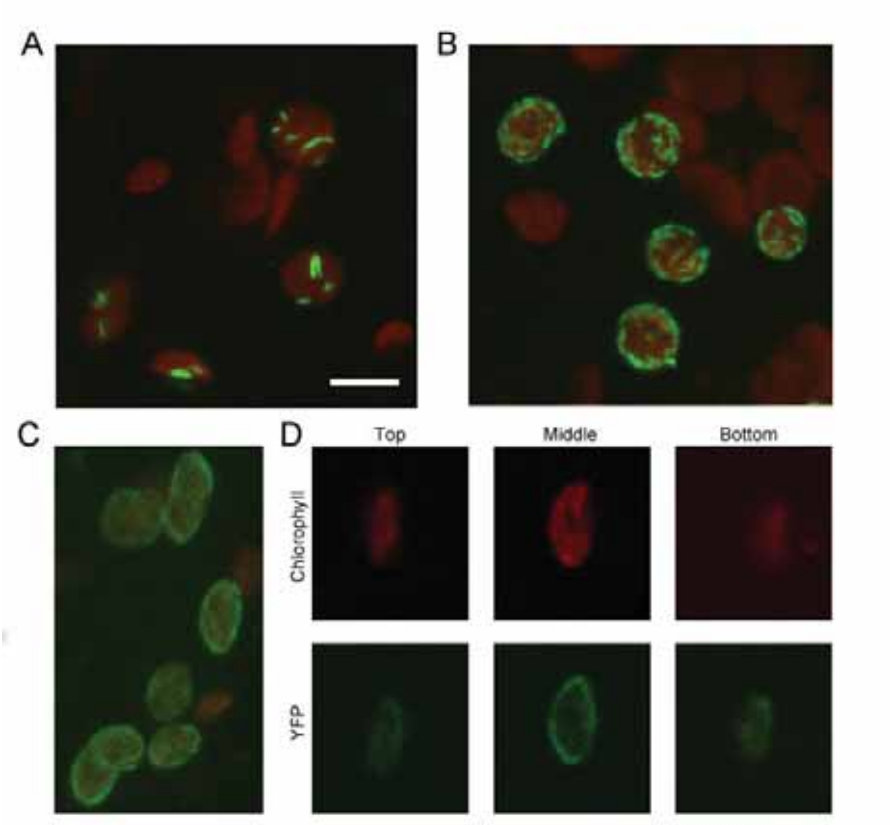


**Figure 3.4 – Localization of TAP1-YFP in tobacco leaf chloroplasts**
AtTAP1-YFP fusion expressed in tobacco leaf cells detected exclusively in chloroplasts. (A and B) Extended focus images showing AtTAP1-YFP distributed as short filaments. (C) The protein AtTAP1-YFP uniformly associated with the envelope. (D) Enlargement of C displaying single chloroplast in three section images; top, middle and bottom of an individual chloroplast showing TAP1-YFP localized is association with the chloroplast envelope.

Green, YFP; Red, chlorophyll; Scale bar is 5 μm

To stably express the AtTAP1-YFP fusion protein in *Arabidopsis*, transgenic plants were generated using the Agrobacterium-mediated floral dip method (Clough and Bent 1998). The plasmid 35S-AtTAP1-YFP/pBA002a was transformed to ABI bacteria, before floral dipping. Microscopy studies were performed on leaves of first generation

transformants and, as was observed in tobacco, AtTAP1-YFP localized to short filaments in proximity to the chloroplast membrane (Figure 3.5).

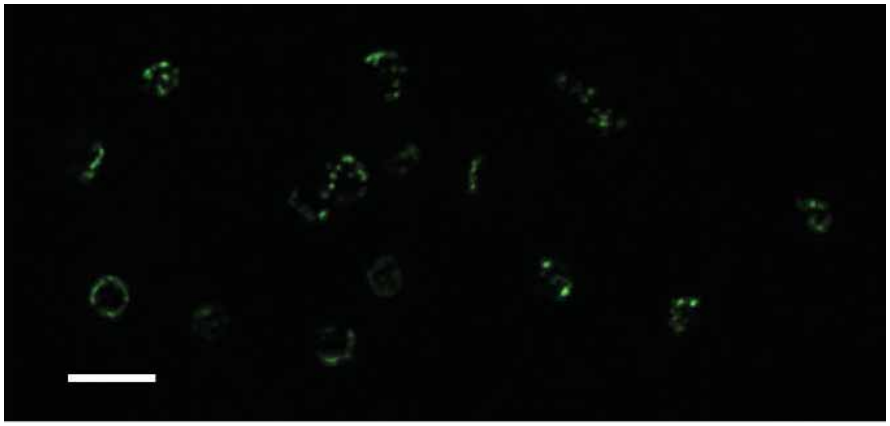

**Figure 3.5 – Localization of AtTAP1-YFP fusion in leaves of *Arabidopsis***
The protein is associated in the proximity of the chloroplast membrane. Green, YFP; Scale bar is 10 μm.

### 3.1.4 Characterization of an AtTAP1 T-DNA Insertion Line, attap1

To analyze the function of AtTAP1 we identified homozygous plants of the *attap1* knockout mutant line SAIL_8_B04 (subsequently referred to as the *attap1* knockout mutant). *Arabidopsis* T-DNA insertion lines were obtained and tested by PCR, using primers designed to anneal within the T-DNA and to the *Arabidopsis* genome flanking the insert site (Figure 3.6A). The position of the insert T-DNA was determined by sequencing, and was shown to be located in an intron near the N-terminal of the gene, between Exon 1 and Exon 2 (Figure 3.6A).

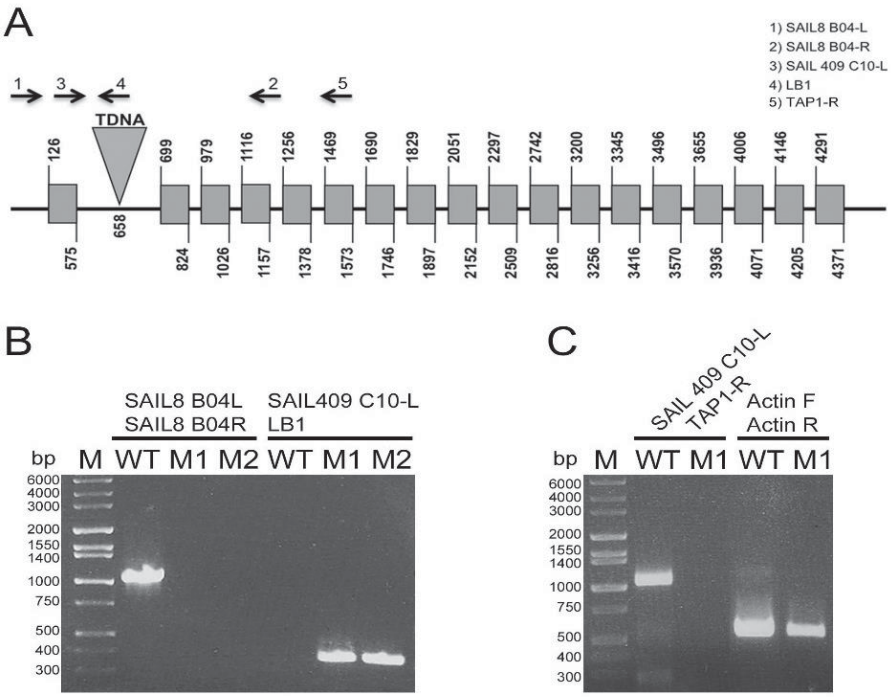


**Figure 3.6 – Identification and localization of the T-DNA**
(A) Schematic of *AtTAP1* genomic DNA showing the location of primers used in this study (1–5), and the site of the T-DNA insertion of the mutant line SAIL_8_B04. Exon boxes in grey color. Numbers indicate nucleotide positions, ATG at position 126. (B) PCR analysis showed bands using primers flanking the insertion in WT seedlings, but not in *attap1* knockout mutant seedlings (SAIL_8_B04-L and R). The T-DNA insert was detected using primers in Exon 1 and in the T-DNA in the mutant line (SAIL_409_C10-L and LB1), whilst no bands was detected in WT. (C) RT-PCR showed that the TAP1 cDNA was absent in the mutant line (M1) but present in WT (SAIL_409_C10-L and TAP1-R primers). Actin primers were used as a control. The M1 and M2 denote two parallels of the *attap1* knockout mutant.

To determine if the insertion in SAIL_8_B04 affected the transcription of *AtTAP1,* RT-PCR was performed (Figure 3.6B). *AtTAP1* transcript was detected using primers specific to the *AtTAP1* cDNA, and expression of *AtTAP1* was clearly detected in wild-type seedlings, but was absent in the *attap1* knockout mutant (Figure 3.6C). Positive controls in the RT-PCR assays using actin primers (Actin Forward/Actin Reverse), on wildtype and mutant DNA show distinct bands.

## 3.1.5 Phenotypic Analysis of the attap1 Knockout Mutant Line of Arabidopsis

Having obtained homozygous *attap1* knockout mutants, we next sought to probe the function of the *AtTAP1* by comparing the phenotypes of WT (Col-0) and the knockout mutant. Seedlings and plants were exposed to different exogenous factors as $Al^{3+}$, $Fe^{3+}$, $Ca^{2+}$, $Mg^{2+}$, $Cu^{2+}$, methyl viologen (MV), $H_2O_2$, auxin and heat stress as described in the Materials and Methods.

### 3.1.5.1 Root Length and Treatment with Different Concentrations of Metal Ions

To analyze the effects of metal ions on root length in the *attap1* knockout mutant, seeds from WT (Col-0) and the *attap1* mutant, were sown on ½MS medium (adjusted to pH 5.8) containing different metal ions, and control ½MS media with and without 1% sucrose added. Sterilized seeds were sown out and placed in the fridge at 4 ºC for four days, before transferring to a growth cabinet at 21 ºC, 16 hrs light and 8 hrs dark, in a vertical position, for 16 days, then inspected and measured.

The differences in root length between the WT and the *attap1* knockout mutant are not significant for any treatment after 16 days of growth, considering a P value $<0.05$ as significant (Table 3.5, Figure 3.7 and Figure 3.8).

**Table 3.5 – Mean root length of seedlings of WT and attap1 knockout mutant (MUT) grown for 16 days on ½MS with/without sucrose, and selected metals**

| | Mean root length (SD[a]) | | |
|---|---|---|---|
| **Treatment** | **WT** | **MUT** | **P value[b]** |
| 0 % sucrose | 8.5 (5.07) | 8.8 (5.56) | 0.343 |
| 1 % sucrose | 18.3 (0.50) | 14.0 (4.55) | 0.340 |
| 0.5 mM $Al^{3+}$ | 37.5 (6.45) | 38.0 (6.73) | 0.686 |
| 2 mM $Al^{3+}$ | 30.0 (4.55) | 38.0 (8.29) | 0.200 |
| 0.5 mM $Fe^{3+}$ | 17.3 (2.50) | 23.0 (3.61) | 0.114 |
| 2 mM $Fe^{3+}$ | 31.3 (0.58) | 32.5 (7.78) | 1.000 |
| 0.5 mM $Mg^{2+}$ | 22.0 (0.82) | 18.5 (5.07) | 0.343 |
| 2 mM $Mg^{2+}$ | 18.8 (3.86) | 19.3 (7.68) | 0.486 |
| 0.5 mM $Ca^{2+}$ | 12.8 (1.89) | 12.7 (4.04) | 0.857 |
| 2 mM $Ca^{2+}$ | 19.3 (3.30) | 17.5 (6.56) | 0.886 |

WT (Col-0) and the *attap1* mutant (MUT). [a]Standard deviation. [b]P value for independent samples by Mann Whitney U is shown. A P value < 0.05 was required to be considered significant. n=4.

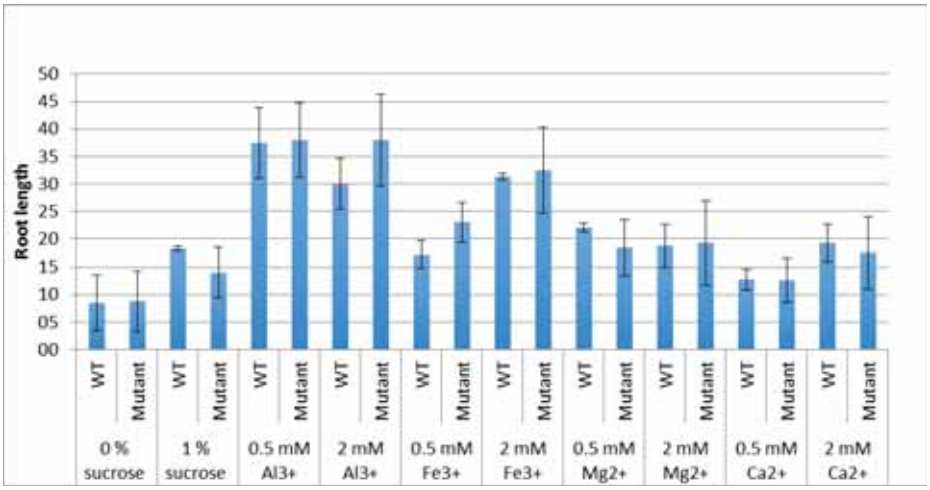


**Figure 3.7 – Root length of seedlings grown for 16 days on ½MS with/without sucrose, and selected metals**
The mean of main root length (mm) of wild type (WT) and *attap1* knockout (mutant) seedlings on the treatment indicated (Blue columns). Standard deviations are shown. n=4.

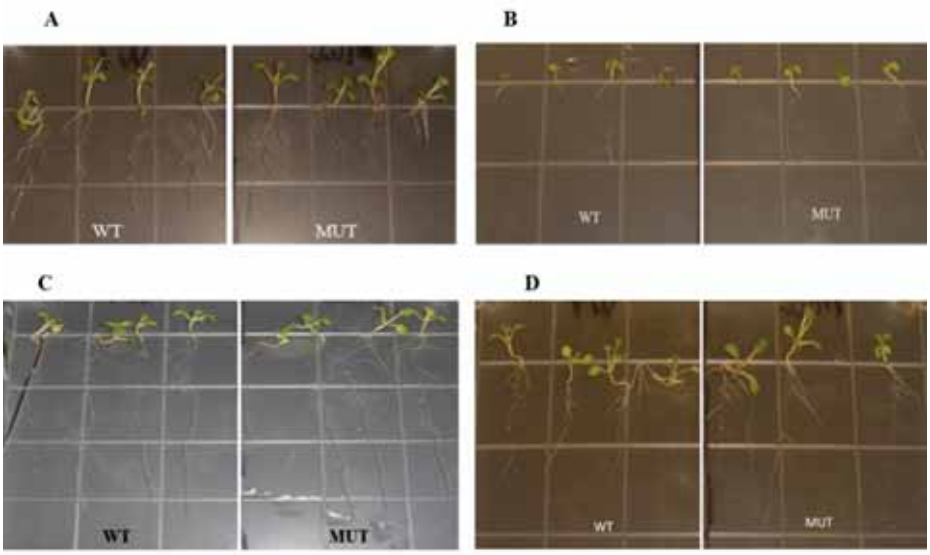


**Figure 3.8 – Seedlings grown on ½MS media with or without metal ions added**
(A) 1% sucrose, (B) 0% sucrose, (C) 0.5 mM $Al^{3+}$, (D) 0.5 mM $Fe^{3+}$. Wild type (WT) and *attap1* knockout mutant (MUT) indicated. Scale: Inner square 13.3x13.3 mm.

To test if growing the seedlings for longer would reveal any differences, the experiment was repeated. Sterilized seeds were sown and placed in fridge at 4 ºC for four days, before being placed horizontally in a cabinet for 12 days. Subsequently the seedlings were transplanted to new dishes, which were placed vertically for an additional 21 days. As observed in the first experiment, there were no differences in root length between WT and *attap1* knockout mutant seedlings (Table 3.6, Figure 3.9 and Figure 3.10). Side roots obviously developed in this second experiment (Figure 3.10).

**Table 3.6 – Mean root length of seedlings grown for 35 days on ½MS with sucrose, and selected metals**

| | Mean root length (SD[a]) | | |
|---|---|---|---|
| **Treatment** | **WT** | **MUT** | **P value[b]** |
| 1 % sucrose | 14.3 (3.79) | 14.7 (3.21) | 1.000 |
| 0.2 mM $Al^{3+}$ | 41.3 (4.16) | 42.0 (7.21) | 1.000 |
| 2 mM $Al^{3+}$ | 24.0 (4.58) | 36.7 (7.37) | 0.100 |
| 0.2 mM $Fe^{3+}$ | 38.7 (9.29) | 38.3 (6.51) | 1.000 |
| 2 mM $Fe^{3+}$ | 17.0 (4.58) | 13.0 (1.00) | 0.400 |
| 0.2 mM $Mg^{2+}$ | 11.3 (2.08) | 11.3 (2.31) | 1.000 |
| 2 mM $Mg^{2+}$ | 10.7 (3.21) | 10.3 (3.21) | 1.000 |
| 0.2 mM $Ca^{2+}$ | 16.0 (4.58) | 15.0 (1.00) | 1.000 |
| 2 mM $Ca^{2+}$ | 16.0 (5.00) | 15.7 (1.53) | 1.000 |

WT (Col-0) and the *attap1* mutant (MUT). [a]Standard deviation. [b]P value for independent samples by Mann Whitney U is shown. A P value < 0.05 considered significant. n=3.

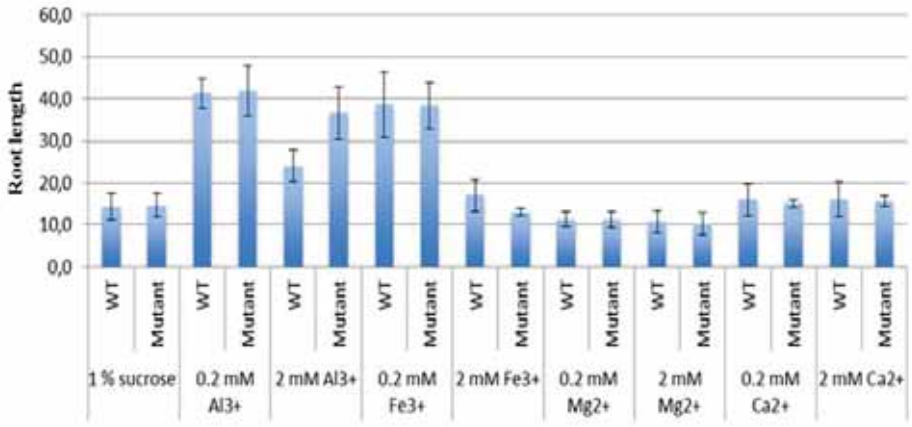


**Figure 3.9 – Root length of seedlings grown for 33 days on ½MS with sucrose, and selected metals**
The mean of main root length (mm) of wild type (WT) and *attap1* knockout mutant (Mutant) seedlings on the treatment indicated (Blue columns). Standard deviations are shown. n=3.

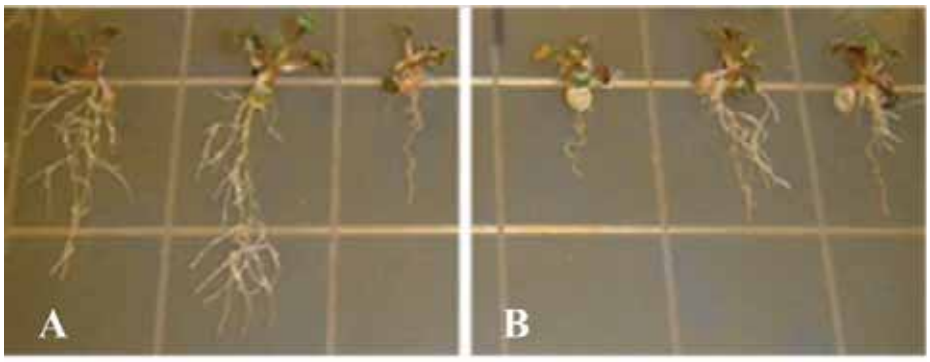


**Figure 3.10 – Seedlings of three replicas grown for 33 days on sucrose and ½MS media added 2.0 mM Fe3+**
(A) Wild type. (B) *attap1* knockout mutant. Scale: Inner square 13.3x13.3 mm.

Our data reveal longer main roots of both WT and mutant seedlings when grown on media containing aluminum, compared to other media (Figure 3.7 and Figure 3.9). This is in contrast to the literature, where it is shown that aluminum toxicity can inhibit root growth (Larsen et al. 2007). This fundamental difference is interesting, and may be as a result of differing acidity of the media, since experiments Larsen et al used pH 4.2 (Larsen

et al. 2007), while pH 5.8 in MS medium was used in this study. Further experiments will therefore be of interest.

#### 3.1.5.2 Stress Treatment of Plants grown on MS Media

To study phenotypic differences and response to different stress treatments, WT and *attap1* knockout mutant seedlings were exposed to exogeneous stress factors. Seedlings were grown for 14 days on ½MS media, before being treated with 10 µM MV (methyl viologen), 10 µM $H_2O_2$, 2.0 mM $CuSO_4$ , heat in darkness at 37 ºC, or grown under standard conditions. 3 ml of solutions were added to each plate, before replacement into the growth chamber. Seedlings were inspected and photographed every second day for 10 days, and 3 ml treatment solutions added every second day. Pictures of the treated and control seedlings after 6 days are shown in Figure 3.11. Detailed phenotypic analysis of the *attap1* knockout mutant compared to WT plants, revealed no differences of overall morphology in response to the exogenouos stress factors (Figure 3.11).

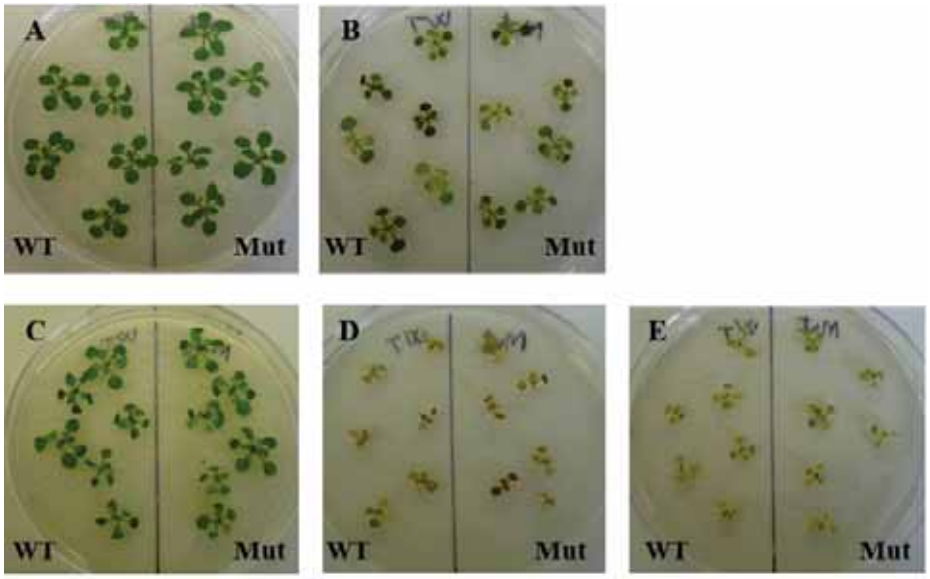


**Figure 3.11 – Seedlings of wild-type (WT) and mutant (Mut) 6 days after treatment**
Grown in Petri dishes containing ½MS media. (A) Control plants. No treatment added. (B) 10 µM MV added. (C) 10 µM $H_2O_2$ added. (D) 2.0 mM $CuSO_4$ added. (E) Heat 37 ºC treated.

### 3.1.5.3 Exposure to $Fe^{3+}$ of Seedlings and Plants on Soil

To study phenotypic differences and response to iron stress treatment, two-week old WT and *attap1* knockout mutant seedlings were transferred to soil and watered regularly with 2.0 mM $FeCl_3$ for six weeks and inspected every fifth day (Figure 3.12). Detailed phenotypic analysis of the *attap1* knockout mutant compared with WT plants revealed no differences of overall morphology in response to the $Fe^{3+}$ treatment (Figure 3.12).

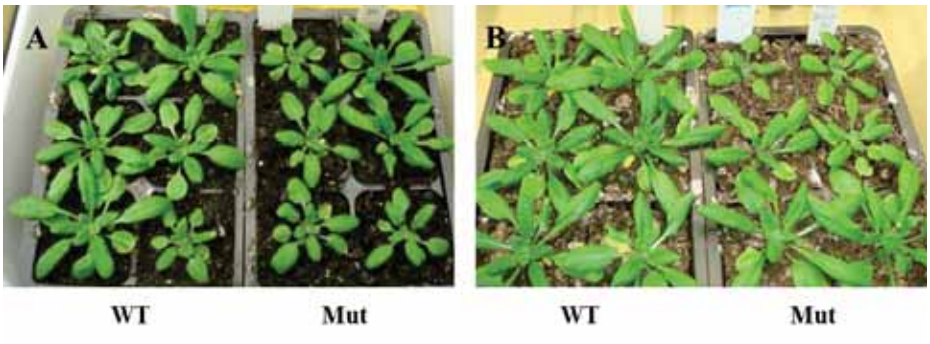


**Figure 3.12 – Phenotypic patterns of young plants on soil after (A) Fe3+ treatment and (B) no treatment, control**
Wild type plants (WT) and *attap1* knockout mutant plants (Mut) indicated.

## 3.1.6 AtTAP1 Expression Analysis

### 3.1.6.1 *AtTAP1* Expression in different Plant Tissues

Firstly, to investigate the expression of *AtTAP1* in different aerial tissues and roots, semi-quantitative RT-PCR experiments were performed using WT plants. Results show expression of *AtTAP1* in both aerial tissues and in roots, with highest expression in flower structures, and considerable lower expression in roots and leaves (Figure 3.13A).

The upstream promoter region of the *AtTAP1* gene (At1g70610) was cloned into the vector pBADG, for GUS expression. The pBADG vector contains a GFP (Green fluorescent protein) and a GUS (β-Glucuronidase) reporter gene. The resulting construct, *PromoterTAP1-pBADG*, places the GUS gene under the control of the *TAP1 promoter.* Using floral dipping, WT *Arabidopsis* plants were transformed with the construct, and transgenic seedlings selected on media containing BASTA, to obtain plants expressing the *AtTAP1 promoter-GUS reporter* ("GUS-plants").

Following this, GUS expression was observed in roots, leaves, siliques and flowers, coming from different GUS-plants, by inspection in the dissecting microscope after GUS staining (Jefferson 1987; Jefferson, Kavanagh, and Bevan 1987) (Figure 3.13). An interesting observation is the expression of *AtTAP1* in roots is confined to site of lateral root initiation (Figure 3.13B-D). This may indicate local enhanced activities of the gene during specific times of plant development. The GUS-reporter experiments clearly demonstrate *AtTAP1* expression in flowers, which supports the RT-PCR results (Figure 3.13E), as well as siliques (Figure 3.13F) and leaves (Figure 3.13G and H).

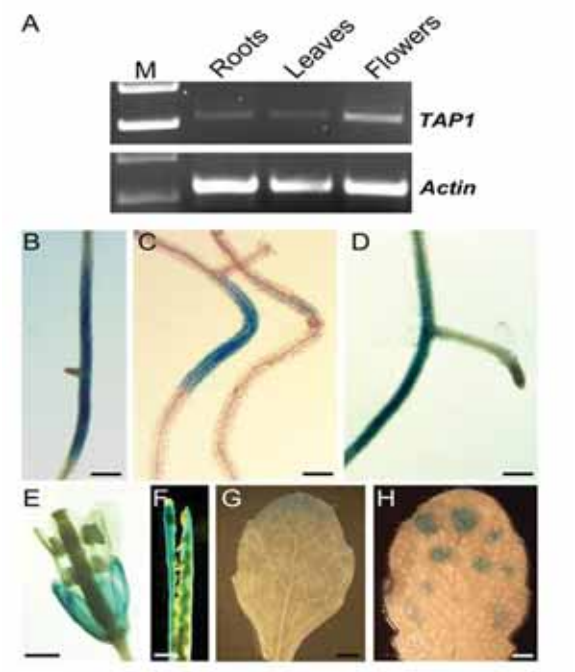


**Figure 3.13 – RT-PCR and GUS expressions of TAP1 in *Arabidopsis***
(A) RT-PCR analysis on different organs with actin references, M indicates marker. (B-D) GUS expressions of TAP1 in main roots near buddings of side roots, (E) in flowers/sepals, (F) in siliques and (G, H) in leaves. Scale bars: 300 μm (B-D) and 2 mm (E-H).

### 3.1.6.2 Effects of Auxin Treatment

To analyze the possible auxin induced expression of the *AtTAP1* gene, sterilized seeds of WT Col-0 were sown out on ½MS media, and seedlings transferred to wells containing ½MS with 1% sucrose and 50 µM auxin, and placed on bench at room temperature and continuous light. Seedlings were harvested after 6, 12 and 24 hrs, and RT-PCR performed using primers TAP1-L/R and Actin F/R (Table 2.1) to detect *AtTAP1* (744 bp) and *Actin* (544 bp) as a control.

The level of *AtTAP1* expression was normalized against the control seedlings. After 6 hrs of treatment with auxin, the levels of *AtTAP1* expression were reduced, relative to the untreated control. The level of *AtTAP1* was restored after 24 hrs, suggesting that *AtTAP1* expression is controlled by auxin, and suggesting a role in plant development (Figure 3.14 and Figure 3.15). The data are highly preliminary due to no control seedlings in liquid media without auxin, following the 6, 12 and 24 hrs treatments. The control in the pilot is seedlings harvested at the same time as the auxin treated ones, then stored at -80 ºC until RT-PCR was executed at the same time of the whole pilot.

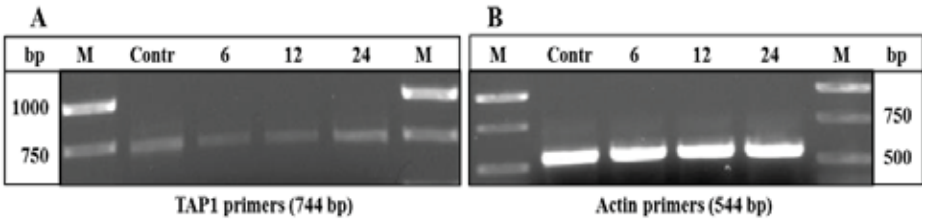


**Figure 3.14 – Auxin treatment of seedlings of Arabidopsis for 6, 12 and 24 hrs**
RT-PCR 25 cycles. Distinct bands show AtTAP1 (A) and Actin (B).

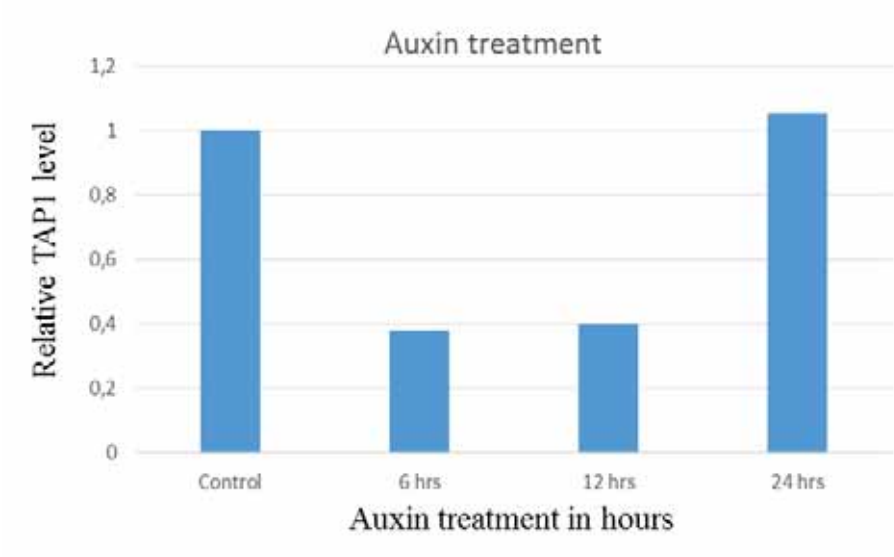


**Figure 3.15 – Auxin treatment of seedlings**
Graph columns from intensities of electrophoretic bands. RT-PCR for 25 cycles indicating lower expressions induced after 6 and 12 hrs of 50 µM auxin treatment, compared to control.

### 3.1.6.3 Effects of Iron treatment

Plants expressing *PromoterAtTAP1-pBADG* were regularly watered with 2.0 mM $FeCl_3$ solution, or only water (control), and leaves were inspected after 20 days. There were no visible differences in the observed phenotypes between the exposed and control plants (Figure 3.16).

Thereafter, leaves from the iron treatment or control plants were subject to histochemical staining with X-Gluc, (Jefferson 1987; Jefferson, Kavanagh, and Bevan 1987). Tubes with leaves in X-Gluc substrate were placed in a water bath at 37 ºC, and the leaves inspected after 1:00, 2:00, 6:30, 7:15 and 24:00 hrs for the development of GUS stain. A faintly bluish color was observed in both $Fe^{3+}$ treated and control leaves after 6:30 and 7:15 hrs, and stronger color was detected after 24 hrs. There

were no visible differences between treated and untreated plants (data not shown).

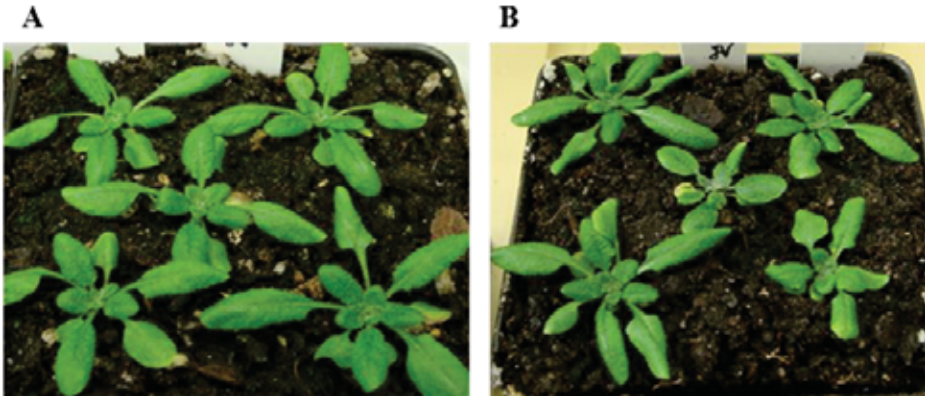


**Figure 3.16 – Wild-type (WT) plants transformed with *promoterAtTAP1*-pBADG after 20 days on soil**
(A) Plants treated with $Fe^{3+}$. (B) Untreated plants.

### 3.1.6.4 Effects of Wounding

Leaves from WT plants expressing *PromoterAtTAP1-pBADG* (GUS plants) were mechanically wounded by tearing with a needle, and the GUS expression compared to control leaves (Jefferson 1987; Jefferson, Kavanagh, and Bevan 1987). Inspection by microscopy revealed an increased expression of the *AtTAP1* gene in wounded leaves, compared to the control leaves (Figure 3.17). In control leaves, which were not wounded, feint bluish color, i.e. weak GUS expression, was observed in the periphery, to the leaf apex, and to some extent in the middle of the leaves, and not in the petiole (Figure 3.17A and C). Wounded leaves show the same pattern of GUS expression, but with a stronger blue color, especially in the periphery of the leaves. Increased expression was not observed in close proximity to the wound (Figure 3.17B and D). This indicates that wounding results in distinct and enhanced GUS expression of the *AtTAP1* gene in leaves, as has been indicated for other genes

(Bohlmann et al. 1998; Mwenda et al. 2015). Leaves of control plants (without the construct *PromoterAtTAP1-pBADG* transformed) did not show any GUS expression (data not shown).

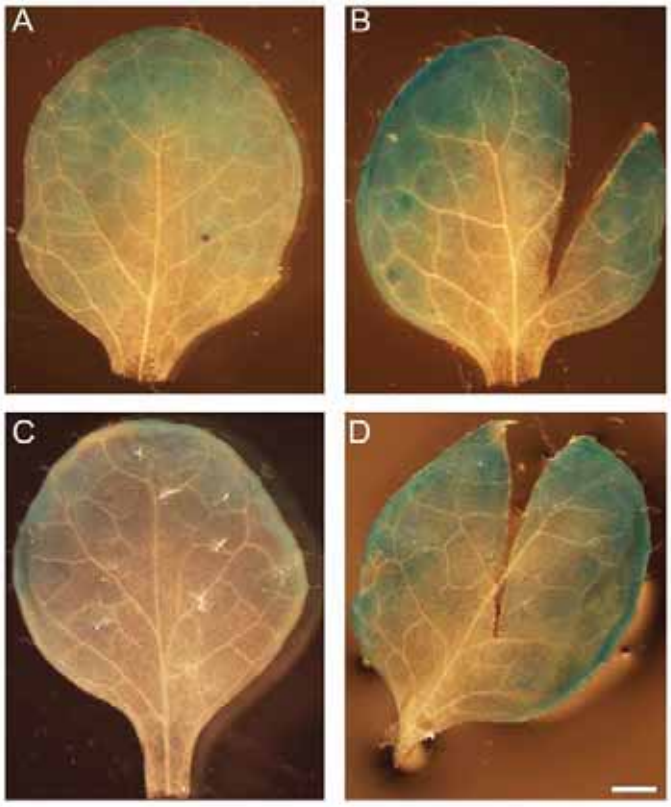


**Figure 3.17 – Leaves from GUS plants (WT) of *Arabidopsis***
(B and D) Wounded leaves by tearing with a needle. (A and C) Leaves not wounded. Scale bar is 2 mm.

## 3.1.7 Comparison of AtTAP1 and AtTAP2

As stated in the Introduction, the two genes *AtTAP1* and *AtTAP2* belong to the transporters associated with antigen processing (TAPs) in the ABCB subfamily of the ABC transporters. Their proteins are half-molecules that localize to the membranes, AtTAP1 in the chloroplast and AtTAP2 in the tonoplast of vacuoles (Ferro et al. 2010; Garcia et al. 2004; Jaquinod et al. 2007; Kang et al. 2011; Rea 2007; Sánchez-Fernández et al. 2001). It has been demonstrated that TAP2 plays an active role in an aluminum toxic environment (Gabrielson et al. 2006; Larsen et al. 2007; Simoes et al. 2012). Therefore, it is of interest to compare the two genes and proteins to reveal any differences and likeliness of function.

### 3.1.7.1 Stress Treatments and AtTAP1 versus AtTAP2 Expressions.

Semi-quantitative RT-PCR was performed to quantify the expression of *AtTAP1* and *AtTAP2* in seedlings treated in ½MS media and 25 µM solutions of $Al^{3+}$, $Fe^{3+}$, $Ca^{2+}$ and $Mg^{2+}$, and incubated for 48 hrs in room temperature and in continuous light (Figure 3.18). The expression of actin was used as a control (Figure 3.19). The experiment was repeated in triplicate and the bands quantified using imageJ software. The expression of *AtTAP1* and *AtTAP2* were normalized against the level of expression in the control seedlings (Figure 3.20).

The expression of both *AtTAP1* and *AtTAP2* was induced in the presence of $Al^{3+}$, $Ca^{2+}$ as well as $Fe^{3+}$, and was reduced in the presence of $Mg^{2+}$ (Figure 3.20). The intensities of the bands shown are visually in accordance with this (Figure 3.19). All the metal treatments show significant differences from the control at the $p = <0.05$ level, except for the *AtTAP1* treated with iron (Figure 3.20).

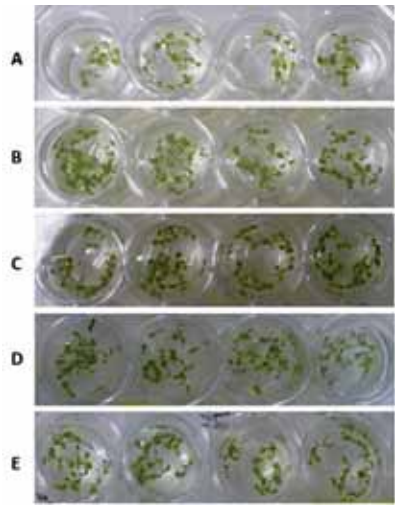


**Figure 3.18 – Seedlings of wildtype (WT) *Arabidopsis* treated in wells with different metal solution for 48 hrs**
25 µM $Fe^{3+}$, (B) 25 µM $Ca^{2+}$, (C) 25 µM $Mg^{2+}$, (D) 25 µM $Al^{3+}$, (E) Control, ½MS media.

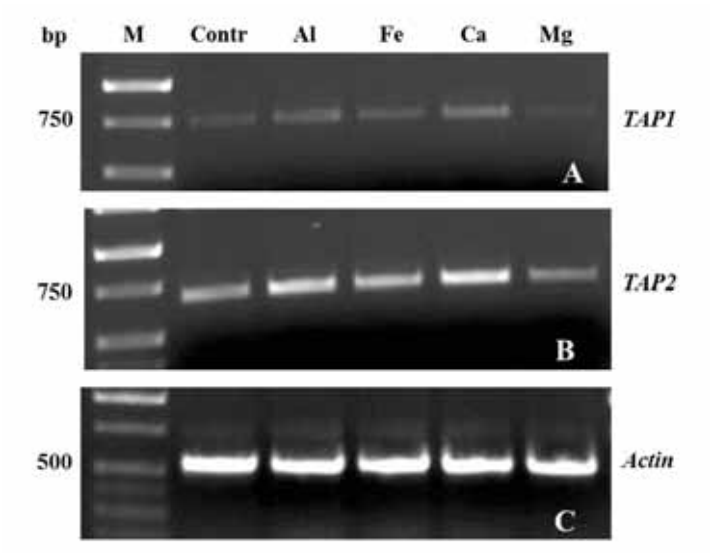


**Figure 3.19 – RT-PCR analysis performed on *Arabidopsis* seedlings treated with different metal ions**
(A) *AtTAP1* expression. (B) *AtTAP2* expression. (C) *Actin* reference.

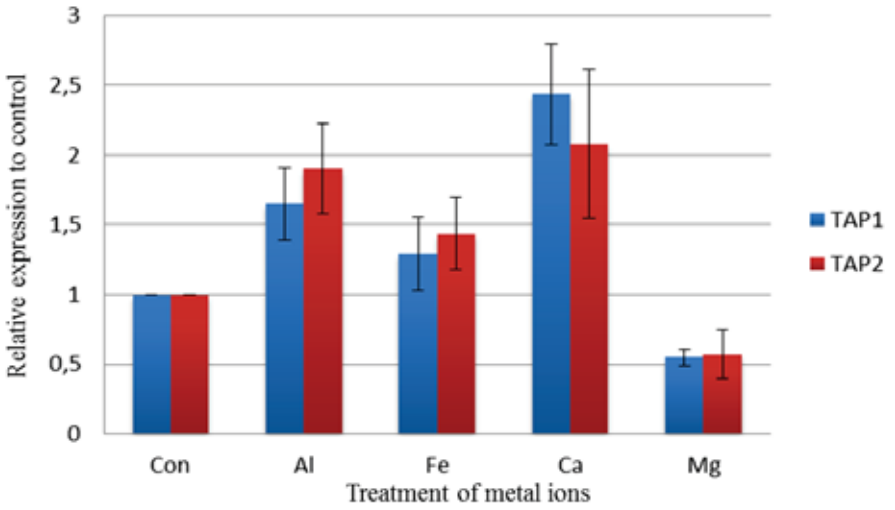


**Figure 3.20 – Expression level of *AtTAP1* and *AtTAP2* in different treatment of metal ions, normalized against the control treatment for each gene**
Graph columns made from intensities of electrophoretic bands and the mean expression level measured in three replicates of 48 hrs grown seedlings. The standard deviations are indicated. All the treatments show significant differences ($P<0.05$) from the control, except for TAP1 treated with Fe.

### 3.1.7.2 Protein Characterization of AtTAP1 and AtTAP2

The aim of this part was to produce and purify AtTAP1 and AtTAP2 proteins for further study of their ATPase activities, determining $V_{max}$ (maximal velocity of enzyme-catalyzed reaction on the substrate) and $K_m$ (substrate concentration that gives the enzyme one-half of its $V_{max}$), in solutions of different pH.

BL21Star$^{TM}$(DE3)pLysS and Rosetta(DE3)pLysS bacteria were transformed with the constructs TAP1-pET and TAP2-pET, and pET-28a(+) for protein production. Different concentrations (5, 10, 50 and 500 µM) of IPTG, were added to induce transcription of the lac operon and protein expression. No clear expression TAP1 (78 kDa) or TAP2

(69 kDa) was observed on protein gels stained with Coomassie Brilliant blue (Figure 3.21).

Following the protocol for Western Blotting using 500 µM IPTG induction, positive bands were detected on the membrane for both TAP1 protein (78 kDa) and TAP2 protein (69 kDa), and no bands detected on these locations in control, i.e. pET plasmid without TAP inserts, (Figure 3.22). The loading volumes were equal in each experiment (Figure 3.21 and Figure 3.22).

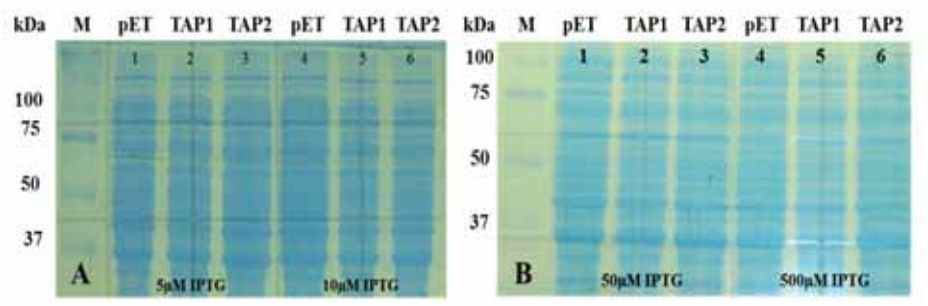


**Figure 3.21 – Protein gels after staining with 0.1% Coomassie Brilliant Blue R250**
(A) Proteins from cultures induced with 5 µM IPTG (1,2,3) or 10 µM IPTG (4,5,6). (B) Proteins from cultures induced with 50 µM IPTG (1,2,3) or 500 µM IPTG (4,5,6). Controls (1,4) refer pET plasmid without inserts. TAP1 (2,5) refer pET with TAP1 insert and TAP2 (3,6) refer pET plasmid with TAP2 insert.

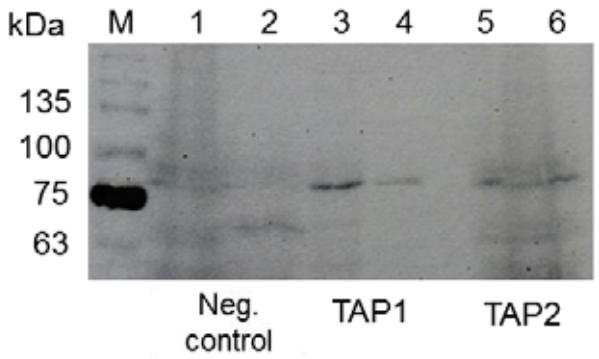


**Figure 3.22 – Western Blotting**
(1,2) Negative control (pET without TAP inserts. (3,4) TAP1, 78 kDa (two parallels). (5,6) TAP2, 69 kDa (two parallels). (M) Marker *BLUEstain™ 2 Protein ladder* from Gold Biotechnology (Goldbio.com). Administered 500 µM IPTG induction in cultures.

Purification of TAP1 and TAP2 proteins, following the protocol for purifying the proteins from the soluble phases as outlined in Section 2.2.7.4 was without any success. Subsequently the plasmids were sent to Prof. Dr. Mark Odell (University of Westminster, London, UK), to repeat the procedure. The collaborating laboratory expressed AtTAP1 and performed Western analysis, but were unable to obtain positive results.

## 3.2 AtNAP14

The objective of studying AtNAP14, a non-intrinsic protein of the ABC transporters (NAP), also named ABCI11 according to the ABC transporter nomenclature (Verrier et al. 2008), was primarily to focus on ATPase activity of the protein and compare it with AtTAP1 and AtTAP2 activities, in addition to analyzing the localization pattern of the protein at the subcellular level.

### 3.2.1 AtNAP14 and Homolog ABCI Proteins

The AtNAP14 protein (encoded by the gene *At5g14100)* is shown to harbor the four classic ATPase domains: Walker A, Signature (ABC transporter signature motif), Walker B and H-loop, and therefore predicted to be an active ATPase enzyme (Sánchez-Fernández et al. 2001). These conserved domains were investigated in homologous or putative similar ABC proteins of plants, to reveal the evolutionary relationship of NAP14 and related proteins. Sequences of homologous proteins from key laboratory and commercial plant species obtained from NCBI were analyzed. Included are proteins from the same six plants as in the study of AtTAP1, *Nicotiana tabacum* (tobacco), *Solanum lycopersicum* (tomato), *Oryza sativa* (rice), *Triticum aestivum* (wheat), *Physcomitrella patens* (moss) and *Chlamydomonas reinhardtii* (green algae) (Table 3.7).

No homologues of NAP14 were detected in selected non-plant model organisms, confirming the findings of (Hwang et al. 2016), that NAP14 and other NAPs are unique to plants.

**Table 3.7 – AtNAP14 and related proteins from different plant species**

| Species | Protein name | Amino acid length | Accession code |
|---|---|---|---|
| **Higher Plants** | | | |
| A. thaliana | AtNAP14 | 278 | NP_196914 |
| N. tabacum | Predicted ABCI11 | 278 | XP_016473541 |
| S. lycopersicum | Predicted ABCI11 | 274 | XP_004233288 |
| O. sativa | ABC protein, expressed | 276 | ABA93815 |
| T. aestivum | Unnamed protein | 267 | CDM85279 |
| **Lower Plants** | | | |
| P. patens | Comp. prot. PpABCI7 | 223 | XP_001780838 |
| C. reinhardtii | Hypoth. partial protein | 198 | XP_001691954 |

### 3.2.2 Alignment of AtNAP14 Protein with Four Essential Motifs and Homologs

Comparisons of sequences of NAP14 proteins from different plant species show to what extent similarities exist. Each group of NAP14 proteins were aligned using BioEdit software. Alignments with the mentioned four essential motifs emphasized, are shown in Figure 3.23. The four highly conserved motifs present are enlarged and aligned (Figure 3.23B).

Inspecting all the four motifs of the NAP14 proteins reveal a perfect conservation of all. The few differences are of no importance for the consensus. These differences are: in the second amino acid of the Walker A (only AtNAP14), in the fifth and sixth amino acid of the Signature, in third amino acid of the Walker B, and in the first and second amino acid of the H-loop.

An interesting detail is that the AtNAP14 protein together with AtNAP11 share identity of about 30% with a protein, SynFutC, from the *Synechocystis* 6803 sequence of the cyanobacteria *Synechocystis sp.* The protein is involved in cyanobacterial Fe transport, and the Signature domain are conserved in all three proteins (Linton 2007; Shimoni-Shor et al. 2010).

Originally, it was thought that ABC proteins of the NAP subfamily encode a heterogeneous group of soluble and non-intrinsic ABC membrane proteins, with no close resemblance to each other or to proteins belonging to specific subfamilies of ABC proteins of other organisms than *Arabidopsis* (Sánchez-Fernández et al. 2001). The NAPs are small molecules containing only one single NBF each, and are reminiscent of peripheral ATP-binding quarter subunits of prokaryotic ABC transporters (Higgins 1992; Sánchez-Fernández et al. 2001). As mentioned, no proteins from the ABCI subfamily are detected in model

animals indicate these proteins to be specific in plants (Hwang et al. 2016).

**A**


**B**

| | | | | |
|---|---|---|---|---|
| **AtNAP14** | GKSGSGKT | LSGGYKRRLA | LLILDE | LVVSHDL |
| **N. tabacum** | GRSGSGKT | LSGGYKRRLA | LLILDE | LVVSHDL |
| **S. lycopersicum** | GRSGSGKT | LSGGYKRRLA | LLILDE | LVVSHDL |
| **O. sativa** | GRSGSGKT | LSGGFKRRLA | LLLLDE | LAVSHDL |
| **T. aestivum** | GRSGSGKT | LSGGFKRRLA | LLLLDE | LVVSHDL |
| **P. patens** | GRSGSGKT | LSGGYKRRLA | LLLLDE | IIVSHDL |
| **C. reinhardtii** | GRSGSGKT | LSGGQQRRLA | LLLLDE | LVVSHDL |
| | **Walker A** | **Signature** | **Walker B** | **H-loop** |

**Figure 3.23 – Alignment of AtNAP14 with six ABCI proteins from other plant species**
(A) Alignment of seven ABCI proteins with the four motifs Walker A, Signature (ABC transporter signature motif), Walker B and the H-loop are underlined. (B) The four motifs enlarged.

### 3.2.3 Evolutionary Relationship and Phylogenetic Tree of seven ABCI proteins

Further analysis of the alignments shows that the likeness between NAP14 proteins is more prominent between AtNAP14 and the higher plant proteins, than between AtNAP14 and lower plant proteins (Figure 3.22). Analysis shows AtNAP14 to be between 59.5% and 66.2% identical, and between 73.5% and 75.8% similar, to the higher plant NAP14 proteins analyzed (Table 3.9), whilst AtNAP14 identity and similarity is lower in the two lower plants examined (Table 3.8).

A phylogenetic tree built from the alignments, indicating the evolutionary relationships and distances of the putative homolog NAP14 plant proteins, is presented in Figure 3.24.

**Table 3.8 – Percentage identity and similarity to AtNAP14a of six similar ABCI proteins from different plant species**

| Species | Protein name | Amino acid length | Id (%) | Sim (%) |
|---|---|---|---|---|
| **Higher Plants** | | | | |
| N. tabacum | Predicted ABCI11 | 278 | 66.2 | 75.8 |
| S. lycopersicum | Predicted ABCI11 | 274 | 66.0 | 75.7 |
| O. sativa | ABC protein, expressed | 276 | 59.5 | 73.5 |
| T. aestivum | Unnamed protein | 267 | 62.7 | 75.6 |
| **Lower Plants** | | | | |
| P. patens | Comp. prot. PpABCI7 | 223 | 48.8 | 59.6 |
| C. reinhardtii | Hypoth. partial protein | 198 | 35.3 | 47.8 |

[a]AtNAP14 protein is also named ABCI11 according to ABC transporter nomenclature (Verrier et al. 2008).

The phylogenetic tree shows the NAP14 proteins of *N. tabacum* and *S. lycopersicum* to have closer evolutionary protein distance to each other than to *P. patens, O. sativa* and *T. aestivum* (Figure 3.24). The evolutionary distance to AtNAP14 is closer for *N. tabacum* and *S. lycopersicum,* than for any of the other four proteins (Figure 3.24). The

longest evolutionary distance is between *C. reinhardtii* and any of the other proteins.

Parallel to the former presentation of the TAP1 proteins, the presented data on NAP14 proteins, can be interpreted as indications and support of the theory that ABC transporter genes have undergone diversification events during evolution, before plants adapted to land environment (Hwang et al. 2016).

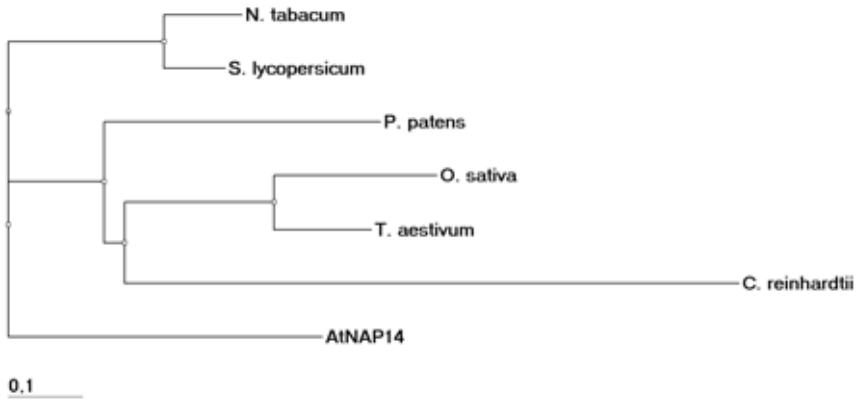


**Figure 3.24 – Phylogenetic tree indicating relationship of AtNAP14**
Branch lengths correspond to sequence differences as indicated by the scale bar.

## 3.2.4 Localization of AtNAP14

### 3.2.4.1 *In silico* Prediction of Subcellular Localization - Chloroplast Transit Peptides and NAP14

Among the NAP14 homologues in plants there are relatively low levels of identity and similarity in the first 50-60 amino acids (Figure 3.23), indicating that plant proteins might harbor a transit peptide, as it is known that sequence similarities between such motifs can be diverse and

low (Kunze and Berger 2015; Lee et al. 2015; Schein, Kissinger, and Ungar 2001).

The presence of a cTP was estimated using the prediction server ChloroP (Emanuelsson, Nielsen, and von Heijne 1999). As shown in Table 3.9, all the NAP proteins are predicted to harbor a cTP, except for *P. patens,* which has the value 0.467, lying under the threshold of 0.500. *P. patens* and *C. reinhardtii* do not have extensions in the N-terminal (Figure 3.23A), and both will therefore probably not harbor a cTP, which value of the *C. reinhardtii* (0.503) is close to the threshold.

**Table 3.9 – Predicting chloroplast transit peptides and their cleavage sites of seven NAP14 homolog proteins**

| Species | Accession code | Amino acid length[a] | Score[b] | cTP[c] | cTP length[d] |
|---|---|---|---|---|---|
| AtNAP14 | NP_196914 | 278 | 0.531 | Y | 49 |
| N. tabacum | XP_016473541 | 278 | 0.566 | Y | 54 |
| S. lycopersicum | XP_004233288 | 274 | 0.554 | Y | 50 |
| O. sativa | ABA93815 | 276 | 0.580 | Y | 40 |
| T. aestivum | CDM85279 | 267 | 0.528 | Y | 29 |
| P. patens | XP_001780838 | 223 | 0.467 | - | 66 |
| C. reinhardtii | XP_001691954 | 198 | 0.503 | Y | 61 |

[a]Length of protein sequence (amino acids), [b]ChloroP prediction score and [c]Result. Scores higher than 0.500 result Y (yes) and positive cTP. [d]Predicted chloroplast transit peptide length (Emanuelsson, Nielsen, and von Heijne 1999).

### 3.2.4.2 *In vivo* Subcellular Localization Analysis of AtNAP14 and Microscopy

Analysis of the AtNAP14 protein sequence revealed prediction of the protein to harbor a cTP. The subcellular localization of AtNAP14 was subsequently determined using a NAP14-YFP fusion. *AtNAP14* was cloned into pWEN18 vector containing *YFP* reporter under control of the 35S promoter.

Sequencing two parallels of *AtNAP14-YFP/pWEN18* plasmids, showed perfect identity to the *AtNAP14* cDNA (*At5g14100*), except for the introduction of a point mutation (c.547 G>A) (Figure 3.25A). This introduces a missense mutation, at position 183 in the protein (p.D183N), changing an aspartic acid (D) in *AtNAP14* to asparagine (N) in the vectors constructed (Figure 3.25B). The amino acid in question is not a part of the four essential motifs of the protein (Figure 3.23), and is not predicted to affect the cTP. Therefore, the construct was used to assess chloroplast localization.


**Figure 3.25 – Comparing NAP14 (At5g14100) and inquiries after sequencing**
(A) An exert of aligned sequences from the two sequenced vectors (*AtNAP14-YFP/pWEN18,* 1 and 2) compared to the expected AtNAP12 sequence. The guanine to adenine substitution at position 547 is highlighted. (B) The c.547 G>A substitution changes the GAC codon to AAC (highlighted), resulting in a p.D183N missense mutation. The WT amino acid (D) is indicated in the red box.

The construct *AtNAP14-YFP/pWEN18* was transiently expressed in tobacco leaf cells by particle bombardment (Kost, Spielhofer, and Chua 1998). YFP fluorescence and auto fluorescence were then detected using Nikon A1R confocal laser scanning microscope. For all samples the same acquisition settings were employed, and signals of similar intensity compared (Hanson and Kohler 2001).

The AtNAP14-YFP fusion protein was observed to localize exclusively in the chloroplasts, to small spots near the chloroplast envelope (Figure 3.26). This is in accordance with the localization described in the literature (Shimoni-Shor et al. 2010), and the prediction results referring to ChloroP 1.1 Prediction Server, which reveal a prediction of the

presence of a putative cTP of AtNAP14 (Table 3.9). We cannot localize AtNAP14-YFP fusion more precisely than being enriched at the chloroplast membrane.

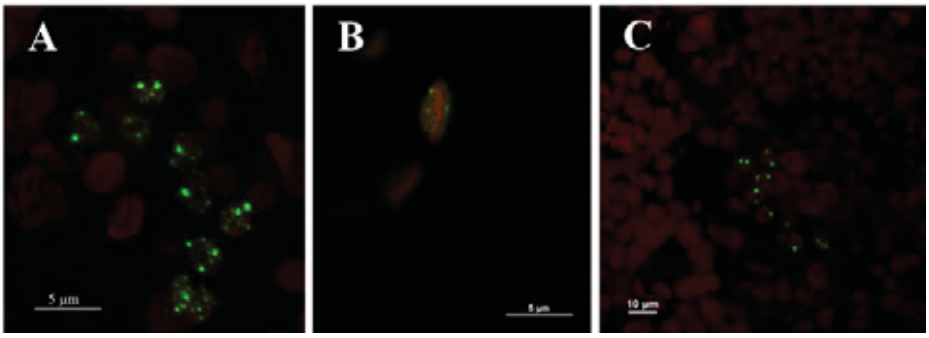


**Figure 3.26 – Localization of NAP14.YFP in tobacco leaf chloroplasts**
(A-C) AtNAP14.YFP fusion expressed in tobacco leaf cells by bombardment detected exclusively in chloroplasts. (B) A single chloroplast with NAP14.YFP in association with the envelope.

Green, YFP; Red, chlorophyll. Scale bar = 5 or 10 µm as shown.

## 3.2.5 Protein Characterization of AtNAP14 in A. thaliana

### 3.2.5.1 Western Blotting, AtNAP14 Protein Production and ATPase Activity

The aim of this part was, as for the two TAP proteins (Section *3.1.7.2*), to produce and purify the NAP14 protein for further study of the ATPase activity, determining $V_{max}$ (maximal velocity of enzyme-catalyzed reaction on the substrate) and $K_m$ (substrate concentration that gives the enzyme one-half of its $V_{max}$), in solutions of different pH.

NAP14-pET and pET-28a(+) were transformed to Rosetta(DE3)pLysS bacteria for protein production, following the basic transformation procedure. NAP14-His proteins from the soluble phase of two parallel experiments were detected by Western Blotting (Figure 3.27).

The literature has classified the *Arabidopsis* NAPs as soluble ABC proteins (Rea 2007; Sánchez-Fernández et al. 2001). However, an experiment testing both soluble and insoluble phases of the protein, showed distinct protein bands from the insoluble phase, and no distinct bands from the soluble phase (Figure 3.28), which led us to use the insoluble phase for purification.

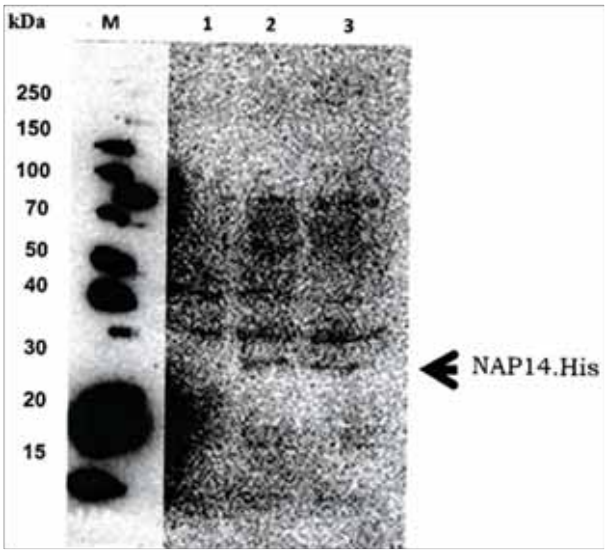


**Figure 3.27 – Western Blotting showing bands of NAP14-His (30.7 kDa)**
(1) Control pET-28a(+). (2) pET-28a(+)/NAP14-His from colony I. (3) pET28a(+)/NAP14-His from colony II.

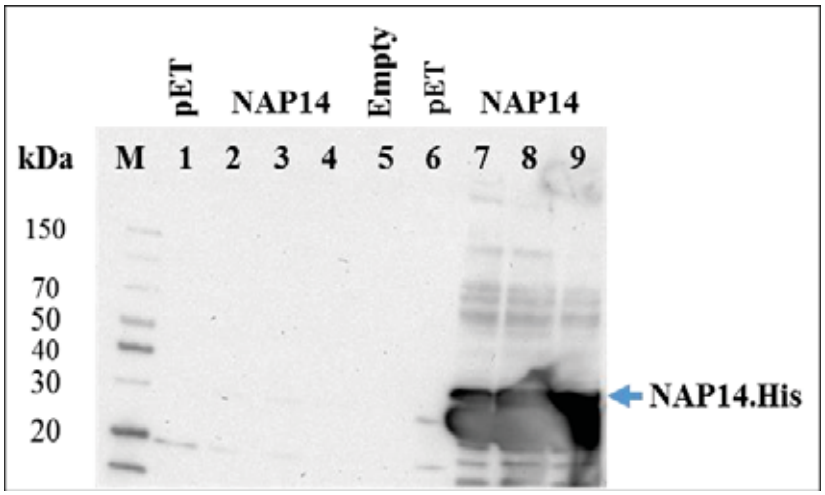


**Figure 3.28 – Western Blotting showing distinct NAP14**
Three replicas from the soluble phase (1-4) or insoluble phase (6-9). NAP14-His (30.7 kDa) detectable in all three replicas of insoluble phase (7-9). Control pET with no detectable NAP14 protein (1 and 6). Empty well (5) loaded with 20µl 1xdye without protein.

Protein purification was executed using Agarose Columns (Gold Biotechnology, USA), equilibrated using Binding/Wash Buffer including 8 M urea, and elution buffer including 6 M urea, before carrying out SDS-Page and Western Blotting (Figure 3.29).

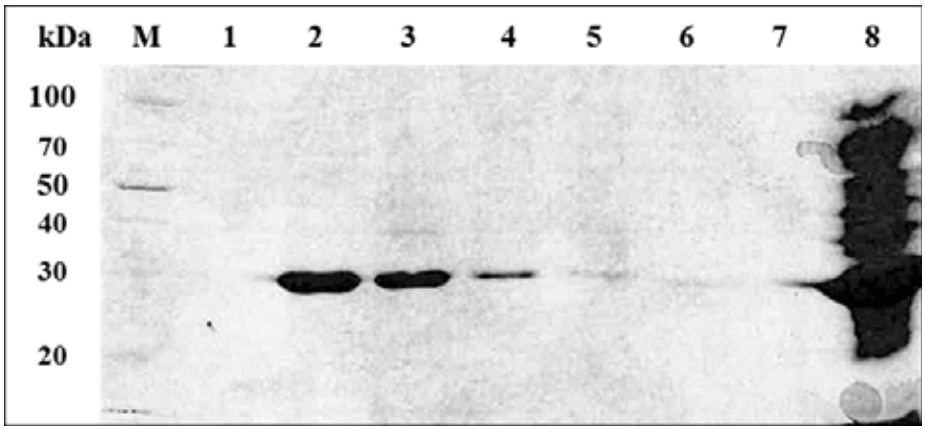


**Figure 3.29 – Western Blotting after purification of NAP14 protein (30.7 kDa)**
Elute pET control (1), Elute NAP14 (2) with distinct protein band. 1st wash (3), 2nd wash (4), 3rd – 6th wash (5), 7th – 10th wash (6) of NAP14. Empty well (7) loaded with 20µl 1xdye without protein. Flow through NAP14 (8).

To refold the purified and eluted denatured NAP14 protein, dialysis cassettes were used as described in the Materials and Methods. Control extracts from cells harboring pET28a(+) with no NAP14 protein, went through the same procedure.

ATPase activity measurements were carried out using ATP and the $P_i$ColorLock™ assay from Innova Biosciences on the enzyme NAP14. The results were inconclusive (data not shown).

A new series of experiments to achieve purified NAP14 protein, starting with the construct NAP14/pET in Rosetta and pET plasmid in Rosetta as a control, was performed. The execution followed the same procedure, with NAP14-His protein induced by 0.5 mM IPTG. Samples of NAP14 protein and pET (control) were prepared for SDS-PAGE and Western Blotting, using the soluble phase of the samples. One parallel with 2% glucose in media (LB + Kan + Cam) were executed in addition of two parallels without glucose added (Figure 3.30).

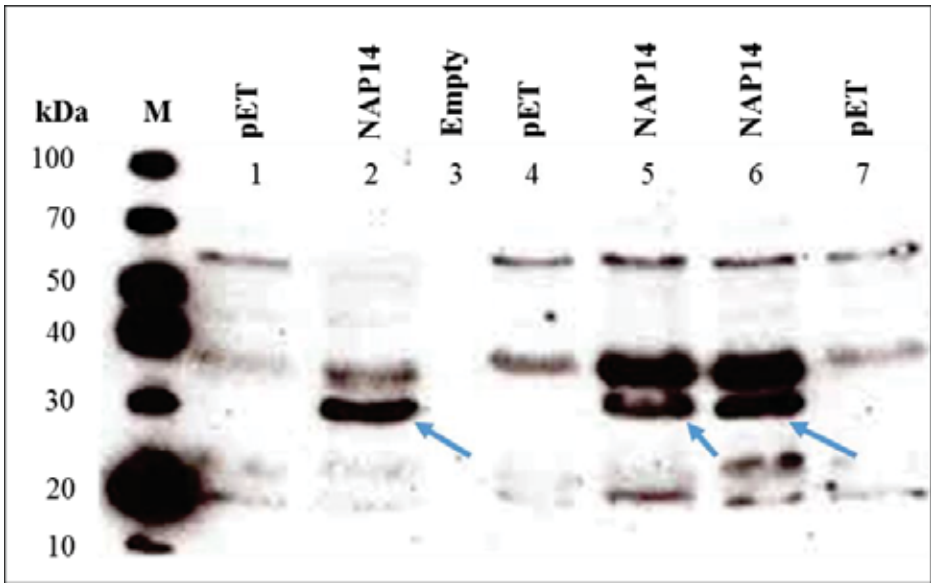


**Figure 3.30 – Western Blotting of three replicas of NAP14 protein and pET (control)**
NAP14 and pET (control) from cultures enriched with 2% glucose (1 and 2), and cultures without added glucose (4-7). Blue arrows: distinct bands of NAP14, 30.7 kDa, protein indicated (2, 5, 6). Empty well (3) loaded with 20 µl 1xdye without protein.

### 3.2.5.2 Purification of NAP14 Protein by Ion-Exchange Chromatography

Purification of NAP14 by ion-exchange chromatography (Section 2.2.7.3) was started using Äkta™ Pure system equipment from GE healthcare Bio-Sciences AB (Figure 3.31). The technique rests on interactions, which are reversible, between charged molecules or ion exchange groups of different charge. Charged molecules bind to the separation medium at low ionic strength and are eluted with a pH gradient or a salt. The practical execution was performed by the PhD student Rashed Abdullah at St. John's University, Queens, NY, USA. A first run (Figure 3.32) shows eight peaks of proteins (Figure 3.32C). Samples of protein from tubes referring to each peak, were examined by

Western Blotting. A gel picture using Coomassie staining is shown in Figure 3.32A, and a membrane from Western Blotting shows distinct NAP14 bands (30.7 kDa) from tubes around peak number 5 and 6 (Figure 3.32B). The contents of these tubes were pooled for further purification (Figure 3.32C), which was not carried out.

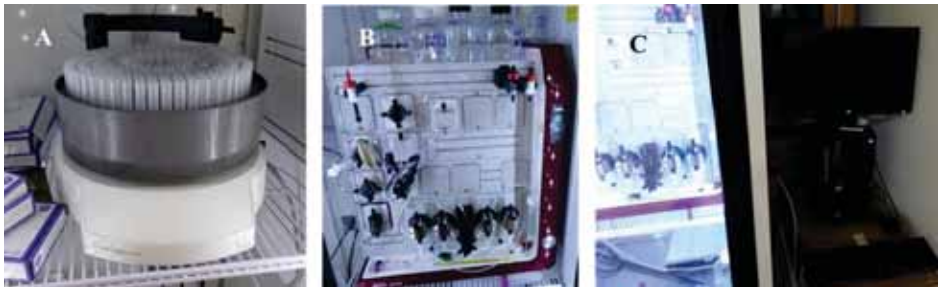


**Figure 3.31 – Ion-exchange chromatography equipment Äkta™ Pure from GE Healthcare Bio-Sciences AB at St. John's University, USA**
(A) Fraction collector F9-R. (B,C) Äkta™ Pure chromatography system (C, right) IT equipment with software.

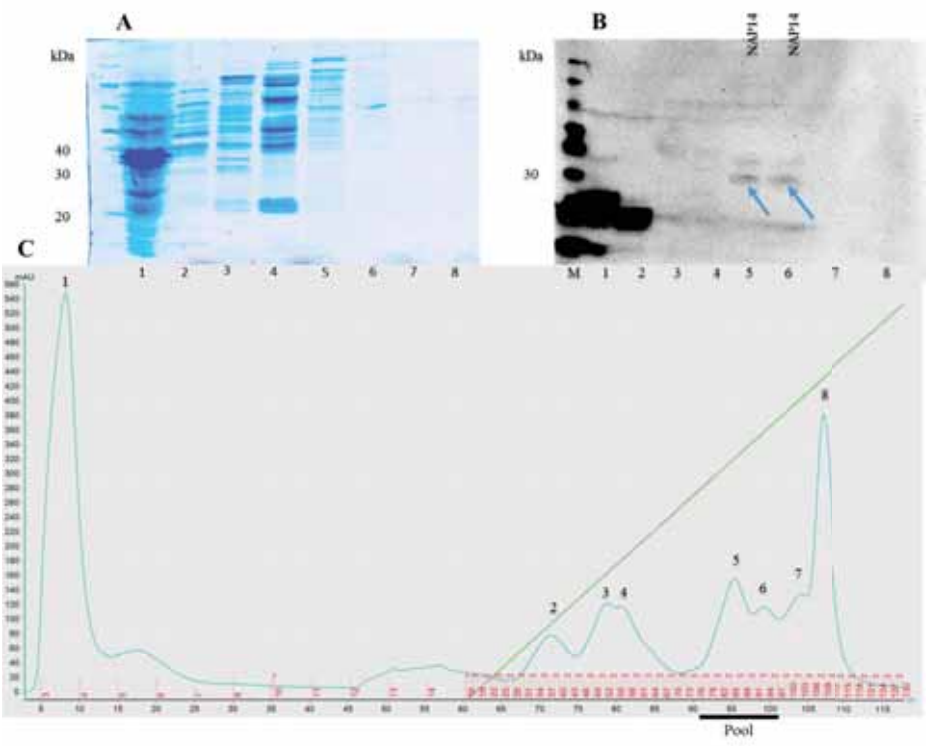


**Figure 3.32 – Isolation of NAP14 protein (30.7 kDa) by Western Blotting and protein purification**

(A) Coomassie gel picture. (B) Membrane picture showing NAP14 protein bands corresponding to peaks 5 and 6 (blue arrows). (C) Ion-exchange chromatogram with protein peaks and corresponding numbered gradient tubes (red number). Blue line indicates absorbance at 280 nm (mAU), and fractions are indicated by short red vertical lines in the chromatogram. Pooled tubes containing NAP14 protein are indicated.

Intentionally left blank

# 4 Discussion

## 4.1 Evolution of ABC transporters

### 4.1.1 General Aspects

Terrestrial plants have many more ABC transporter genes than vertebrates like human and mouse, invertebrates like the fruit fly, and roundworm and no-terrestrial lower plants like *Chlamydomonas*. While terrestrial plants, for example moss, rice and *Arabidopsis* have about 130 transporter genes, the other groups have only 50-60 (Hwang et al. 2016). We may ask why terrestrial plants have many more ABC transporter proteins than other organisms. Why are genes from the subfamily ABCB and ABCG in particular over represented? Reviewing the functions of many plant ABC proteins, and trying to decipher their evolutionary paths, gives a good basis for answering these questions. One indication comparing with animals, is that plant genomes enriched in genes encoding ABC transporters are particularly suited to helping plants survive and become competitive under dry land conditions (Hwang et al. 2016). The ABC transporter genes might have undergone a simultaneous multiplication and diversification during evolution and adaptation of plants to terrestrial environment. During this time plants developed wide surface areas for photosynthesis, and a sessile lifestyle. These characteristics increase the risks of desiccation, damage due to toxins and chemical stress, and diseases acquired from microorganisms. The best defense of land plants against xenobiotics, such as heavy metals, might come from the ability of ABCB transporters to sequester, to transport, or to export stressing foreign chemicals, for example an *Arabidopsis* export protein allowing some tolerance to cadmium and lead when overexpressed (Lane et al. 2016).

An interesting suggestion based on current data on the origin of ABCI subfamily transporter, of which the NAP14 is a member, propose it to evolve from prokaryotic genomes, and may result from movement of genes in mitochondria and plastids to the nuclear genome (Lane et al. 2016; Verrier et al. 2008). The hypothesis that the NBD motifs of many transporter families derive form common ancestor of prokaryotes and eukaryotes is proposed (Igarashi et al. 2004). Investigations of the phylogeny of the superfamily and analyzing domain features to trace the evolution of structures, reveal all eukaryote ABC transporter families to be present in the genomes of all 79 eukaryotic species inspected, suggesting the structures may have originated before the last eukaryotic common ancestor (Xiong et al. 2015).

## 4.2 AtTAP1

### 4.2.1 Conservation of TAP1 and NAP14 Domains and Evolution

The essentials domains of the ABC proteins were earlier used to identify the closest protein structures as homologs in different organisms (Walker et al. 1982), and tentatively assign the *Arabidopsis* proteins to subfamilies (Sánchez-Fernández et al. 2001). To investigate conservation and similarities of TAP1 and NAP14, protein sequences were obtained from NCBI. Our study focused on relationships between sequences selected from key laboratory and commercial plant species, and from other non-plant model organisms. AtTAP2 was included because of the close relationship to AtTAP1.

Comparing protein sequences in the alignments, and calculating the identities and similarities made it possible to present a phylogenetic tree indicating the evolutionary relationships and distances of the homologous TAP1 and NAP14 proteins. The study indicates a closer evolutionary protein distance between the TAP1 proteins of *N. tabacum*

and *S. lycopersicum* than to the other homolog proteins of TAP1, and the AtTAP1 protein is shown to be most closely related to the two mentioned proteins than to the other four proteins (Figure 3.3, Section 3.1.2). The percentage identities and similarities between the proteins of *N. tabacum* and *S. lycopersicum* and AtTAP1 are higher than between AtTAP1 and the other four proteins (Table 3.3, Section 3.1.2). In addition, the AtTAP1 is more similar to the other higher plant proteins, than to the lower plant proteins (Table 3.3), and higher plants proteins show a closer evolutionary relationship to each other than to the lower plant proteins (Figure 3.3). The non-plant proteins have a lesser similarity and identity to AtTAP1 than the plant homologs have (Table 3.3).

The NAP14 homolog proteins show a similar pattern. *N. tabacum* and *S. lycopersicum* show a closer evolutionary distance to each other than to the other homologs, and the AtNAP14 protein also is closer to these two proteins than it is to the other four proteins (Figure 3.24, Section 3.2.3). The percentage identities and similarities between the proteins of *N. tabacum* and *S. lycopersicum* compared to AtNAP14 are higher than between AtNAP14 and the other four proteins (Table 3.9, Section 3.2.3). In addition, the AtNAP14 is more similar to the other higher plant proteins, than to the lower plant proteins (Table 3.9), and except partly for *O. sativa*, higher plants proteins show a closer evolutionary relationship to each other than to the lower plant proteins (Figure 3.24).

Inspection of the essential domains regarding the amino acids, reveal a distinct conservation and consensus of the motifs (Rea 2007; Sánchez-Fernández et al. 2001) in all the proteins, both TAP1s and NAP14s. The motifs are nearly identical and placed in the same part of the TAP1 proteins, towards the C-terminal. The motifs of the NAP14 proteins are placed in the same end, except for the Walker A motif, which is localized nearer to the N-terminal (Figure 3.23).

All motifs of TAP1 and NAP14 are conserved with respect to the frame formulas (Introduction, Section 1.1.2). Some variations of amino acids

inside the motifs do not alter the validity of the conservation (Figure 3.1, Figure 3.2 and Figure 3.23). The difference between the motifs of the AtTAP1 and AtTAP2 proteins are very low, and much lower than between these motifs and the NAP14 motifs. Similarly, the NAP14 motifs are more alike each other than they are compared to the TAP1 (Figure 3.1, Figure 3.2 and Figure 3.23). AtTAP2 is included to the TAP1s because of the near relationship. These differences and likenesses of the motifs may indicate molecular changes at different times or rates inside the TAP1 the NAP14 proteins during evolution.

Concerning the transit peptides, suggestion of a basic functional module in plastid protein import established prior to the divergence evolution of the three distinct evolutionary branches, is proposed (Kohler et al. 2015; Steiner and Loffelhardt 2005). Acquisition of transit peptides is among the most critical events in in plastid evolution, making their evolutionary origin significant and of considerably interest (Lee et al. 2008; McFadden 1999).

Our study showed a lack of N-terminal extensions in TAP1 of *C. reinhardii* and *P. patens* (Figure 3.1, Section 3.1.1) and a predicting score of cTP lower than 0.5, which indicates an abscence of cTP (Table 3.5, Section 3.1.3). Likewise, we find NAP14 of *C. reinhardii* and *P. patens* lacking N-terminal extension (Figure 3.23, Section 3.2.2) and a predicting score of cTP lower than 0.5 (*P. patens*) and to 0.503 (*C. reinhardii*) (Table 3.10, Section 3.2.4). These observations predict the TAP1 and NAP14 protein homologs in the lower plants *C. reinhardii* and *P. patens* not evolve a cTP, with consequences on their functions to be different from those of the higher plants discussed.

The presented data on similarities and diversities on TAP1 and NAP14 proteins, may be interpreted as support of the theory that ABC transporter genes might have undergone diversification and multiplication events during evolution, and may be before plants adapted

to the land environment (Hwang et al. 2016), with different targeting locations of homolog proteins in higher and lower plants.

### 4.2.2 In vivo Subcellular Localization

The subcellular localization of the AtTAP1 protein was observed exclusively in the chloroplasts, by observation of the AtTAP1-YFP fusion protein in leaf cells of tobacco (Figure 3.4) and in leaf cells of *Arabidopsis* (Figure 3.5). The enrichment at the chloroplast envelope suggests that the protein has a role in transport into the chloroplast stroma, which agrees with the predictions that AtTAP1 harbors a chloroplast transit peptide, and is enriched in the chloroplast envelope (Ferro et al. 2010; Kang et al. 2011).

Two different patterns of localization were observed: AtTAP1-YFP localized as short filaments in close association with the envelope (Figure 3.4A and Figure 3.4B), or AtTAP1-YFP uniformly distributed with the entire surface of the chloroplast (Figure 3.4C). Sectional images of an individual chloroplast show that the fusion protein is clearly associated with the chloroplast envelope, and not throughout the stroma (Figure 3.4D). However, it was impossible in this study to determine if AtTAP1 is an integral membrane protein, or is only enriched near the membrane. Further investigations, including studies on chloroplast extracts and AtTAP1 analysis, may reveal more details on the exact position occupied by the protein in the chloroplast structure.

The closest homolog in *Arabidopsis*, AtTAP2, does not have a N-terminal extension (Figure 3.1), and is detected in vacuolar (tonoplast) membranes, not in chloroplasts (Jaquinod et al. 2007), which indicates a divergent function compared to AtTAP1.

### 4.2.3 T-DNA Establishment of the Mutant attap1

In our study, we identified a T-DNA insert in the *AtTAP1* gene in the mutant line *attap1,* SAIL_8_B04 (Mut). The T-DNA was located between two exons, directly after nucleotide 658 of the genomic DNA (Figure 3.6A). Mutant and wild type plants were used in analysis for characterization of the AtTAP1 protein.

### 4.2.4 Phenotypic Analysis

The literature shows a diversity of studies concerning stress treatments, expressions and impacts on processes in mutants of *A. thaliana*. The main interests and focus in this study are to examine phenotypic differences in expressions of *attap1* compared to WT, mainly by use of metals, like aluminum (Gabrielson et al. 2006; Larsen et al. 2007; Larsen et al. 2005), but other stress treatments, like MV, $H_2O_2$, auxin, and heat. Aluminum toxicity is an agricultural problem worldwide, because the $Al^{3+}$ as a predominant form in environments of low-pH, will inhibit root growth (Kochian 1995; Kochian, Hoekenga, and Pineros 2004; Vardar and Ünal 2007). Roots of *Arabidopsis* show characteristic aluminum hypersensitivity when mutants of *ALS1*, and others like *ALS3*, are compared to wild type (Gabrielson et al. 2006; Larsen et al. 2007). An indication of these studies is that the *AtTAP2* gene is required for root growth in an environment of aluminum, and GUS analyses reveal that *ALS1* expression is primarily localized to the root tip and the vasculature throughout the plant. Based on that TAP1 and TAP2 are located in the same half type family of ABC transporters of the superfamily of ABC proteins (Rea 2007; Sánchez-Fernández et al. 2001), we assumed the TAP1 gene to have similar responses.

The study shows no significant differences in root length between WT and *attap1* when exposed to aluminum, as well as to any of the other abiotic and biotic treatments (Table 3.6, Table 3.7, Figure 3.7 and Figure 3.9). This indicates that AtTAP1 is not, as AtTAP2 involved in

aluminum sensitivity of the root, nor is it involved in sensitivity reactions of the other stress factors used. However, the root length of the aluminum treated seedlings, both WT and mutants, are significantly longer than the non-treated seedlings. This was not expected as the literature reports considerable inhibition of root growth in aluminum acid environments, in experiments with seedlings grown hydroponically or on soaked gel plates with a pH 4.2 (Gabrielson et al. 2006; Larsen et al. 2007; Larsen et al. 2005). My study uses MS agar plates and pH 5.8. Differences in acidity may influence the state of the aluminum ion and thereby have influence on the root growth. Aluminum presents itself in a normal environment as the $Al^{3+}$-cation (Sarpola 2007), in water solutions as monomeric $[Al(OH)_2]^+$, $Al(OH)_3$, $[Al(OH)_4]^-$ , and AlO(OH) forms, or polymerizing by bridging to dimers, trimers, etc. (Sarpola 2007). Distribution of aluminum in dilute solutions, shows a much higher and dominating $Al^{3+}$ fraction at pH 4.2 than at pH 5.8, while the $[Al(OH)_2]^+$, $Al(OH)_3$, $[Al(OH)_4]^-$ and AlO(OH) forms dominate at pH 5.8 (Sarpola 2007). This view is of interest, and further studies on root growth in more alkaline environments may give more information on genes and proteins subcellular reactions.

Different solutions of metal ions were employed on seedlings, and root length measured (Table 3.6, Table 3.7, Figures 3.7 and Figure 3.9), seedlings grown on media containing MV, $H_2O_2$, $CuSO_4$, or heat treated, were inspected every second day (Figure 3.11), and plants grown on soil were exposed by watering with $Fe^{3+}$ solution (Figure 3.12). The study revealed no phenotypic differences in expressions of *attap1* seedlings compared to WT seedlings in any experiment. We conclude from this that neither of the stress factors have impact on the *AtTAP1* gene to produce phenotypic changes in environmental conditions as described. Thus, we cannot from the results, tell the impact on transport, storage and co-factor assembly in plastids, or on cellular homeostasis (Lopez-Millan, Duy, and Philippar 2016).

### 4.2.5 Expression Analysis

Studies of the plant growth hormone auxin, which has ability to stimulate differential growth in repose to light stimuli, have led to discoveries of several genes in the auxin biosynthesis pathway (Zhao 2010). The preliminary study executed in this work, shows a lower expression level of *AtTAP1* in seedlings after six hours auxin treatment than after 24 hours. The experiment suffers from lack of appropriate controls, but can give a suggestion and preliminary indication that the gene expression firstly is suppressed by the auxin, and then is recovering to a "normal" level (adjusted and compared to the control) after 24 hrs (Figure 3.14 and Figure 3.15). An interesting study based on two phenotypes of the 35S::PID lines, shows decreased expression of the auxin responsive DR::GUS reporter combined with reduced lateral root initiation upon exogenous application of auxin (Christensen et al. 2000). In this study Christensen et al. concluded that PID acts as a negative regulator of auxin signaling. However, later observations have argued against such a function for PID (Benjamins et al. 2001). Laskowski et al. (Laskowski et al. 2006) have reported microarray experiments revealing nearly hundred genes (*AtTAP1* not included) that are substantially up-regulated in the root following auxin treatment. Benjamins et al. (Benjamins et al. 2001; Benjamins and Scheres 2008) have asserted overexpression of other genes resulting in phenotypes observed in mutants with altered sensitivity to or transport of auxin. On this basis, it is of interest to perform further experiments on the gene *AtTAP1* to reveal if it participates in any auxin biosynthesis pathways.

During evolution chloroplasts, which originated about three billion years ago, in higher plants established as site for photosynthesis to become the basis for all life dependent on oxygen and carbohydrate supply, and in consequence represent the iron-richest system in plant cells (Lopez-Millan, Duy, and Philippar 2016). This study looked at plants expressing *PromoterAtTAP1-pBADG* after watering regularly with an iron solution or only water for 20 days, and compared leaves phenotypes of GUS-

staining after different times. There were no visible differences between treated and untreated plants (Figure 3.16).

From this preliminary experiments, we can draw the conclusion and suggest that AtTAP1 reveal no special biotic functions or reactions, on the basis of no observed differences between WT and mutant *attap1,* when exposed to the different stress factors described. Nevertheless, further studies may show functions of the AtTAP1 protein in cells and chloroplasts biosynthetic reactions (Lopez-Millan, Duy, and Philippar 2016).

Analysis using RT-PCR and the GUS expression indicate a higher induction of the *AtTAP1* gene in flowers compared to roots and leaves (Figure 3.13). Highest expression of the gene in main roots is remarkably concentrated near the sites of lateral root initiation (Figure 3.13B-D). In comparison, *AtTAP2* expression is mainly localized to the root tip and the vasculature of the plant, and therefore, it will be of interest to analyze the function of AtTAP1 in root cell plastids. Studies on stages of root developments are of particular interest, referring to discussions on other gene activities involving root hair formation (Bernhardt and Tierney 2000), root and root tips (Singh, Kaloudas, and Raines 2008) and detections of sites of lateral root initiation and junctions between primarily and secondary roots (Cunillera, Boronat, and Ferrer 2000).

### 4.2.6 Wounding

GUS expression after mechanical wounding has been reported in different transgenic lines of *Arabidopsis* (Bohlmann et al. 1998). Other studies indicate wound-inducible gene expressions as predominantly in particular organs and tissues (Gupta et al. 2012).

In this study leaves from WT plants expressing *PromoterAtTAP1-pBADG* (GUS plants) were mechanically wounded by tearing with a needle. In control leaves, *AtTAP1* was shown to be expressed throughout

the leaf, with the highest expression along the periphery, to the leaf apex, and to some extent to the middle of the leaves, and not to the petiole (Figure 3.17A and C). Mechanically wounded leaves resulted in the same pattern of GUS expression, but with a stronger blue color, especially in the periphery of the leaves, and not at the wounding site (Figure 3.17B and D). This demonstrates that wounding results in distinct and enhanced GUS expression of *AtTAP1* in leaves. The evidence that the higher expression observed throughout the leaf, and not increased at the wounding site, may suggest it as part of a systematic response with a role in plant defense.

Induction of the wounding response has been shown for other ABC proteins, for example AtABCG11, which is upregulated in response to wounding, as well as to glucose, salt, and ABA treatments, and gibberellin-mediated down-regulation of ABA-induced expression (Panikashvili et al. 2007). Moreover, this protein plays a role in cutin and wax secretion, as well as vascular patterning in conjunction with AtABCG9 and AtABCG14 (Le Hir et al. 2013). A second example is the ABC transporter AtABCD1, which is involved in peroxisomal import of jasmonate precursors, and to basal and wound-induced jasmonic acid biosynthesis in leaves (Theodoulou et al. 2005).

Several wound-responsive genes in *Arabidopsis* encode proteins that are also involved in pathogen responses, comprising for example genes for signaling and regulatory components and for effector proteins, together with interactions between wounding, pathogen, abiotic stress, and hormonal responses (Cheong et al. 2002). Moreover, water stress on wounded carrot plants has been shown to exert a synergetic effect on the wound-response at the gene level (Becerra-Moreno et al. 2015).

Further investigations on different area localized induction expressions of the *AtTAP1* gene in the leaves and other tissues, with possible connected biochemical regeneration pathways, are of highly interest.

### 4.2.7 AtTAP1 Expression and Comparison to AtTAP2

Using semi-quantitative RT-PCR we found a significantly higher induction of the *AtTAP1* gene when stressed to $Ca^{2+}$, compared to control expression (Figure 3.20). $Al^{3+}$ and $Fe^{3+}$ treatments also induced *AtTAP1* to some degree, while $Mg^{2+}$ significantly reduced the induction (Figure 3.20). The calcium response upregulation may indicate that AtTAP1, like many other plant proteins, can be classified as $Ca^{2+}$ sensor proteins, which are involved in mediating responses to various biotic and abiotic environmental signals and in regulation of many developmental processes in plants (Hashimoto and Kudla 2011; Steinhorst and Kudla 2013). Many prominent calcium sensors described exist in complex gene families and form intricate signaling networks in plants that are capable of robust and flexible information processing (Hashimoto and Kudla 2011).

Wound-induced resistance in *Arabidopsis* is shown to be preceded by, and dependent upon, a burst of calcium, and that systematic cytosolic calcium elevation is activated upon wounding (Beneloujaephajri et al. 2013; Kiep et al. 2015). Therefore, the induction of AtTAP1 by calcium could form part of a stress response.

Figure 3.20 also shows expression of the *AtTAP2* gene, which, like *AtTAP1* may also be involved in responses to calcium regulations. Bioinformatic analysis has shown that at least four promoter motifs were calcium-regulated in *Arabidopsis*, and totally 269 genes are upregulated by calcium (Whalley et al. 2011).

Otherwise, differences and similarities in response to metal stresses between TAP1 and TAP2 genes and proteins is not possible to extract out from this study. Interestingly, induced expression of *AtTAP1* and *AtTAP2* caused by the iron, may indicate their proteins and plastids to be involved in sensing and regulation of iron concentration within the plant (Lopez-Millan, Duy, and Philippar 2016). Chloroplasts represent the iron-richest system in plant cells, and several families of proteins provide

and play a role in the transport across the two envelope membranes (Lopez-Millan, Duy, and Philippar 2016). On this basis, as the AtTAP1 is a chloroplast transporter protein, it may be possible to have iron regulating functions in or associated to chloroplasts. AtTAP2 is not a chloroplast transporter protein (Jaquinod et al. 2007), but may have other iron-acquisition or iron-regulatory activities (Brumbarova, Bauer, and Ivanov 2015; Lopez-Millan, Duy, and Philippar 2016). The protein plays a role in the internal detoxification of aluminum, transporting it between the cytoplasm and vacuole. Storage of aluminum in the vacuole enables plants to survive in an aluminum-toxic environment, an important factor for agriculture, given that aluminum-toxicity is a distinct growth-limiting factor for crop production on acid soils worldwide.

Magnesium is one of the most important and core macronutrients in plant growth and development, which has diverse biological functions, and it plays a central role in plant chlorophyll biosynthesis, and is able to alleviate aluminum toxicity (Chen and Ma 2013; Guo et al. 2015). Magnesium homeostasis in plant cells has been elaborated with discovery of magnesium transporters, and microarray studies have revealed that transcriptional levels of these transporters surprisingly changed little under magnesium stresses, either deficiency or excess/toxicity (Guo et al. 2015). Treatment of seedling with $Mg^{2+}$ in this study shows significantly reduced induction of both *AtTAP1* and *AtTAP2* genes (Figure 3.20). There is no evidence for other genes or proteins to suppress the expressions of these two TAP genes, but we promote the idea that high magnesium concentrations may initiate activity of other proteins, which as secondary effects lower the *AtTAP* expressions. Interactions between high magnesium concentrations to displace or compete with aluminum from binding sites on tissue, plasma membrane, and other components, protecting the roots from aluminum toxicity, are described (Chen and Ma 2013). However, there are no references to lowering of any gene expressions in this context, but further

investigations may reveal connections between magnesium excess/toxicity and lowering of gene expressions.

In conclusion, a comparison of TAP1 and TAP2 has revealed that the function of the two proteins are highly divergent in Arabidopsis. Further studies involving biotic and abiotic environmental stress situations, with respect to the similarities and differences will be important for more understanding of the two proteins' functions.

## 4.3 AtNAP14

AtNAP14 is a member of a family of plant specific NAP proteins, and early reports suggest that it plays a role in regulating transition metal homeostasis (Shimoni-Shor et al. 2010). Analysis of conserved motifs essential for ATPase activity, predict that AtNAP14 is a functional enzyme (Figure 3.23, Section 3.2.2). Efforts to confirm the enzyme activity were unsuccessful (Section 3.2.5), but much can still be gleaned from the study of the conservation of AtNAP14, and analysis of its localization.

This study and others have shown that AtNAP14 is specific to plants, lacking homologs in other species. Because NAP14 and its homologs are not found in non-plants, the protein relationships can be interpreted as indications of evolutionary adaptions of beneficial homeostatic balances, favorable to plants.

Insertional mutants in both *AtNAP14* and *AtNAP11* shows plants exhibiting severe growth defects. The two proteins are orthologs of the ATPase FutC protein, which functions as a part of the FutABC transporter involved in iron binding processes in Cyanobacteria (Badarau et al. 2008; Katoh et al. 2001; Shimoni-Shor et al. 2010). Studies on insertional mutants of *AtNAP14* have detected significant changes in transition metal homeostasis, reporting approximately 18 times more iron in the shoot tissue than in WT plants (Shimoni-Shor et al. 2010). A

specific loss of chloroplast structures and a reduction in transcript levels of iron homeostasis-related genes accompanied the increased shoot transition metal content. Based on these reported results, it is likely that AtNAP14 plays an important role in plastid transition metal homeostasis as a part of a chloroplast transporter complex or, alternatively, in the regulation of transition metal homeostasis (Shimoni-Shor et al. 2010).

Although preliminary, an unpublished study (Dr. Sarah Rottet, University of Neuchâtel, Switzerland) hypothesize AtNAP14, together with AtNAP13, is involved in lipid exchange between thylakoid membranes and plastoglobules. This is particularly interesting, as the closely related AtNAP11 (also known as TGD3, trigalactosyldiacylglycerol 3) has also been shown to have a role in chloroplast lipid import, required in a functional complex together with TGD1 (ABCI14) and TGD2 (ABCI15). The TGD lipid transporter complex, forming an ABC transporter, is proposed to be a lipid translocator, residing at the inner chloroplast envelope membrane. AtNAP11 is the ATPase component containing a NBD, associated with TDG1, containing permease domain, and TGD2, containing the substrate-binding domain (Lu et al. 2007; Roston et al. 2012). The latter two proteins are required for the biosynthesis of ER-derived thylakoids in *Arabidopsis* (Lu et al. 2007). AtNAP14 did not show association to the TGD1/TGD2 complex (Lu et al. 2007). Other TGD proteins, like TGD4 and TGD5, are reported to be involved in lipid transfers and interact with the TGD complex (Fan et al. 2015). Interestingly, further investigations may reveal that AtNAP14 also has a role in lipid trafficking and exchange functions.

This study and others have shown that AtNAP14 is localized to plastids. The localization of the NAP14-YFP fusion protein in tobacco leaves was shown exclusively in the chloroplasts, to small spots near the chloroplast envelope (Figure 3.26, Section 3.2.4). The chloroplast localization for the AtNAP14 protein provide strong support from reported fluorescence of the fusion protein co-localized with chlorophyll fluorescence

(Shimoni-Shor et al. 2010), and additional support for the plastid localization found in proteomic analysis of isolated chloroplasts in two independent studies (Mitra et al. 2007; Zybailov et al. 2008).

The closest Arabidopsis homologs of AtNAP14 are NAP8, NAP11 and NAP13 (Sánchez-Fernández et al. 2001), and are shown to be located to the chloroplast membrane too (Ferro et al. 2003; Froehlich et al. 2003; Shimoni-Shor et al. 2010). As has been discussed, AtNAP14 may function with AtNAP11 in both metal homeostasis and lipid import, and the localization of both these proteins to the chloroplast envelope supports this idea. It would be interesting to determine if they co-localize, and which, if in case existing, other proteins possibly are co-operating with AtNAP14 in the regulating homeostasis.

Intentionally left blank

# 5 Future Perspectives

The identification of *AtTAP1* as a gene that is induced by wounding, gives new information on the mechanisms by which plants adapt to reduce wound-triggered trauma. A motivating question to track: How is the *AtTAP1* gene and its protein involved in stress response in wound-induced resistance and calcium elevation? Comparisons to the *AtTAP2* will also be of interest. To investigate this further it may be interesting to determine timing of the *AtTAP1* induction, referring to microarray analysis that wound-induced genes of *Arabidopsis* are transcriptionally-activated in two temporal waves (Cheong et al. 2002). The preliminary study on auxin indicates a time restoring response after treatment. A similar and late-expressing transcript may be a response to wounding. The response of the gene to calcium, may be investigated together with wounding, using calcium solutions as treatment of wounded plant tissue, and examine transcription responses at different times.

Expression of *AtTAP1* is found to be induced throughout the leaf (Figure 3.17). This suggests that the protein functions in helping the plant adapt to reduce wound-induced trauma. Injury to the leaf causes dramatic changes in water availability, which may induce restoring.. The water loss and water stress has been shown to initiate wound signaling (Becerra-Moreno et al. 2015). It would be interesting to create experiments with additional water stress in calcium environments together wounding, to study their impact on the *AtTAP1* expression.

Studies on protein characterizations will reveal enzyme (ATPase) activities of the AtTAP1. In this context, the activities in different calcium concentration environments, together with different pH, are most interesting, and may reveal further understanding of the *AtTAP1* wounding expression processes.

Finally, it is known that activation of the wound-induced is not limited to the locally damaged leaf, but also occurs in the undamaged distal

systemic leaves. In this setting, it will be important to establish if *AtTAP1* induction is parts of the plants response distal from the wounding site.

These aspects of further work on the expression of the gene *AtTAP1* may reveal interesting understanding in agriculture, to the benefit of crop development and yields.

The present study has revealed some characteristic functions of the *AtTAP1* gene and its protein. Phylogenetic studies demonstrate that essential domains are highly conserved and that the protein is in closer evolutionary relationship to certain species' homolog proteins than to others. Comparing homologs and study their genes' expression patterns may reveal potential applications to diseases. For example, the human ABCB9, closely related to TAP1 and TAP2, is associated with the leukemia (GeneCards, Human Gene Database, ABCB9 Gene). Subsequently, such discoveries can implement important knowledge to medical treatment of diseases. Additionally, significant information may be given on similarities of defense response strategies between plants and animals.

# 6 References

Abele, R., and R. Tampe. 2004. 'The ABCs of immunology: structure and function of TAP, the transporter associated with antigen processing', *Physiology (Bethesda)*, 19: 216-24.

Al-Quraan, N. A., R. D. Locy, and N. K. Singh. 2011. 'Implications of paraquat and hydrogen peroxide-induced oxidative stress treatments on the GABA shunt pathway in Arabidopsis thaliana calmodulin mutants', *Plant Biotechnology Reports*, 5: 225-34.

Almen, M. S., K. J. Nordstrom, R. Fredriksson, and H. B. Schioth. 2009. 'Mapping the human membrane proteome: a majority of the human membrane proteins can be classified according to function and evolutionary origin', *BMC Biol*, 7: 50.

Ames, G. F., and J. Lever. 1970. 'Components of histidine transport: histidine-binding proteins and hisP protein', *Proc Natl Acad Sci U S A*, 66: 1096-103.

Asahina, M., K. Azuma, W. Pitaksaringkarn, T. Yamazaki, N. Mitsuda, M. Ohme-Takagi, S. Yamaguchi, Y. Kamiya, K. Okada, T. Nishimura, T. Koshiba, T. Yokota, H. Kamada, and S. Satoh. 2011. 'Spatially selective hormonal control of RAP2.6L and ANAC071 transcription factors involved in tissue reunion in Arabidopsis', *Proc Natl Acad Sci U S A*, 108: 16128-32.

Badarau, A., S. J. Firbank, K. J. Waldron, S. Yanagisawa, N. J. Robinson, M. J. Banfield, and C. Dennison. 2008. 'FutA2 is a ferric binding protein from Synechocystis PCC 6803', *Journal of Biological Chemistry*, 283: 12520-27.

Balk, J., and T. A. Schaedler. 2014. 'Iron cofactor assembly in plants', *Annu Rev Plant Biol*, 65: 125-53.

Baniwal, S. K., K. Bharti, K. Y. Chan, M. Fauth, A. Ganguli, S. Kotak, S. K. Mishra, L. Nover, M. Port, K. D. Scharf, J. Tripp, C. Weber, D. Zielinski, and P. von Koskull-Doring. 2004. 'Heat stress response in plants: a complex game with chaperones and more than twenty heat stress transcription factors', *J Biosci*, 29: 471-87.

Becerra-Moreno, A., M. Redondo-Gil, J. Benavides, V. Nair, L. Cisneros-Zevallos, and D. A. Jacobo-Velazquez. 2015.

'Combined effect of water loss and wounding stress on gene activation of metabolic pathways associated with phenolic biosynthesis in carrot', *Front Plant Sci*, 6: 837.

Belal, R., R. Tang, Y. Li, Y. Mabrouk, E. Badr, and S. Luan. 2015. 'An ABC transporter complex encoded by Aluminum Sensitive 3 and NAP3 is required for phosphate deficiency responses in Arabidopsis', *Biochem Biophys Res Commun*, 463: 18-23.

Beneloujaephajri, E., A. Costa, F. L'Haridon, J. P. Metraux, and M. Binda. 2013. 'Production of reactive oxygen species and wound-induced resistance in Arabidopsis thaliana against Botrytis cinerea are preceded and depend on a burst of calcium', *BMC Plant Biol*, 13: 160.

Benjamins, R., A. Quint, D. Weijers, P. Hooykaas, and R. Offringa. 2001. 'The PINOID protein kinase regulates organ development in Arabidopsis by enhancing polar auxin transport', *Development*, 128: 4057-67.

Benjamins, R., and B. Scheres. 2008. 'Auxin: the looping star in plant development', *Annu Rev Plant Biol*, 59: 443-65.

Bernhardt, C., and M. L. Tierney. 2000. 'Expression of AtPRP3, a proline-rich structural cell wall protein from Arabidopsis, is regulated by cell-type-specific developmental pathways involved in root hair formation', *Plant Physiol*, 122: 705-14.

Birnbaum, K. D., and A. Sanchez Alvarado. 2008. 'Slicing across kingdoms: regeneration in plants and animals', *Cell*, 132: 697-710.

Bohlmann, H., A. Vignutelli, B. Hilpert, O. Miersch, C. Wasternack, and K. Apel. 1998. 'Wounding and chemicals induce expression of the Arabidopsis thaliana gene Thi2.1, encoding a fungal defense thionin, via the octadecanoid pathway', *FEBS Lett*, 437: 281-6.

Briat, J. F. 2010. 'Arsenic tolerance in plants: "Pas de deux" between phytochelatin synthesis and ABCC vacuolar transporters', *Proc Natl Acad Sci U S A*, 107: 20853-4.

Brumbarova, T., P. Bauer, and R. Ivanov. 2015. 'Molecular mechanisms governing Arabidopsis iron uptake', *Trends Plant Sci*, 20: 124-33.

Burkhead, J. L., K. A. Reynolds, S. E. Abdel-Ghany, C. M. Cohu, and M. Pilon. 2009. 'Copper homeostasis', *New Phytologist*, 182: 799-816.

Chen, C. C., Y. Y. Chen, I. C. Tang, H. M. Liang, C. C. Lai, J. M. Chiou, and K. C. Yeh. 2011. 'Arabidopsis SUMO E3 ligase SIZ1 is involved in excess copper tolerance', *Plant Physiol*, 156: 2225-34.

Chen, Z. C., and J. F. Ma. 2013. 'Magnesium transporters and their role in Al tolerance in plants', *Plant and Soil*, 368: 51-56.

Cheong, Y. H., H. S. Chang, R. Gupta, X. Wang, T. Zhu, and S. Luan. 2002. 'Transcriptional profiling reveals novel interactions between wounding, pathogen, abiotic stress, and hormonal responses in Arabidopsis', *Plant Physiol*, 129: 661-77.

Choi, H., J. Y. Jin, S. Choi, J. U. Hwang, Y. Y. Kim, M. C. Suh, and Y. Lee. 2011. 'An ABCG/WBC-type ABC transporter is essential for transport of sporopollenin precursors for exine formation in developing pollen', *Plant J*, 65: 181-93.

Christensen, S. K., N. Dagenais, J. Chory, and D. Weigel. 2000. 'Regulation of auxin response by the protein kinase PINOID', *Cell*, 100: 469-78.

Clough, S. J., and A. F. Bent. 1998. 'Floral dip: a simplified method for Agrobacterium-mediated transformation of Arabidopsis thaliana', *Plant J*, 16: 735-43.

Coleman, J. A., F. Quazi, and R. S. Molday. 2013. 'Mammalian P4-ATPases and ABC transporters and their role in phospholipid transport', *Biochim Biophys Acta*, 1831: 555-74.

Cunillera, N., A. Boronat, and A. Ferrer. 2000. 'Spatial and temporal patterns of GUS expression directed by 5' regions of the Arabidopsis thaliana farnesyl diphosphate synthase genes FPS1 and FPS2', *Plant Mol Biol*, 44: 747-58.

Davidson, A. L., E. Dassa, C. Orelle, and J. Chen. 2008. 'Structure, function, and evolution of bacterial ATP-binding cassette systems', *Microbiol Mol Biol Rev*, 72: 317-64, table of contents.

Davies, T. G. E., and J. O. D. Coleman. 2000. 'The Arabidopsis thaliana ATP-binding cassette proteins: an emerging superfamily', *Plant Cell and Environment*, 23: 431-43.

Dean, J. V., and J. D. Mills. 2004. 'Uptake of salicylic acid 2-O-beta-D-glucose into soybean tonoplast vesicles by an ATP-binding cassette transporter-type mechanism', *Physiol Plant*, 120: 603-12.

Dean, M., A. Rzhetsky, and R. Allikmets. 2001. 'The human ATP-binding cassette (ABC) transporter superfamily', *Genome Res*, 11: 1156-66.

Desikan, R., A. H-Mackerness S, J. T. Hancock, and S. J. Neill. 2001. 'Regulation of the Arabidopsis transcriptome by oxidative stress', *Plant Physiol*, 127: 159-72.

Divol, F., D. Couch, G. Conejero, H. Roschzttardtz, S. Mari, and C. Curie. 2013. 'The Arabidopsis YELLOW STRIPE LIKE4 and 6 transporters control iron release from the chloroplast', *Plant Cell*, 25: 1040-55.

Dizdarevic, S., and A. M. Peters. 2011. 'Imaging of multidrug resistance in cancer', *Cancer Imaging*, 11: 1-8.

Duy, D., R. Stube, G. Wanner, and K. Philippar. 2011. 'The chloroplast permease PIC1 regulates plant growth and development by directing homeostasis and transport of iron', *Plant Physiol*, 155: 1709-22.

El-Awady, R., E. Saleh, A. Hashim, N. Soliman, A. Dallah, A. Elrasheed, and G. Elakraa. 2016. 'The Role of Eukaryotic and Prokaryotic ABC Transporter Family in Failure of Chemotherapy', *Front Pharmacol*, 7: 535.

Emamverdian, A., Y. Ding, F. Mokhberdoran, and Y. Xie. 2015. 'Heavy metal stress and some mechanisms of plant defense response', *ScientificWorldJournal*, 2015: 756120.

Emanuelsson, O., H. Nielsen, and G. von Heijne. 1999. 'ChloroP, a neural network-based method for predicting chloroplast transit peptides and their cleavage sites', *Protein Sci*, 8: 978-84.

Fan, J., Z. Zhai, C. Yan, and C. Xu. 2015. 'Arabidopsis TRIGALACTOSYLDIACYLGLYCEROL5 Interacts with TGD1, TGD2, and TGD4 to Facilitate Lipid Transfer from the Endoplasmic Reticulum to Plastids', *Plant Cell*, 27: 2941-55.

Ferenci, T., W. Boos, M. Schwartz, and S. Szmelcman. 1977. 'Energy-coupling of the transport system of Escherichia coli dependent on maltose-binding protein', *Eur J Biochem*, 75: 187-93.

Ferro, M., S. Brugiere, D. Salvi, D. Seigneurin-Berny, M. Court, L. Moyet, C. Ramus, S. Miras, M. Mellal, S. Le Gall, S. Kieffer-Jaquinod, C. Bruley, J. Garin, J. Joyard, C. Masselon, and N. Rolland. 2010. 'AT_CHLORO, a comprehensive chloroplast proteome database with subplastidial localization and curated information on envelope proteins', *Mol Cell Proteomics*, 9: 1063-84.

Ferro, M., D. Salvi, S. Brugiere, S. Miras, S. Kowalski, M. Louwagie, J. Garin, J. Joyard, and N. Rolland. 2003. 'Proteomics of the chloroplast envelope membranes from Arabidopsis thaliana', *Mol Cell Proteomics*, 2: 325-45.

Fischer, M., Q. Y. Zhang, R. E. Hubbard, and G. H. Thomas. 2010. 'Caught in a TRAP: substrate-binding proteins in secondary transport', *Trends Microbiol*, 18: 471-8.

Froehlich, J. E., C. G. Wilkerson, W. K. Ray, R. S. McAndrew, K. W. Osteryoung, D. A. Gage, and B. S. Phinney. 2003. 'Proteomic study of the Arabidopsis thaliana chloroplastic envelope membrane utilizing alternatives to traditional two-dimensional electrophoresis', *J Proteome Res*, 2: 413-25.

Gabrielson, K. M., J. D. Cancel, L. F. Morua, and P. B. Larsen. 2006. 'Identification of dominant mutations that confer increased aluminium tolerance through mutagenesis of the Al-sensitive Arabidopsis mutant, als3-1', *J Exp Bot*, 57: 943-51.

Garcia, O., P. Bouige, C. Forestier, and E. Dassa. 2004. 'Inventory and comparative analysis of rice and Arabidopsis ATP-binding cassette (ABC) systems', *J Mol Biol*, 343: 249-65.

Garmory, H. S., and R. W. Titball. 2004. 'ATP-binding cassette transporters are targets for the development of antibacterial vaccines and therapies', *Infect Immun*, 72: 6757-63.

Gayet, L., N. Picault, A. C. Cazale, A. Beyly, P. Lucas, H. Jacquet, H. P. Suso, A. Vavasseur, G. Peltier, and C. Forestier. 2006. 'Transport of antimony salts by Arabidopsis thaliana protoplasts over-

expressing the human multidrug resistance-associated protein 1 (MRP1/ABCC1)', *FEBS Lett*, 580: 6891-7.

Goldberg, J., H. B. Huang, Y. G. Kwon, P. Greengard, A. C. Nairn, and J. Kuriyan. 1995. 'Three-dimensional structure of the catalytic subunit of protein serine/threonine phosphatase-1', *Nature*, 376: 745-53.

Guo, W., S. Chen, N. Hussain, Y. Cong, Z. Liang, and K. Chen. 2015. 'Magnesium stress signaling in plant: just a beginning', *Plant Signal Behav*, 10: e992287.

Gupta, N. C., P. K. Jain, S. R. Bhat, and R. Srinivasan. 2012. 'Upstream sequence of fatty acyl-CoA reductase (FAR6) of Arabidopsis thaliana drives wound-inducible and stem-specific expression', *Plant Cell Rep*, 31: 839-50.

Haley, T. J. 1979. 'Review of the toxicology of paraquat (1,1'-dimethyl-4,4'-bipyridinium chloride)', *Clin Toxicol*, 14: 1-46.

Hall, T. 2011. 'BioEdit: An important software for molecular biology', *GERF Bulletin of Biosciences*, 2: 60-61.

Han, H. J., R. H. Peng, B. Zhu, X. Y. Fu, W. Zhao, B. Shi, and Q. H. Yao. 2014. 'Gene expression profiles of Arabidopsis under the stress of methyl viologen: a microarray analysis', *Mol Biol Rep*, 41: 7089-102.

Hanson, M. R., and R. H. Kohler. 2001. 'GFP imaging: methodology and application to investigate cellular compartmentation in plants', *J Exp Bot*, 52: 529-39.

Hanson, P. I., and S. W. Whiteheart. 2005. 'AAA+ proteins: have engine, will work', *Nat Rev Mol Cell Biol*, 6: 519-29.

Harper, J. F., G. Breton, and A. Harmon. 2004. 'Decoding Ca(2+) signals through plant protein kinases', *Annu Rev Plant Biol*, 55: 263-88.

Hashimoto, K., and J. Kudla. 2011. 'Calcium decoding mechanisms in plants', *Biochimie*, 93: 2054-9.

Hayashi, M., K. Nito, R. Takei-Hoshi, M. Yagi, M. Kondo, A. Suenaga, T. Yamaya, and M. Nishimura. 2002. 'Ped3p is a peroxisomal ATP-binding cassette transporter that might supply substrates for fatty acid beta-oxidation', *Plant Cell Physiol*, 43: 1-11.

Henderson, D. P., and S. M. Payne. 1994. 'Vibrio cholerae iron transport systems: roles of heme and siderophore iron transport in virulence and identification of a gene associated with multiple iron transport systems', *Infect Immun*, 62: 5120-5.

Henderson, M. J., M. Haber, A. Porro, M. A. Munoz, N. Iraci, C. Xue, J. Murray, C. L. Flemming, J. Smith, J. I. Fletcher, S. Gherardi, C. K. Kwek, A. J. Russell, E. Valli, W. B. London, A. B. Buxton, L. J. Ashton, A. C. Sartorelli, S. L. Cohn, M. Schwab, G. M. Marshall, G. Perini, and M. D. Norris. 2011. 'ABCC multidrug transporters in childhood neuroblastoma: clinical and biological effects independent of cytotoxic drug efflux', *J Natl Cancer Inst*, 103: 1236-51.

Henikoff, S., E. A. Greene, S. Pietrokovski, P. Bork, T. K. Attwood, and L. Hood. 1997. 'Gene families: the taxonomy of protein paralogs and chimeras', *Science*, 278: 609-14.

Hepler, P. K. 2005. 'Calcium: a central regulator of plant growth and development', *Plant Cell*, 17: 2142-55.

Higgins, C. F. 1992. 'ABC transporters: from microorganisms to man', *Annu Rev Cell Biol*, 8: 67-113.

———. 2001. 'ABC transporters: physiology, structure and mechanism--an overview', *Res Microbiol*, 152: 205-10.

Hjorth, E., K. Hadfi, S. Zauner, and U. G. Maier. 2005. 'Unique genetic compartmentalization of the SUF system in cryptophytes and characterization of a SufD mutant in Arabidopsis thaliana', *FEBS Lett*, 579: 1129-35.

Holland, I. B., and M. A. Blight. 1999. 'ABC-ATPases, adaptable energy generators fuelling transmembrane movement of a variety of molecules in organisms from bacteria to humans', *J Mol Biol*, 293: 381-99.

Hu, X. L., M. Y. Jiang, J. H. Zhang, A. Y. Zhang, F. Lin, and M. P. Tan. 2007. 'Calcium-calmodulin is required for abscisic acid-induced antioxidant defense and functions both upstream and downstream of H2O2 production in leaves of maize (Zea mays) plants', *New Phytologist*, 173: 27-38.

Hwang, J. U., W. Y. Song, D. Hong, D. Ko, Y. Yamaoka, S. Jang, S. Yim, E. Lee, D. Khare, K. Kim, M. Palmgren, H. S. Yoon, E.

Martinoia, and Y. Lee. 2016. 'Plant ABC Transporters Enable Many Unique Aspects of a Terrestrial Plant's Lifestyle', *Mol Plant*, 9: 338-55.

Igarashi, Y., K. F. Aoki, H. Mamitsuka, K. Kuma, and M. Kanehisa. 2004. 'The evolutionary repertoires of the eukaryotic-type ABC transporters in terms of the phylogeny of ATP-binding domains in eukaryotes and prokaryotes', *Molecular Biology and Evolution*, 21: 2149-60.

Jaquinod, M., F. Villiers, S. Kieffer-Jaquinod, V. Hugouvieux, C. Bruley, J. Garin, and J. Bourguignon. 2007. 'A proteomics dissection of Arabidopsis thaliana vacuoles isolated from cell culture', *Mol Cell Proteomics*, 6: 394-412.

Jefferson, R. A. 1987. 'Assaying Chimeric Genes in Plants: The GUS Gene Fusion System', *Plant Molecular Biology Reporter*, 5: 387-405.

Jefferson, R. A., T. A. Kavanagh, and M. W. Bevan. 1987. 'GUS fusions: beta-glucuronidase as a sensitive and versatile gene fusion marker in higher plants', *EMBO J*, 6: 3901-7.

Kang, B. G., X. Ye, L. D. Osburn, C. N. Stewart, Jr., and Z. M. Cheng. 2010. 'Transgenic hybrid aspen overexpressing the Atwbc19 gene encoding an ATP-binding cassette transporter confers resistance to four aminoglycoside antibiotics', *Plant Cell Rep*, 29: 643-50.

Kang, J., J. Park, H. Choi, B. Burla, T. Kretzschmar, Y. Lee, and E. Martinoia. 2011. 'Plant ABC Transporters', *Arabidopsis Book*, 9: e0153.

Katoh, H., N. Hagino, A. R. Grossman, and T. Ogawa. 2001. 'Genes essential to iron transport in the cyanobacterium Synechocystis sp. strain PCC 6803', *J Bacteriol*, 183: 2779-84.

Kellermann, O., and S. Szmelcman. 1974. 'Active transport of maltose in Escherichia coli K12. Involvement of a "periplasmic" maltose binding protein', *Eur J Biochem*, 47: 139-49.

Kiep, V., J. Vadassery, J. Lattke, J. P. Maass, W. Boland, E. Peiter, and A. Mithofer. 2015. 'Systemic cytosolic Ca(2+) elevation is activated upon wounding and herbivory in Arabidopsis', *New Phytologist*, 207: 996-1004.

Kloch, M., M. Milewski, E. Nurowska, B. Dworakowska, G. R. Cutting, and K. Dolowy. 2010. 'The H-loop in the second nucleotide-binding domain of the cystic fibrosis transmembrane conductance regulator is required for efficient chloride channel closing', *Cell Physiol Biochem*, 25: 169-80.

Kochian, L. V. 1995. 'Cellular Mechanisms of Aluminum Toxicity and Resistance in Plants', *Annual Review of Plant Physiology and Plant Molecular Biology*, 46: 237-60.

Kochian, L. V., O. A. Hoekenga, and M. A. Pineros. 2004. 'How do crop plants tolerate acid soils? - Mechanisms of aluminum tolerance and phosphorous efficiency', *Annual Review of Plant Biology*, 55: 459-93.

Kohler, D., D. Dobritzsch, W. Hoehenwarter, S. Helm, J. M. Steiner, and S. Baginsky. 2015. 'Identification of protein N-termini in Cyanophora paradoxa cyanelles: transit peptide composition and sequence determinants for precursor maturation', *Front Plant Sci*, 6: 559.

Kosova, K., P. Vitamvas, I. T. Prasil, and J. Renaut. 2011. 'Plant proteome changes under abiotic stress--contribution of proteomics studies to understanding plant stress response', *J Proteomics*, 74: 1301-22.

Kost, B., P. Spielhofer, and N. H. Chua. 1998. 'A GFP-mouse talin fusion protein labels plant actin filaments in vivo and visualizes the actin cytoskeleton in growing pollen tubes', *Plant J*, 16: 393-401.

Kovalchuk, A., and A. J. Driessen. 2010. 'Phylogenetic analysis of fungal ABC transporters', *BMC Genomics*, 11: 177.

Kretzschmar, T., B. Burla, Y. Lee, E. Martinoia, and R. Nagy. 2011. 'Functions of ABC transporters in plants', *Essays Biochem*, 50: 145-60.

Kunze, M., and J. Berger. 2015. 'The similarity between N-terminal targeting signals for protein import into different organelles and its evolutionary relevance', *Frontiers in Physiology*, 6.

Lane, T. S., C. S. Rempe, J. Davitt, M. E. Staton, Y. Peng, D. E. Soltis, M. Melkonian, M. Deyholos, J. H. Leebens-Mack, M. Chase, C. J. Rothfels, D. Stevenson, S. W. Graham, J. Yu, T. Liu, J. C. Pires, P. P. Edger, Y. Zhang, Y. Xie, Y. Zhu, E. Carpenter, G. K.

Wong, and C. N. Stewart, Jr. 2016. 'Diversity of ABC transporter genes across the plant kingdom and their potential utility in biotechnology', *BMC Biotechnol*, 16: 47.

Larsen, P. B., J. Cancel, M. Rounds, and V. Ochoa. 2007. 'Arabidopsis ALS1 encodes a root tip and stele localized half type ABC transporter required for root growth in an aluminum toxic environment', *Planta*, 225: 1447-58.

Larsen, P. B., M. J. Geisler, C. A. Jones, K. M. Williams, and J. D. Cancel. 2005. 'ALS3 encodes a phloem-localized ABC transporter-like protein that is required for aluminum tolerance in Arabidopsis', *Plant J*, 41: 353-63.

Laskowski, M., S. Biller, K. Stanley, T. Kajstura, and R. Prusty. 2006. 'Expression profiling of auxin-treated Arabidopsis roots: toward a molecular analysis of lateral root emergence', *Plant Cell Physiol*, 47: 788-92.

Le Hir, R., C. Sorin, D. Chakraborti, T. Moritz, H. Schaller, F. Tellier, S. Robert, H. Morin, L. Bako, and C. Bellini. 2013. 'ABCG9, ABCG11 and ABCG14 ABC transporters are required for vascular development in Arabidopsis', *Plant J*, 76: 811-24.

Lee, D. W., J. K. Kim, S. Lee, S. Choi, S. Kim, and I. Hwang. 2008. 'Arabidopsis nuclear-encoded plastid transit peptides contain multiple sequence subgroups with distinctive chloroplast-targeting sequence motifs', *Plant Cell*, 20: 1603-22.

Lee, D. W., S. Woo, K. R. Geem, and I. Hwang. 2015. 'Sequence Motifs in Transit Peptides Act as Independent Functional Units and Can Be Transferred to New Sequence Contexts', *Plant Physiol*, 169: 471-84.

Lewis, H. A., S. G. Buchanan, S. K. Burley, K. Conners, M. Dickey, M. Dorwart, R. Fowler, X. Gao, W. B. Guggino, W. A. Hendrickson, J. F. Hunt, M. C. Kearins, D. Lorimer, P. C. Maloney, K. W. Post, K. R. Rajashankar, M. E. Rutter, J. M. Sauder, S. Shriver, P. H. Thibodeau, P. J. Thomas, M. Zhang, X. Zhao, and S. Emtage. 2004. 'Structure of nucleotide-binding domain 1 of the cystic fibrosis transmembrane conductance regulator', *EMBO J*, 23: 282-93.

Li, G. J., W. F. Xu, H. J. Kronzucker, and W. M. Shi. 2015. 'Ethylene is critical to the maintenance of primary root growth and Fe homeostasis under Fe stress in Arabidopsis', *Journal of Experimental Botany*, 66: 2041-54.

Li, J., J. Mu, J. Bai, F. Fu, T. Zou, F. An, J. Zhang, H. Jing, Q. Wang, Z. Li, S. Yang, and J. Zuo. 2013. 'Paraquat Resistant1, a Golgi-localized putative transporter protein, is involved in intracellular transport of paraquat', *Plant Physiol*, 162: 470-83.

Linton, K. J. 2007. 'Structure and function of ABC transporters', *Physiology (Bethesda)*, 22: 122-30.

Lopez-Millan, A. F., D. Duy, and K. Philippar. 2016. 'Chloroplast Iron Transport Proteins - Function and Impact on Plant Physiology', *Front Plant Sci*, 7: 178.

Lu, B., C. Xu, K. Awai, A. D. Jones, and C. Benning. 2007. 'A small ATPase protein of Arabidopsis, TGD3, involved in chloroplast lipid import', *J Biol Chem*, 282: 35945-53.

Magalhaes, J. V., J. Liu, C. T. Guimaraes, U. G. Lana, V. M. Alves, Y. H. Wang, R. E. Schaffert, O. A. Hoekenga, M. A. Pineros, J. E. Shaff, P. E. Klein, N. P. Carneiro, C. M. Coelho, H. N. Trick, and L. V. Kochian. 2007. 'A gene in the multidrug and toxic compound extrusion (MATE) family confers aluminum tolerance in sorghum', *Nat Genet*, 39: 1156-61.

Majoul, T., E. Bancel, E. Triboi, J. Ben Hamida, and G. Branlard. 2004. 'Proteomic analysis of the effect of heat stress on hexaploid wheat grain: characterization of heat-responsive proteins from non-prolamins fraction', *Proteomics*, 4: 505-13.

McFadden, G. I. 1999. 'Endosymbiosis and evolution of the plant cell', *Curr Opin Plant Biol*, 2: 513-9.

Meyer, S., A. De Angeli, A. R. Fernie, and E. Martinoia. 2010. 'Intra- and extra-cellular excretion of carboxylates', *Trends Plant Sci*, 15: 40-7.

Mitra, S. K., J. A. Gantt, J. F. Ruby, S. D. Clouse, and M. B. Goshe. 2007. 'Membrane proteomic analysis of Arabidopsis thaliana using alternative solubilization techniques', *J Proteome Res*, 6: 1933-50.

Mogami, J., Y. Fujita, T. Yoshida, Y. Tsukiori, H. Nakagami, Y. Nomura, T. Fujiwara, S. Nishida, S. Yanagisawa, T. Ishida, F. Takahashi, K. Morimoto, S. Kidokoro, J. Mizoi, K. Shinozaki, and K. Yamaguchi-Shinozaki. 2015. 'Two distinct families of protein kinases are required for plant growth under high external Mg2+ concentrations in Arabidopsis', *Plant Physiol*, 167: 1039-57.

Moller, S. G., T. Kunkel, and N. H. Chua. 2001. 'A plastidic ABC protein involved in intercompartmental communication of light signaling', *Genes Dev*, 15: 90-103.

Moussatova, A., C. Kandt, M. L. O'Mara, and D. P. Tieleman. 2008. 'ATP-binding cassette transporters in Escherichia coli', *Biochim Biophys Acta*, 1778: 1757-71.

Mutch, D. M., P. Anderle, M. Fiaux, R. Mansourian, K. Vidal, W. Wahli, G. Williamson, and M. A. Roberts. 2004. 'Regional variations in ABC transporter expression along the mouse intestinal tract', *Physiol Genomics*, 17: 11-20.

Mwenda, C. M., A. Matsuki, K. Nishimura, T. Koeduka, and K. Matsui. 2015. 'Spatial expression of the Arabidopsis hydroperoxide lyase gene is controlled differently from that of the allene oxide synthase gene', *Journal of Plant Interactions*, 10: 1-10.

Nagane, T., A. Tanaka, and R. Tanaka. 2010. 'Involvement of AtNAP1 in the regulation of chlorophyll degradation in Arabidopsis thaliana', *Planta*, 231: 939-49.

Nagy, R., H. Grob, B. Weder, P. Green, M. Klein, A. Frelet-Barrand, J. K. Schjoerring, C. Brearley, and E. Martinoia. 2009. 'The Arabidopsis ATP-binding cassette protein AtMRP5/AtABCC5 is a high affinity inositol hexakisphosphate transporter involved in guard cell signaling and phytate storage', *J Biol Chem*, 284: 33614-22.

Pan, I. C., H. H. Tsai, Y. T. Cheng, T. N. Wen, T. J. Buckhout, and W. Schmidt. 2015. 'Post-Transcriptional Coordination of the Arabidopsis Iron Deficiency Response is Partially Dependent on the E3 Ligases RING DOMAIN LIGASE1 (RGLG1) and RING DOMAIN LIGASE2 (RGLG2)', *Mol Cell Proteomics*, 14: 2733-52.

Panikashvili, D., S. Savaldi-Goldstein, T. Mandel, T. Yifhar, R. B. Franke, R. Hofer, L. Schreiber, J. Chory, and A. Aharoni. 2007. 'The Arabidopsis DESPERADO/AtWBC11 transporter is required for cutin and wax secretion', *Plant Physiol*, 145: 1345-60.

Peelman, F., C. Labeur, B. Vanloo, S. Roosbeek, C. Devaud, N. Duverger, P. Denefle, M. Rosier, J. Vandekerckhove, and M. Rosseneu. 2003. 'Characterization of the ABCA transporter subfamily: identification of prokaryotic and eukaryotic members, phylogeny and topology', *J Mol Biol*, 325: 259-74.

Pisarev, A. V., M. A. Skabkin, V. P. Pisareva, O. V. Skabkina, A. M. Rakotondrafara, M. W. Hentze, C. U. Hellen, and T. V. Pestova. 2010. 'The role of ABCE1 in eukaryotic posttermination ribosomal recycling', *Mol Cell*, 37: 196-210.

Poolman, B., J. J. Spitzer, and J. M. Wood. 2004. 'Bacterial osmosensing: roles of membrane structure and electrostatics in lipid-protein and protein-protein interactions', *Biochim Biophys Acta*, 1666: 88-104.

Quazi, F., S. Lenevich, and R. S. Molday. 2012. 'ABCA4 is an N-retinylidene-phosphatidylethanolamine and phosphatidylethanolamine importer', *Nature Communications*, 3.

Rayapuram, N., J. Hagenmuller, J. M. Grienenberger, P. Giege, and G. Bonnard. 2007. 'AtCCMA interacts with AtCcmB to form a novel mitochondrial ABC transporter involved in cytochrome c maturation in Arabidopsis', *J Biol Chem*, 282: 21015-23.

Rea, P. A. 2007. 'Plant ATP-binding cassette transporters', *Annu Rev Plant Biol*, 58: 347-75.

Rees, D. C., E. Johnson, and O. Lewinson. 2009. 'ABC transporters: the power to change', *Nat Rev Mol Cell Biol*, 10: 218-27.

Reid, J. B., and J. J. Ross. 2011. 'Regulation of tissue repair in plants', *Proc Natl Acad Sci U S A*, 108: 17241-2.

Reits, E. A., J. C. Vos, M. Gromme, and J. Neefjes. 2000. 'The major substrates for TAP in vivo are derived from newly synthesized proteins', *Nature*, 404: 774-8.

Robinson, C., and R. J. Ellis. 1984. 'Transport of proteins into chloroplasts. Partial purification of a chloroplast protease

involved in the processing of important precursor polypeptides', *Eur J Biochem*, 142: 337-42.

Roston, R. L., J. Gao, M. W. Murcha, J. Whelan, and C. Benning. 2012. 'TGD1, -2, and -3 proteins involved in lipid trafficking form ATP-binding cassette (ABC) transporter with multiple substrate-binding proteins', *J Biol Chem*, 287: 21406-15.

Ryan, P. R., S. D. Tyerman, T. Sasaki, T. Furuichi, Y. Yamamoto, W. H. Zhang, and E. Delhaize. 2011. 'The identification of aluminium-resistance genes provides opportunities for enhancing crop production on acid soils', *J Exp Bot*, 62: 9-20.

Saier, M. H., Jr. 2000. 'A functional-phylogenetic classification system for transmembrane solute transporters', *Microbiol Mol Biol Rev*, 64: 354-411.

Sánchez-Fernández, R., T. G. Davies, J. O. Coleman, and P. A. Rea. 2001. 'The Arabidopsis thaliana ABC protein superfamily, a complete inventory', *J Biol Chem*, 276: 30231-44.

Sarpola, A. 2007. 'The Hydrolysis of Aluminium, a Mass Spectrometric Study', *University of Oulu, Finland*, Acta Univ. Oul., C 279: 19-22.

Sato, H., J. Mizoi, H. Tanaka, K. Maruyama, F. Qin, Y. Osakabe, K. Morimoto, T. Ohori, K. Kusakabe, M. Nagata, K. Shinozaki, and K. Yamaguchi-Shinozaki. 2014. 'Arabidopsis DPB3-1, a DREB2A interactor, specifically enhances heat stress-induced gene expression by forming a heat stress-specific transcriptional complex with NF-Y subunits', *Plant Cell*, 26: 4954-73.

Saurin, W., M. Hofnung, and E. Dassa. 1999. 'Getting in or out: early segregation between importers and exporters in the evolution of ATP-binding cassette (ABC) transporters', *J Mol Evol*, 48: 22-41.

Schein, A. I., J. C. Kissinger, and L. H. Ungar. 2001. 'Chloroplast transit peptide prediction: a peek inside the black box', *Nucleic Acids Res*, 29: E82.

Schneider, E., and S. Hunke. 1998. 'ATP-binding-cassette (ABC) transport systems: functional and structural aspects of the ATP-hydrolyzing subunits/domains', *FEMS Microbiol Rev*, 22: 1-20.

Scholz, C., D. Parcej, C. S. Ejsing, H. Robenek, I. L. Urbatsch, and R. Tampe. 2011. 'Specific lipids modulate the transporter associated with antigen processing (TAP)', *J Biol Chem*, 286: 13346-56.

Schroeder, J. I., E. Delhaize, W. B. Frommer, M. L. Guerinot, M. J. Harrison, L. Herrera-Estrella, T. Horie, L. V. Kochian, R. Munns, N. K. Nishizawa, Y. F. Tsay, and D. Sanders. 2013. 'Using membrane transporters to improve crops for sustainable food production', *Nature*, 497: 60-66.

Shimoni-Shor, E., M. Hassidim, N. Yuval-Naeh, and N. Keren. 2010. 'Disruption of Nap14, a plastid-localized non-intrinsic ABC protein in Arabidopsis thaliana results in the over-accumulation of transition metals and in aberrant chloroplast structures', *Plant Cell and Environment*, 33: 1029-38.

Shitan, N., I. Bazin, K. Dan, K. Obata, K. Kigawa, K. Ueda, F. Sato, C. Forestier, and K. Yazaki. 2003. 'Involvement of CjMDR1, a plant multidrug-resistance-type ATP-binding cassette protein, in alkaloid transport in Coptis japonica', *Proc Natl Acad Sci U S A*, 100: 751-6.

Simoes, C. C., J. O. Melo, J. V. Magalhaes, and C. T. Guimaraes. 2012. 'Genetic and molecular mechanisms of aluminum tolerance in plants', *Genet Mol Res*, 11: 1949-57.

Singh, B. R., S. K. Gupta, H. Azaizeh, S. Shilev, D. Sudre, W. Y. Song, E. Martinoia, and M. Mench. 2011. 'Safety of food crops on land contaminated with trace elements', *J Sci Food Agric*, 91: 1349-66.

Singh, P., D. Kaloudas, and C. A. Raines. 2008. 'Expression analysis of the Arabidopsis CP12 gene family suggests novel roles for these proteins in roots and floral tissues', *J Exp Bot*, 59: 3975-85.

Singh, S., P. Parihar, R. Singh, V. P. Singh, and S. M. Prasad. 2015. 'Heavy Metal Tolerance in Plants: Role of Transcriptomics, Proteomics, Metabolomics, and Ionomics', *Front Plant Sci*, 6: 1143.

Soll, J., and R. Tien. 1998. 'Protein translocation into and across the chloroplastic envelope membranes', *Plant Mol Biol*, 38: 191-207.

Song, W. Y., J. Park, D. G. Mendoza-Cozatl, M. Suter-Grotemeyer, D. Shim, S. Hortensteiner, M. Geisler, B. Weder, P. A. Rea, D.

Rentsch, J. I. Schroeder, Y. Lee, and E. Martinoia. 2010. 'Arsenic tolerance in Arabidopsis is mediated by two ABCC-type phytochelatin transporters', *Proc Natl Acad Sci U S A*, 107: 21187-92.

Steiner, J. M., and W. Loffelhardt. 2005. 'Protein translocation into and within cyanelles (review)', *Mol Membr Biol*, 22: 123-32.

Steinhorst, L., and J. Kudla. 2013. 'Calcium and reactive oxygen species rule the waves of signaling', *Plant Physiol*, 163: 471-85.

Sugiyama, A., N. Shitan, S. Sato, Y. Nakamura, S. Tabata, and K. Yazaki. 2006. 'Genome-wide analysis of ATP-binding cassette (ABC) proteins in a model legume plant, Lotus japonicus: comparison with Arabidopsis ABC protein family', *DNA Res*, 13: 205-28.

Suzuki, N., E. Bassil, J. S. Hamilton, M. A. Inupakutika, S. I. Zandalinas, D. Tripathy, Y. T. Luo, E. Dion, G. Fukui, A. Kumazaki, R. Nakano, R. M. Rivero, G. F. Verbeck, R. K. Azad, E. Blumwald, and R. Mittler. 2016. 'ABA Is Required for Plant Acclimation to a Combination of Salt and Heat Stress', *Plos One*, 11.

Szmelcman, S., M. Schwartz, T. J. Silhavy, and W. Boos. 1976. 'Maltose transport in Escherichia coli K12. A comparison of transport kinetics in wild-type and lambda-resistant mutants as measured by fluorescence quenching', *Eur J Biochem*, 65: 13-9.

Taylor, R. G., D. C. Walker, and R. R. McInnes. 1993. 'E. coli host strains significantly affect the quality of small scale plasmid DNA preparations used for sequencing', *Nucleic Acids Res*, 21: 1677-8.

ter Beek, J., A. Guskov, and D. J. Slotboom. 2014. 'Structural diversity of ABC transporters', *J Gen Physiol*, 143: 419-35.

Theodoulou, F. L., K. Job, S. P. Slocombe, S. Footitt, M. Holdsworth, A. Baker, T. R. Larson, and I. A. Graham. 2005. 'Jasmonic acid levels are reduced in COMATOSE ATP-binding cassette transporter mutants. Implications for transport of jasmonate precursors into peroxisomes', *Plant Physiol*, 137: 835-40.

van Veen, H. W. . 2016. 'Bacterial ABC Multidrug Exporters: From Shared Proteins Motifs and Features to Diversity in Molecular

Mechanisms.' in A. M. George (ed.), *ABC Transporters - 40 years on* (Springer International Publishing Switzerland 2016).

Vardar, F., and M. Ünal. 2007. 'Aluminium toxicity and resistance in higher plants', *Advances in Molecular Biology*: 1-12.

Vasiliou, V., K. Vasiliou, and D. W. Nebert. 2009. 'Human ATP-binding cassette (ABC) transporter family', *Hum Genomics*, 3: 281-90.

Verbruggen, N., C. Hermans, and H. Schat. 2009. 'Mechanisms to cope with arsenic or cadmium excess in plants', *Curr Opin Plant Biol*, 12: 364-72.

Verrier, P. J., D. Bird, B. Burla, E. Dassa, C. Forestier, M. Geisler, M. Klein, U. Kolukisaoglu, Y. Lee, E. Martinoia, A. Murphy, P. A. Rea, L. Samuels, B. Schulz, E. J. Spalding, K. Yazaki, and F. L. Theodoulou. 2008. 'Plant ABC proteins--a unified nomenclature and updated inventory', *Trends Plant Sci*, 13: 151-9.

Vranova, E., D. Inze, and F. Van Breusegem. 2002. 'Signal transduction during oxidative stress', *J Exp Bot*, 53: 1227-36.

Walker, J. E., M. Saraste, M. J. Runswick, and N. J. Gay. 1982. 'Distantly related sequences in the alpha- and beta-subunits of ATP synthase, myosin, kinases and other ATP-requiring enzymes and a common nucleotide binding fold', *EMBO J*, 1: 945-51.

Whalley, H. J., A. W. Sargeant, J. F. Steele, T. Lacoere, R. Lamb, N. J. Saunders, H. Knight, and M. R. Knight. 2011. 'Transcriptomic analysis reveals calcium regulation of specific promoter motifs in Arabidopsis', *Plant Cell*, 23: 4079-95.

Wilkens, S. 2015. 'Structure and mechanism of ABC transporters', *F1000Prime Rep*, 7: 14.

Woehlecke, H., A. Pohl, N. Alder-Baerens, H. Lage, and A. Herrmann. 2003. 'Enhanced exposure of phosphatidylserine in human gastric carcinoma cells overexpressing the half-size ABC transporter BCRP (ABCG2)', *Biochem J*, 376: 489-95.

Xiong, J., J. Feng, D. Yuan, J. Zhou, and W. Miao. 2015. 'Tracing the structural evolution of eukaryotic ATP binding cassette transporter superfamily', *Sci Rep*, 5: 16724.

Xu, X. M., S. Adams, N. H. Chua, and S. G. Moller. 2005. 'AtNAP1 represents an atypical SufB protein in Arabidopsis plastids', *J Biol Chem*, 280: 6648-54.

Xu, X. M., and S. G. Moller. 2004. 'AtNAP7 is a plastidic SufC-like ATP-binding cassette/ATPase essential for Arabidopsis embryogenesis', *Proceedings of the National Academy of Sciences of the United States of America*, 101: 9143-48.

Zhang, F., W. Zhang, L. Liu, C. L. Fisher, D. Hui, S. Childs, K. Dorovini-Zis, and V. Ling. 2000. 'Characterization of ABCB9, an ATP binding cassette protein associated with lysosomes', *J Biol Chem*, 275: 23287-94.

Zhang, H. Y., X. Zhao, J. G. Li, H. Q. Cai, X. W. Deng, and L. Li. 2014. 'MicroRNA408 Is Critical for the HY5-SPL7 Gene Network That Mediates the Coordinated Response to Light and Copper', *Plant Cell*, 26: 4933-53.

Zhang, M., G. Li, W. Huang, T. Bi, G. Chen, Z. Tang, W. Su, and W. Sun. 2010. 'Proteomic study of Carissa spinarum in response to combined heat and drought stress', *Proteomics*, 10: 3117-29.

Zhao, J., D. Huhman, G. Shadle, X. Z. He, L. W. Sumner, Y. Tang, and R. A. Dixon. 2011. 'MATE2 mediates vacuolar sequestration of flavonoid glycosides and glycoside malonates in Medicago truncatula', *Plant Cell*, 23: 1536-55.

Zhao, Y. 2010. 'Auxin biosynthesis and its role in plant development', *Annu Rev Plant Biol*, 61: 49-64.

Zhu, X. F., G. J. Lei, Z. W. Wang, Y. Z. Shi, J. Braam, G. X. Li, and S. J. Zheng. 2013. 'Coordination between Apoplastic and Symplastic Detoxification Confers Plant Aluminum Resistance', *Plant Physiology*, 162: 1947-55.

Zybailov, B., H. Rutschow, G. Friso, A. Rudella, O. Emanuelsson, Q. Sun, and K. J. van Wijk. 2008. 'Sorting signals, N-terminal modifications and abundance of the chloroplast proteome', *Plos One*, 3: e1994.

# Appendices

Intentionally left blank

## *Appendix 1 – Article submitted to Journal of Plant Research*

Title: "Characterization of the plastid localized ABC protein TAP1 in Arabidopsis".

**Journal of Plant Research**

Draft Manuscript for Review

**Characterization of the plastid localized ABC protein TAP1 in Arabidopsis**

| | |
|---|---|
| Journal: | *Journal of Plant Research* |
| Manuscript ID | Draft |
| Manuscript Type: | Regular Paper |
| Date Submitted by the Author: | n/a |
| Complete List of Authors: | Johansen Hempel, Jan; Universitetet i Stavanger Institutt for matematikk og naturvitskap<br>Maple-Grodem, Jodi; Stavanger University Hospital, Norwegian Center for Movement Disorders<br>Moller, Simon; St John´s University, Biology |
| Keywords: | ABC proteins, Arabidopsis, TAP1, Stress, Wounding |
| | |

**Journal of Plant Research**

**Cover page**

Corresponding author:

Simon Geir Møller

Department of Biological Sciences

St John's University

New York 11439

USA

Phone: 718 990 1697

E-mail: Mollers@stjohns.edu

Membership of the Botanical Society of Japan: No

Subject area: Physiology/Biochemistry/Molecular and Cellular biology

Number of Tables: 3

Number of black and white figures: 3

Number of color figures: 3

**Journal of Plant Research**

# Characterization of the plastid localized ABC protein TAP1 in Arabidopsis

Jan Johansen Hempel,[a,b] Jodi Maple-Grødem,[b,c] and Simon Geir Møller[a,b,c]

[a]Department of Biological Sciences, St John's University, New York, USA

[b]Centre for Organelle Research, University of Stavanger, Stavanger, Norway

[c]Norwegian Centre for Movement Disorders, Stavanger University Hospital, Stavanger, Norway

**Journal of Plant Research**

**Abstract**

The *Arabidopsis* genome contains two TAP-like genes, *AtTAP1* and *AtTAP2*, which belong to the ABC transporter superfamily. AtTAP2/ALS1 has been shown to be important for aluminium metabolism and tolerance however, little is known about the function of AtTAP1. In this study, we investigate the expression dynamics of *AtTAP1*, the intracellular localization patterns of AtTAP1, and possible functional roles of AtTAP1 in response to a variety of biotic and abiotic stress factors. We show through Yellow Fluorescent Protein (YFP) translational fusion approaches that AtTAP1 is localized to chloroplasts, with a clear enrichment at the chloroplast membrane. Using semi-quantitative RT-PCR in wild-type plants and an *AtTAP1* promoter-beta-glucuronidase (GUS) construct in transgenic plants, we show that *AtTAP1* shows elevated expression in aerial tissues, at lateral root initiation sites and in siliques. We further show that *AtTAP1* expression is increased in response to $Ca^{2+}$ exposure, and to a lesser extent by $Al^{3+}$, which is different from *AtTAP2*. Functional analysis, employing an *AtTAP1* loss-of-function *Arabidopsis thaliana* transgenic line, revealed no phenotypic differences as compared to wild-type plants, in response to $Al^{3+}$, $Fe^{3+}$, $Ca^{2+}$, $Mg^{2+}$, $Cu^{2+}$, methyl viologen (MV), $H_2O_2$, auxin and heat exposure, suggesting that AtTAP1 and AtTAP2 harbour very different functions. Interestingly, *AtTAP1* shows elevated expression in wounded leaf tissue indicating a possible involvement in wounding responses.



***Keywords:*** ABC proteins, *Arabidopsis*, TAP1, wounding, stress

**Journal of Plant Research**

**Introduction**

The half-size TAP (transporter associated with antigen processing) proteins belong to the ABC transporter superfamily and the ABCB subfamily, which is also characterized as the multidrug resistance (MDR) family. The ABC proteins are found throughout all genera of the three kingdoms of life (Higgins 2001). ABC proteins share a highly conserved ATPase domain, often referred to as the ATP-binding cassette (ABC) that provides energy for a large number of fundamental biological processes (Holland and Blight 1999; Schneider and Hunke 1998). Since their original discovery and characterization in prokaryotes (Ames and Lever 1970; Szmelcman et al. 1976), ABC proteins have received much attention, mainly because they are involved in several human diseases (Dean et al. 2001). The continued interest is also fuelled by the fact that multidrug resistant cancer cell lines and tumours show overexpression of certain classes of ABC proteins, and the observed chemotherapeutic resistance is due to the presence of elevated ABC proteins levels (Henderson et al. 2011).

ABC proteins play important roles in prokaryotes, transporting essential compounds such as sugars, vitamins and metal ions into the cell (Davidson et al. 2008; Fischer et al. 2010). In eukaryotes ABC proteins also play many essential roles, including the transport of molecules out of cells and into membrane bound organelles (Scholz et al. 2011). Genetic variation in genes that encode ABC proteins can therefore cause or contribute to a wide variety of human disorders, including cystic fibrosis, neurological diseases, retinal degeneration, cholesterol and bile defects, and anaemia (Dizdarevic and Peters 2011).

The ABC transporters represent one of the largest known protein super families, and contain 130 or more members in both Arabidopsis and *Oryza sativa* (Hwang et al. 2016) that are associated with a myriad of biological processes. These include heavy metal and metalloid detoxification (Larsen et al. 2005; Li et al. 1997; Ryan et al. 2011; Zhao et al. 2010), transport of glucosylated compounds and antibiotics across membranes (Dean and Mills 2004; Kang et al. 2010; Zhao et al. 2011), in polar auxin transport, lipid catabolism, xenobiotic detoxification, disease resistance and stomatal function (Rea 2007). Although, functional predictions of plant ABC transporters based on subfamily

classifications have yielded some success, a strict structure-function relationship is often found to be obscure (Rea 2007).

The TAP proteins belong to one of five subfamilies of the half-molecule ABC transporters (Kang et al. 2011; Sánchez-Fernández et al. 2001). Mammalian TAP proteins participate in peptide secretion and translocation from the cytosol to the endoplasmic reticulum lumen, ultimately associated with the presentation of major histocompatibility complex class I (MHC1) molecules on the surface of the cell. TAP1 and TAP2 form a heterodimer, and mutations in either *TAP* gene can prevent antigen presentation by MHC class I molecules (Abele and Tampe 2004; Reits et al. 2000). The Arabidopsis genome contains two *TAP*-like genes that encode half-molecule proteins (Garcia et al. 2004; Sánchez-Fernández et al. 2001). Proteomic analysis has indicated that AtTAP1 may be localized to chloroplasts (Ferro et al. 2010; Kang et al. 2011), while AtTAP2 (ALS1; At5g39040) is detected in the vacuolar membrane (Jaquinod et al. 2007).

The precise functions of the two TAP proteins of Arabidopsis are unknown although it has been postulated that they may have similarities to their mammalian counterparts (Rea 2007). It has been demonstrated that AtTAP2 is associated with in root growth in response to aluminium exposure (Gabrielson et al. 2006; Larsen et al. 2007; Simoes et al. 2012). To reveal possible functional similarities between AtTAP1 and AtTAP2 in Arabidopsis, and to further understand the role of TAP1 in plants, we have performed gene expression, localization, and functional analysis, which have revealed that AtTAP1 and AtTAP2 in Arabidopsis are highly divergent.

**Journal of Plant Research**

**Materials and methods**

*Plants and growth conditions*

*Arabidopsis thaliana* ecotype Columbia was used for all experiments. Wild-type, *attap1* insertion lines (SAIL_8_B04) and transgenic plants were propagated in an identical manner unless otherwise stated. Surface-sterilised seeds were sown on MS medium (Murashige and Skoog 1962), and placed at 4°C in darkness for 2–4 days, followed by germination under continuous white light at 22°C. Seedlings were then transferred to 12-h light/12-h dark cycles at 22 °C, or transferred to soil and grown under standard greenhouse conditions. Transgenic Arabidopsis plants were generated using the Agrobacterium-mediated floral dip method (Clough and Bent 1998), and primary transformants were selected on 15 $\mu$g ml$^{-1}$dl-phosphinotricin (BASTA) (Melford Laboratories, Ipswich, UK) and transplanted onto fresh MS medium or soil.

For stress treatments, plants were grown on MS media (with or without 1 % sucrose) or media with 1 % sucrose containing 0.5 mM or 2.0 mM $AlCl_3$, $FeCl_3$, $CaCl_2$ or $MgCl_2$, 0.1 mM or 10 µM methyl viologen (MV), or 0.1mM or 10 µM $H_2O_2$, and grown under standard conditions, or heat treated in darkness at 37°C. All dishes were inspected every fifth day for 6 weeks, and phenotypical differences noted. For root measurements seedlings were grown in a vertical orientation in square dishes, on media including 1% sucrose and 0.5 mM or 2.0 mM $AlCl_3$, $FeCl_3$, $CaCl_2$ or $MgCl_2$. Plants were inspected and photographed after 17 days, main root length measured and values expressed in mm as the mean ± SE (n=3).

*Mutant Analysis*

Homozygous insert lines of the SAIL line SAIL_8_B04 (Stock: CS800375) were identified by PCR of genomic DNA extracted from individual plants using the primers SAIL_8_B04-L, SAIL_8_B04-R, SAIL_409_C10-L and LB1 (Table 1). The position of the T-DNA insert in the genome was determined by PCR amplifying a fragment of genomic DNA spanning the T-DNA insertion border using primers LB3 and SAIL_8_B04-L (Table 1). The fragment was cloned into pJET vector (Fermentas Life Sciences) and subject to sequencing (GENEWIZ Inc., NJ, US).

**Journal of Plant Research**

*Bioinformatics methods*

Protein sequences were obtained from ncbi.nlm.nih.gov, and aligned with BioEdit v. 7.2.5.0 (Hall 2011). Percentage identity and similarity of proteins were determined using the EMBOSS Needle pairwise sequence alignment tool (http:www.ebi.ac.uk/Tools/psa/emboss_needle), and the prediction of chloroplast transit peptides was performed using the ChloroP 1.1 Predicting Server (Emanuelsson et al. 1999).

*Cloning and Vector Construction*

Total RNA was isolated using SurePrep™ Plant/Fungi Total RNA Purification Kit, and first strand cDNA were made using the RevertAid™ First Strand cDNA Synthesis Kit (ThermoFisher Scientific). *AtTAP1* was amplified using the primers 1g70610-KpnI-L and 1g70610-KpnI-R (Table 1), and cloned into the pPCR-Script vector (Stratagene, CA, US). *AtTAP1* was subsequently cloned into the *Kpn*I site of pWEN18 (containing YFP under the control of the 35S promoter) to generate pWEN18/TAP1. The promoter region of *AtTAP1*, the 701 bp sequence directly upstream of the start codon, was amplified with primers TAP1-Promoter-L and TAP1-Promoter-R (Table 1), and cloned into *Asc*I and *Nco*I of pBADG upstream of GFP-GUS to generate PromoterTAP1-pBADG. PromoterTAP1-pBADG was subsequently used to generate stable transgenic Arabidopsis plants for GUS expression analysis. All plasmids were sequenced (Genewiz Inc., NJ, US).

*Semi quantitative RT-PCR*

*AtTAP1* transcript was quantified by semi quantitative RT-PCR, using 2.0 µl of cDNA, and the primers SAIL_409_C10-L and TAP1-R, and Actin Forward and Reverse (Table 1). RT-PCR images were acquired by VisiDoc-It™ Imaging System (UVP, Cambridge, UK), and densitometry was performed with ImageJ software and relative band intensity normalized to Actin set to 1.0.

**Journal of Plant Research**

*Subcellular Localisation Analysis*

For localisation experiments tobacco leaves were bombarded (Kost et al. 1998) with pWEN18/TAP1, incubated in darkness for 24 hrs at 21°C, and YFP fluorescence and autofluorescence detected using a Nikon A1R confocal laser scanning microscope and NIS-Elements software. For all samples the same acquisition settings were employed, and signals of similar intensity compared. Figure montages were compiled in Photoshop.

*GUS Expression and Analysis*

Seeds of WT plants transformed with pBADG/promoterTAP1 were grown under standard conditions. Histochemical localization of GUS activity was achieved as described by (Jefferson 1987). Briefly, flowers, leaves and roots from individual plants, or leaves torn with a needle were inspected by microscopy.

**Journal of Plant Research**

**Results**

*Identification and Localization of AtTAP1*

In Arabidopsis the *AtTAP1* (At1g70610) cDNA encodes a 701 amino acid protein. To gain insight into the evolutionary conservation of AtTAP1 we performed an amino acid sequence alignment of AtTAP1 with TAP1 homolog proteins from five model organisms: *T. aestivum*, *H. sapiens*, *D. rerio*, *D. melanogaster*, and *S. cerevisiae* (Fig. 1). Common to the ABC superfamily are four functional motifs: the Walker A motif, the Signature motif (ABC transporter signature motif), the Walker B motif, and the H-loop motif (Rea 2007; Sánchez-Fernández et al. 2001). Each motif is highly conserved in the TAP1 proteins, and are situated near the C-terminal of the proteins (Fig. 1).

The Walker A and Walker B motifs are known to have highly conserved three-dimensional structures. The Walker A motif is comprised of eight amino acids, and has the pattern G-4x-GK-T/S, where G, K, T and S denote glycine, lysine, threonine, and serine respectively, and x denotes any amino acid (Rea 2007; Walker et al. 1982), whilst the Walker B motif consensus sequence is reported to be hhhhDE (Hanson and Whiteheart 2005), where D and E denotes aspartic acid and glutamate residues respectively, and h denotes a hydrophobic amino acid. Analysis of the Walker A and B motifs in all TAP1 proteins reveals that consensus sequences are perfectly conserved (Fig. 1). The Walker B-site is immediately preceded by a highly conserved Signature motif that is unique to the ABC transport family and has proven to be a valuable tool in identifying putative new members of the family. The Signature motif contains a ten amino acid consensus sequence ([LIVMFY]S[SG]Gx3[RKA][LIVMYA]x[LIVFM][AG]), commonly denoted LSGGQ, but several exceptions have been reported (Kang et al. 2011; Rea 2007; Wilkens 2015). The short consensus sequence of the Signature motif is perfectly conserved in all the TAP proteins. Finally, the H motif or switch region contains a highly conserved histidine residue that is important in the interaction of the ABC domain with ATP (Kloch et al. 2010; Lewis et al. 2004; Schneider and Hunke 1998), and is found in all TAP1 proteins analyzed (Fig. 1).

Notwithstanding the perfect conservation of the functional motifs, analysis of the TAP1 protein sequences shows that overall the likeness is more prominent between AtTAP1 and the higher plant

**Journal of Plant Research**

proteins, than between AtTAP1 and the non-plant proteins (Fig. 1 and Table 2). In a more extensive overview we have found that AtTAP1 is 60-69% identical, and 73-81% similar to the TAP1 proteins of higher plants, whereas AtTAP1 is only 36-50% identical to lower plant proteins, and 29–32% identical to non-plant TAP1 proteins (Table 2). These data reveal that the higher plant TAP1 proteins are highly conserved, indicating that they could have the same function in all species. Additionally, it could support the theory that ABC transporter genes have undergone diversification events during evolution before plants adapted to the land environment (Hwang et al. 2016).

*AtTAP1 localizes to chloroplasts*

Using the ChloroP 1.1 Prediction Server, AtTAP1 was predicted to harbor a 59 amino acid chloroplast transit peptide. To confirm this prediction, we cloned the *AtTAP1* cDNA as a translational fusion to the N-terminus of *YFP*, followed by transient transfection into tobacco leaves using particle bombardment. Using fluorescent microscopy, we found that AtTAP1-YFP was exclusively localized to chloroplasts in tobacco leaves (Fig. 2). The AtTAP1-YFP signal was not uniform but punctate in nature (Fig 2a, b) and further analysis of serial sections through individual chloroplasts showed that AtTAP1 localization was enriched at the chloroplast membrane (Fig. 2c, d). The enrichment of AtTAP1 at the chloroplast membrane suggests that the protein maybe involved in transport mechanisms, transporting substances through the chloroplast envelope.

*AtTAP1 expression analysis*

To investigate the expression of *AtTAP1* in different aerial tissues and roots, semi-quantitative RT-PCR experiments were performed using WT plants. Results show expression of *AtTAP1* in both aerial tissues and in roots, with highest expression observed in flower structures, and lower expression in roots and leaves (Fig. 3a).

The upstream promoter region of *AtTAP1* was cloned into the vector pBADG, to generate PromoterTAP1-pBADG, in which the *GUS* gene is under the control of the *AtTAP1* promoter. Using floral dipping, WT Arabidopsis plants were transformed with the construct, and transgenic seedlings

**Journal of Plant Research**

selected on media containing BASTA, to obtain plants expressing the *AtTAP1* promoter-GUS reporter. Following this, *GUS* expression was observed in the roots, leaves, siliques and flowers of secondary transformants (Fig. 3 b-h). An interesting observation is the expression of *AtTAP1* in roots is confined to sites of lateral root initiation (Fig. 3b–d). This may indicate local enhanced activities of the gene during specific times of plant development. The GUS-reporter experiments clearly demonstrate *AtTAP1* expression in flowers (Fig. 3e), which supports the RT-PCR results, as well as siliques (Fig. 3f) and leaves (Fig. 3g, h).

*Stress treatments and AtTAP1 expression*

To measure changes in *AtTAP1* expression in response to exogenous stress, wild-type seedlings were treated with different solutions of metal ions, and semi-quantitative RT-PCR performed. Seedlings were transferred to wells containing 25 $\mu$M of $Al^{3+}$, $Fe^{3+}$ or $Ca^{2+}$, or ½MS as a control, and incubated in continuous light. After 48 hours RT-PCR was performed using actin as a reference, and expression of *AtTAP1* was normalized against the level of expression of *AtTAP1* in the control seedlings. *AtTAP1* expression was shown to be significantly induced by $Ca^{2+}$, and to a lesser extent by $Al^{3+}$ or $Fe^{3+}$ ($P < 0.05$; Fig. 4a). From these observations, we may anticipate that the *AtTAP1* gene plays a part in calcium homeostasis in Arabidopsis, or that the activity of AtTAP1 may be regulated by calcium, and to a less degree by aluminum and iron.

*Wounding induced expression of AtTAP1*

ABC proteins have been shown to be involved in defense responses towards viral and fungal pathogens in plants (Krattinger et al 2009: Sun et al, 2016). Because of this we sought to test whether *AtTAP1* expression is influenced by mechanical wounding To this end we made use of the transgenic Arabidopsis plants harboring the *AtTAP1* promoter-GUS reporter, and analyzed *AtTAP1* promoter activity in response to mechanical wounding in leaves. As shown in Fig. 3g and 3h, unwounded leaves revealed weak GUS staining throughout the leaves, with the highest expression near the leaf margins, whilst mechanical wounding resulted in a marked increase in GUS staining

**Journal of Plant Research**

(Fig. 5). Interestingly, the localization of GUS staining did not change after mechanical wounding, and the highest level of *GUS* expression was observed along the leaf margins rather than at the wound site (Fig. 5b, d). Although mechanical wounding is different from pathogen attack, transcriptional profiling in Arabidopsis has shown that there are clear interactions between these two responses at the gene expression level. Indeed, several wound-responsive genes encode proteins that are also involved in pathogen responses, including genes for signaling/regulatory components and for effector proteins (Cheong et al, 2002). Collectively, our data suggests that *AtTAP1* expression is induced by mechanical wounding and that AtTAP1 may be associated with defense responses in plants.

*Sequence analysis of the knock-out mutant Arabidopsis line SAIL_8_B04*

Homozygous *AtTAP1* knockout mutant plants (*attap1* insertion line SAIL_8_B04) were identified by PCR, using WT plants as a control (Fig. 6a, b). Subsequently the location of the T-DNA insert, determined by sequencing a fragment spanning the insertion site, and found to be within intron 1 (Fig. 6a). Semi quantitative RT-PCR was used to analyze the effect of the T-DNA-insertion on *AtTAP1* expression, using primers to detect the N-terminal end of the *AtTAP1* cDNA, and using actin as a control. Analysis of WT seedlings revealed clear expression of *AtTAP1*, whilst in the homozygous *attap1* knockout mutant line no expression of *AtTAP1* was detected, indicating that the intronic T-DNA insertion abolished *AtTAP1* expression (Fig. 6c). The *attap1* plants grew to maturity and were fertile (data not shown).

*Phenotypic Analysis of the attap1 knockout mutant*

To probe the function of AtTAP1 we compared WT and *attap1* knockout mutant seedlings and plants when exposed to exogenous stress factors, including $Al^{3+}$, $Fe^{3+}$, $Ca^{2+}$, $Mg^{2+}$, $Cu^{2+}$, methyl viologen (MV), $H_2O_2$, auxin and heat stress, as described. We anticipated that *the* attap1 mutant may have a similar response to aluminum toxicity, as previously described in the literature for *attap1 (als1-1)* and *attap2* (*als1-2*) mutant seedlings (Larsen et al. 2007), or that the function of AtTAP1 may have diverged and that different exogenous stress factors would prove to be important. Detailed analysis of

the *attap1* mutant in our study revealed no phenotypic differences as compared to WT plants in terms of overall morphology in response to the exogenous stress factors applied. Furthermore, comparison of the main root lengths of the mutant and WT seedlings after treatment with two different concentrations of $Al^{3+}$, $Fe^{3+}$, $Mg^{2+}$ and $Ca^{2+}$, did not show any statistically significant differences (Table 3).

**Journal of Plant Research**

**Discussion**

AtTAP1 is a half-sized ABC transporter that is a member of the TAP (transporter associated with antigen processing) sub-group, which has 130 members in the Arabidopsis genome (Hwang et al. 2016). Although most of the Arabidopsis ABC proteins have not been functionally characterized, previous studies have shown that ABC transporters are involved in the transport of a wide variety of substrates, and play fundamental roles in development and interaction with the environment. Here we show that AtTAP1 is induced by wounding, suggesting a role in the plastid associated stress response in Arabidopsis.

AtTAP1 is localized to the chloroplasts and enriched at the chloroplast envelope (Fig. 2), suggesting a role in transport into the chloroplast stroma. This agrees with predictions that AtTAP1 harbors a chloroplast transit peptide, and is enriched in the chloroplast envelope (Ferro et al. 2010). Two different patterns of localization were observed: short filaments in close association with the chloroplast envelope, and uniform distribution with the entire chloroplast envelope (Fig. 2), which may reflect different levels of the fusion protein. The localization of AtTAP1 to chloroplasts contrasts with that of the closest homologue in Arabidopsis AtTAP2 (ALS1; At5g39040), which is localised to the tonoplast membrane (Jaquinod et al. 2007). AtTAP2 plays a role in the internal detoxification of aluminium, transporting aluminum between the cytoplasm and vacuole. Storage of aluminum in the vacuole enables plants to survive in an aluminum-toxic environment, an important factor for agriculture given that aluminum toxicity is a major growth-limiting factor for crop production on acid soils worldwide.

Knockout of *AtTAP1* did not affect the plants sensitivity to metals, or result in a clear phenotype after exposure to exogenous stress factors in comparison to WT plants. Furthermore, there were no significant differences in root length between WT and *attap1* mutant seedlings when exposed to aluminum or other metal ions. This is in sharp contrast to the phenotype displayed by the *als1* mutant, and is further evidence that the function of the two members of the TAP family have diverged in Arabidopsis.

**Journal of Plant Research**

Mechanical wounding resulted in distinct and enhanced expression of *AtTAP1*, measured by the induction of *GUS* expression from an *AtTAP1* promoter *GUS* reporter construct (Fig. 5). In control leaves, *AtTAP1* was shown to be expressed throughout the leaf, with highest expression along the leaf margins. Mechanical wounding, by tearing the leaf with a needle, resulted in an increase in *GUS* expression (Fig. 5). Interestingly the pattern of *GUS* expression did not change, with higher expression observed throughout the leaf, and there was no evidence that *AtTAP1* was increased at the wounding site, but rather part of a systemic response. The induction of AtTAP1 expression in response to wounding, suggests a role in plant defense.

Other ABC proteins have also been shown to be induced in response to wounding, for example AtABCG11 (COF1/DSO/WBC11; At1g17840), a member of the ABCG subfamily, is upregulated in response to wounding, as well as to salt, glucose, and ABA treatments, and gibberellin-mediated down-regulation of ABA-induced expression (Panikashvili et al. 2007). AtABCG11 was identified through a gene trapping approach (Alvarado et al. 2004) to identify novel stress responsive genes, and was subsequently shown to play a role in cutin and wax secretion, as well as vascular patterning in conjunction with AtABCG9 and AtABCG14 (Le Hir et al. 2013). A second example is the peroxisomal ABC transporter AtABCD1 (CTS, COMATOSE; At4g39850), which is involved in peroxisomal import of jasmonate precursors, and contributes both to basal and wound-induced jasmonic acid biosynthesis in leaves (Theodoulou et al. 2005).

ABC transporters are also involved in general stress responses, as part of a massive reprogramming required to bring about a shift from growth-oriented to defense-oriented plant metabolism, and the induction of the defense response genes are equally relevant for both tolerance and induced expression of resistance traits. This illustrates the broad roles of ABC transporters in both stress responses and normal plant development, and it will be important to further clarify the function of AtTAP1.

*AtTAP1* is expressed in both roots and throughout aerial tissue, with highest expression observed in flowers. Interestingly, in roots *AtTAP1* expression is highest at the sites of lateral root initiation. *AtTAP2* expression is primarily localized to root tips and the vasculature of the plant, and it will be interesting to analyze the role of AtTAP1 in root cell plastids. Using semi-quantitative RT-PCR we

found that the expression of *AtTAP1* was induced by calcium, and to a lesser extent by aluminum and iron (Fig. 4). It has been shown that wound-induced resistance in Arabidopsis is preceded by, and dependent upon, a burst of calcium, and that systemic cytosolic calcium elevation is activated upon wounding (Beneloujaephajri et al. 2013; Kiep et al. 2015). The induction of AtTAP1 by calcium could therefore form part of the stress response.

In conclusion, the elevated expression of *AtTAP1* in wounded leaves, and in response to calcium suggests that AtTAP1 may be involved in defense mechanisms in Arabidopsis. Interestingly, TAP2 has also been shown to be involved in defense responses, particularly aluminum detoxification, which suggests a high level commonality between the two TAP proteins. Despite this, our studies also demonstrate marked differences between TAP1 and TAP2 suggesting that the two proteins are highly divergent in Arabidopsis. Further studies are encouraged in order to understand the intreractions and interseactions between these two protens in defense responses and in overall plant development.

**Acknowledgements**

This work was funded by Rogaland County Council, Norway and The Norwegian Research Council, Norway.

**References**


Abele R, Tampe R (2004) The ABCs of immunology: structure and function of TAP, the transporter associated with antigen processing Physiology (Bethesda) 19:216-224 doi:10.1152/physiol.00002.2004

Alvarado MC, Zsigmond LM, Kovacs I, Cseplo A, Koncz C, Szabados LM (2004) Gene trapping with firefly luciferase in Arabidopsis. Tagging of stress-responsive genes Plant Physiol 134:18-27 doi:10.1104/pp.103.027151

Ames GF, Lever J (1970) Components of histidine transport: histidine-binding proteins and hisP protein Proc Natl Acad Sci U S A 66:1096-1103

Beneloujaephajri E, Costa A, L'Haridon F, Metraux JP, Binda M (2013) Production of reactive oxygen species and wound-induced resistance in Arabidopsis thaliana against Botrytis cinerea are preceded and depend on a burst of calcium BMC Plant Biol 13:160 doi:10.1186/1471-2229-13-160

Cheong YH, Chang HS, Gupta R, Wang X, Zhu T, Luan S (2002) Transcriptional profiling reveals novel interactions between wounding, pathogen, abiotic stress, and hormonal responses in Arabidopsis Plant Physiol 129:661-677 doi:10.1104/pp.002857

Clough SJ, Bent AF (1998) Floral dip: a simplified method for Agrobacterium-mediated transformation of Arabidopsis thaliana Plant J 16:735-743

Davidson AL, Dassa E, Orelle C, Chen J (2008) Structure, function, and evolution of bacterial ATP-binding cassette systems Microbiol Mol Biol Rev 72:317-364, table of contents doi:10.1128/MMBR.00031-07

Dean JV, Mills JD (2004) Uptake of salicylic acid 2-O-beta-D-glucose into soybean tonoplast vesicles by an ATP-binding cassette transporter-type mechanism Physiol Plant 120:603-612 doi:10.1111/j.0031-9317.2004.0263.x

Dean M, Rzhetsky A, Allikmets R (2001) The human ATP-binding cassette (ABC) transporter superfamily Genome Res 11:1156-1166 doi:10.1101/gr.184901

Dizdarevic S, Peters AM (2011) Imaging of multidrug resistance in cancer Cancer Imaging 11:1-8 doi:10.1102/1470-7330.2011.0001

Emanuelsson O, Nielsen H, von Heijne G (1999) ChloroP, a neural network-based method for predicting chloroplast transit peptides and their cleavage sites Protein Sci 8:978-984 doi:10.1110/ps.8.5.978

Ferro M et al. (2010) AT_CHLORO, a comprehensive chloroplast proteome database with subplastidial localization and curated information on envelope proteins Mol Cell Proteomics 9:1063-1084 doi:10.1074/mcp.M900325-MCP200

Fischer M, Zhang QY, Hubbard RE, Thomas GH (2010) Caught in a TRAP: substrate-binding proteins in secondary transport Trends Microbiol 18:471-478 doi:10.1016/j.tim.2010.06.009

Gabrielson KM, Cancel JD, Morua LF, Larsen PB (2006) Identification of dominant mutations that confer increased aluminium tolerance through mutagenesis of the Al-sensitive Arabidopsis mutant, als3-1 J Exp Bot 57:943-951 doi:10.1093/jxb/erj080

Garcia O, Bouige P, Forestier C, Dassa E (2004) Inventory and comparative analysis of rice and Arabidopsis ATP-binding cassette (ABC) systems J Mol Biol 343:249-265 doi:10.1016/j.jmb.2004.07.093

Hall T (2011) BioEdit: An important software for molecular biology GERF Bulletin of Biosciences 2:60-61

Hanson PI, Whiteheart SW (2005) AAA+ proteins: have engine, will work Nat Rev Mol Cell Biol 6:519-529 doi:10.1038/nrm1684

Henderson MJ et al. (2011) ABCC multidrug transporters in childhood neuroblastoma: clinical and biological effects independent of cytotoxic drug efflux J Natl Cancer Inst 103:1236-1251 doi:10.1093/jnci/djr256

Higgins CF (2001) ABC transporters: physiology, structure and mechanism--an overview Res Microbiol 152:205-210

**Journal of Plant Research**

Holland IB, Blight MA (1999) ABC-ATPases, adaptable energy generators fuelling transmembrane movement of a variety of molecules in organisms from bacteria to humans J Mol Biol 293:381-399 doi:10.1006/jmbi.1999.2993

Hwang JU et al. (2016) Plant ABC Transporters Enable Many Unique Aspects of a Terrestrial Plant's Lifestyle Mol Plant 9:338-355 doi:10.1016/j.molp.2016.02.003

Jaquinod M, Villiers F, Kieffer-Jaquinod S, Hugouvieux V, Bruley C, Garin J, Bourguignon J (2007) A proteomics dissection of Arabidopsis thaliana vacuoles isolated from cell culture Mol Cell Proteomics 6:394-412 doi:10.1074/mcp.M600250-MCP200

Jefferson RA (1987) Assaying Chimeric Genes in Plants: The GUS Gene Fusion System Plant Molecular Biology Reporter 5:387-405

Kang BG, Ye X, Osburn LD, Stewart CN, Jr., Cheng ZM (2010) Transgenic hybrid aspen overexpressing the Atwbc19 gene encoding an ATP-binding cassette transporter confers resistance to four aminoglycoside antibiotics Plant Cell Rep 29:643-650 doi:10.1007/s00299-010-0850-8

Kang J, Park J, Choi H, Burla B, Kretzschmar T, Lee Y, Martinoia E (2011) Plant ABC Transporters Arabidopsis Book 9:e0153 doi:10.1199/tab.0153

Krattinger SG, Lagudah ES, Spielmeyer W, Singh RP, Huerta-Espino J, McFadden H, Bossolini E, Selter LL, Keller B (2009) A putative ABC transporter confers durable resistance to multiple fungal pathogens in wheat Science 323:1360-1363 doi:10.1126/science.1166453

Kiep V, Vadassery J, Lattke J, Maass JP, Boland W, Peiter E, Mithofer A (2015) Systemic cytosolic Ca(2+) elevation is activated upon wounding and herbivory in Arabidopsis New Phytol 207:996-1004 doi:10.1111/nph.13493

Kloch M, Milewski M, Nurowska E, Dworakowska B, Cutting GR, Dolowy K (2010) The H-loop in the second nucleotide-binding domain of the cystic fibrosis transmembrane conductance regulator is required for efficient chloride channel closing Cell Physiol Biochem 25:169-180 doi:10.1159/000276549

Kost B, Spielhofer P, Chua NH (1998) A GFP-mouse talin fusion protein labels plant actin filaments in vivo and visualizes the actin cytoskeleton in growing pollen tubes Plant J 16:393-401

Larsen PB, Cancel J, Rounds M, Ochoa V (2007) Arabidopsis ALS1 encodes a root tip and stele localized half type ABC transporter required for root growth in an aluminum toxic environment Planta 225:1447-1458 doi:10.1007/s00425-006-0452-4

Larsen PB, Geisler MJ, Jones CA, Williams KM, Cancel JD (2005) ALS3 encodes a phloem-localized ABC transporter-like protein that is required for aluminum tolerance in Arabidopsis Plant J 41:353-363 doi:10.1111/j.1365-313X.2004.02306.x

Le Hir R et al. (2013) ABCG9, ABCG11 and ABCG14 ABC transporters are required for vascular development in Arabidopsis Plant J 76:811-824 doi:10.1111/tpj.12334

Lewis HA et al. (2004) Structure of nucleotide-binding domain 1 of the cystic fibrosis transmembrane conductance regulator EMBO J 23:282-293 doi:10.1038/sj.emboj.7600040

Li ZS, Lu YP, Zhen RG, Szczypka M, Thiele DJ, Rea PA (1997) A new pathway for vacuolar cadmium sequestration in Saccharomyces cerevisiae: YCF1-catalyzed transport of bis(glutathionato)cadmium Proc Natl Acad Sci U S A 94:42-47

Murashige T, Skoog F (1962) A Revised Medium for Rapid Growth and Bio Assays with Tobacco Cultures. Physiologia Plantarum:473-497 doi:10.1111/j.1399-3054.1962.tb08052.x

Panikashvili D et al. (2007) The Arabidopsis DESPERADO/AtWBC11 transporter is required for cutin and wax secretion Plant Physiol 145:1345-1360 doi:10.1104/pp.107.105676

Rea PA (2007) Plant ATP-binding cassette transporters Annu Rev Plant Biol 58:347-375 doi:10.1146/annurev.arplant.57.032905.105406

Reits EA, Vos JC, Gromme M, Neefjes J (2000) The major substrates for TAP in vivo are derived from newly synthesized proteins Nature 404:774-778 doi:10.1038/35008103

Ryan PR, Tyerman SD, Sasaki T, Furuichi T, Yamamoto Y, Zhang WH, Delhaize E (2011) The identification of aluminium-resistance genes provides opportunities for enhancing crop production on acid soils J Exp Bot 62:9-20 doi:10.1093/jxb/erq272

Sánchez-Fernández R, Davies TG, Coleman JO, Rea PA (2001) The Arabidopsis thaliana ABC protein superfamily, a complete inventory J Biol Chem 276:30231-30244 doi:10.1074/jbc.M103104200

Schneider E, Hunke S (1998) ATP-binding-cassette (ABC) transport systems: functional and structural aspects of the ATP-hydrolyzing subunits/domains FEMS Microbiol Rev 22:1-20

Scholz C, Parcej D, Ejsing CS, Robenek H, Urbatsch IL, Tampe R (2011) Specific lipids modulate the transporter associated with antigen processing (TAP) J Biol Chem 286:13346-13356 doi:10.1074/jbc.M110.216416

Simoes CC, Melo JO, Magalhaes JV, Guimaraes CT (2012) Genetic and molecular mechanisms of aluminum tolerance in plants Genet Mol Res 11:1949-1957 doi:10.4238/2012.July.19.14

Sun D, Zhang X, Li S, Jiang CZ, Zhang Y, Niu L (2016) LrABCF1, a GCN-type ATP-binding cassette transporter from Lilium regale, is involved in defense responses against viral and fungal pathogens Planta. 244(6):1185-1199 doi:10.1007/s00425-016-2576-5

Szmelcman S, Schwartz M, Silhavy TJ, Boos W (1976) Maltose transport in Escherichia coli K12. A comparison of transport kinetics in wild-type and lambda-resistant mutants as measured by fluorescence quenching Eur J Biochem 65:13-19

Theodoulou FL et al. (2005) Jasmonic acid levels are reduced in COMATOSE ATP-binding cassette transporter mutants. Implications for transport of jasmonate precursors into peroxisomes Plant Physiol 137:835-840 doi:10.1104/pp.105.059352

Walker JE, Saraste M, Runswick MJ, Gay NJ (1982) Distantly related sequences in the alpha- and beta-subunits of ATP synthase, myosin, kinases and other ATP-requiring enzymes and a common nucleotide binding fold EMBO J 1:945-951

Wilkens S (2015) Structure and mechanism of ABC transporters F1000Prime Rep 7:14 doi:10.12703/P7-14

Zhao FJ, McGrath SP, Meharg AA (2010) Arsenic as a Food Chain Contaminant: Mechanisms of Plant Uptake and Metabolism and Mitigation Strategies Annual Review of Plant Biology, Vol 61 61:535-559 doi:10.1146/annurev-arplant-042809-112152

Zhao J, Huhman D, Shadle G, He XZ, Sumner LW, Tang Y, Dixon RA (2011) MATE2 mediates vacuolar sequestration of flavonoid glycosides and glycoside malonates in Medicago truncatula Plant Cell 23:1536-1555 doi:10.1105/tpc.110.080804

**Journal of Plant Research**

**Table 1** Primers used in this study

| Primer name | Sequence[a] |
|---|---|
| 1g70610-KpnI-L | 5'-AATGGTACCATGGCTCAGCAAGTACTCG-3' |
| 1g70610-KpnI-R | 5'-AATGGTACCTAAGACGGCATCGTTTT-3' |
| TAP1-Promoter-L | 5'-ATCCATGGAGGTTAACGATTGGGCAGAAG-3' |
| TAP1-Promoter-R | 5'-ATGGCGCGCCTTATGTTCGGTGGACTAAAG-3' |
| LB1 | 5'-GCCTTTTCAGAAATGGATAAATAGCCTTGCTTCC-3' |
| LB3 | 5'-AAGCATCTGAATTTCATAACCAATCTCGATACAC-3' |
| SAIL_8_B04-L | 5'-AAGGAAAAAGCTTGAAGCGTC-3' |
| SAIL_8_B04-R | 5'-TGTTTCCCTCATTCGTTTCAC-3' |
| TAP1-R | 5'-CCACTTCACCAGGATGCACGGA-3' |
| SAIL_409_C10-L | 5'-AGGATCGTTGGGTTATCTTCG-3' |
| Actin Forward | 5'-TGCCAATCTACGAGGGTTTC-3' |
| Actin Reverse | 5'-GAACCACCGATCCAGACACT-3' |

[a] Restriction sites are underlined

**Journal of Plant Research**

**Table 2** Identity and similarity of AtTAP1 and TAP1 proteins from different plant and non-plant species.

| Species | Protein name | Length (aa) | Identity (%) | Similarity (%) |
|---|---|---|---|---|
| Higher Plants | | | | |
| N. tabacum | ABCB-26 | 701 | 68.8 | 81.4 |
| S. lycopersicum | ABCB-26 | 689 | 66.5 | 79.3 |
| O. sativa | ABCB-26 | 688 | 61.4 | 75.4 |
| T. aestivum | Unnamed protein | 675 | 60.4 | 72.8 |
| Lower Plants | | | | |
| P. patens | PpABCB-6 | 578 | 49.8 | 66.0 |
| C. reinhardtii | Unnamed protein | 560 | 36.3 | 52.3 |
| Non-plants | | | | |
| H. sapiens | ABCB9; TAPL | 766 | 31.8 | 48.9 |
| D. rerio | ABCB9 | 789 | 32.3 | 48.6 |
| D. melanogaster | CG3156 | 692 | 29.9 | 49.6 |
| C. elegans | Haf-2 | 773 | 30.3 | 48.0 |
| S. cerevisiae | MDL2 | 773 | 28.5 | 41.9 |

Identity and similarity between AtTAP1 and TAP1 proteins from other organisms was assessed using *EMBOSS Needle*. Protein sequences were obtained from NCBI for *A. thaliana* (accession number NP_177218), *N. tabacum* (XP_016492080), S. *lycopersicum* (XP_004252689), *O. sativa* (XP_015613646), *T. aestivum* (CDM85589), *P. patens* (XP_001781344), *C. reinhardtii* (XP_001699295), *H. sapiens* (NP_062571), *D. rerio* (NP_001119906), *D. melanogaster* (NP_569844), *C. elegans* (NP_495537), and *S. cerevisiae* (EDN60878).

**Journal of Plant Research**

**Table 3.** Comparison of main root length of WT and *attap1* knockout mutant in response to metal treatments

| | Root length [a] | |
|---|---|---|
| **Treatment** | **WT** | **MUT** |
| 0 % sucrose | 8.5 (5.07) | 8.8 (5.56) |
| 1 % sucrose | 18.3 (0.50) | 14.0 (4.55) |
| 0.5 mM $Al^{3+}$ | 37.5 (6.45) | 38.0 (6.73) |
| 2 mM $Al^{3+}$ | 30.0 (4.55) | 38.0 (8.29) |
| 0.5 mM $Fe^{3+}$ | 17.3 (2.50) | 23.0 (3.61) |
| 2 mM $Fe^{3+}$ | 31.3 (0.58) | 32.5 (7.78) |
| 0.5 mM $Mg^{2+}$ | 22.0 (0.82) | 18.5 (5.07) |
| 2 mM $Mg^{2+}$ | 18.8 (3.86) | 19.3 (7.68) |
| 0.5 mM $Ca^{2+}$ | 12.8 (1.89) | 12.7 (4.04) |
| 2 mM $Ca^{2+}$ | 19.3 (3.30) | 17.5 (6.56) |

WT (*Col-0*) and the *attap1* mutant (MUT).

[a]The mean root length and standard deviation are shown. n = 4

**Journal of Plant Research**

**Figure Legends**

**Fig. 1**. Alignment of AtTAP1 protein with TAP1 proteins from different plant and non-plant species. The Walker A, Signature, Walker B and H-loop motifs are underlined. Protein sequences were obtained from NCBI for *A. thaliana* (AtTAP1, accession number NP_177218), *T. aestivum* (TaTAP1, CDM85589), *H. sapiens* (HsABCB9, NP_062571), *D. rerio* (DrABCB9, NP_001119906), *D. melanogaster* (DmDME1, NP_569844), and *S. cerevisiae* (ScMDL2, EDN60878), and aligned using Clustal W.

**Fig. 2.** Localization of AtTAP1-YFP in tobacco leaf chloroplasts. (**a,b**) Extended focus images showing AtTAP1-YFP distributed as short filaments. (**c**) AtTAP1-YFP uniformly associated with the envelope. (**d**) Enlargement of **c** displaying a single chloroplast in three cross-sections; top, middle and bottom, showing AtTAP1-YFP is enriched at the chloroplast envelope. Green, YFP; Red, chlorophyll; *Scale bar*: 5 μm

**Fig. 3**. *AtTAP1* expression in aerial tissues and roots of Arabidopsis. **a**) RT-PCR analysis of *AtTAP1* expression in different organs with actin used as a reference gene; M indicates marker. GUS expression driven by the *AtTAP1* promoter in main roots near the sites of lateral root formation (**b-d**), in flowers, predominantly sepals (**e**), in siliques (**f**) and in leaves (**g, h**). *Scale bars*: 0.3 mm in **b-d** and 2 mm in (**e-h**)

**Fig. 4**. *AtTAP1* expression in Arabidopsis seedlings treated with metal ions. (**a**) RT-PCR analysis was performed on seedlings treated with different metal ions to measure *AtTAP1* expression (TAP1), and using Actin as a reference gene. M, marker. (**b**) Quantification of *AtTAP1* expression normalized against the control. The standard error is shown. n = 3

**Journal of Plant Research**

**Fig. 5**. Wounding induced *AtTAP1* expression. Leaves from plants expressing an *AtTAP1* promoter-GUS reporter were used as a control (**a** and **c**), or were wounded by tearing with a needle (**b** and **d**), and the expression of *GUS* assessed by histochemical analysis. *Scale bar*: 2 mm

**Fig. 6**. Characterization of T-DNA insertion lines of *AtTAP1*. (**a**) A schematic of *AtTAP1* genomic DNA showing the location of primers used in this study (1–5), and the site of the T-DNA insertion in the *attap1* mutant line, SAIL_8_B04. Exons shown as grey boxes, numbers indicate nucleotide positions, with ATG starting at position 126 (not drawn to scale). (**b**) PCR analysis to determine the presence or absence of the T-DNA insertion. Primers flanking the insertion site (SAIL8_B04-L and -R) generate a PCR product in WT seedlings, but not in *attap1* knockout mutant seedlings. In contrast the T-DNA insert was detected only in the mutant line using primers SAIL_409_C10-L and LB1. (**c**) RT-PCR analysis using primers SAIL_409_C10-L and TAP1-R showed that the *AtTAP1* cDNA was absent in the mutant line (M1) but present in WT. Actin primers were used as a control. M1 and M2 denote two parallels of the *attap1* knockout mutant.

**Journal of Plant Research**

Figure 1

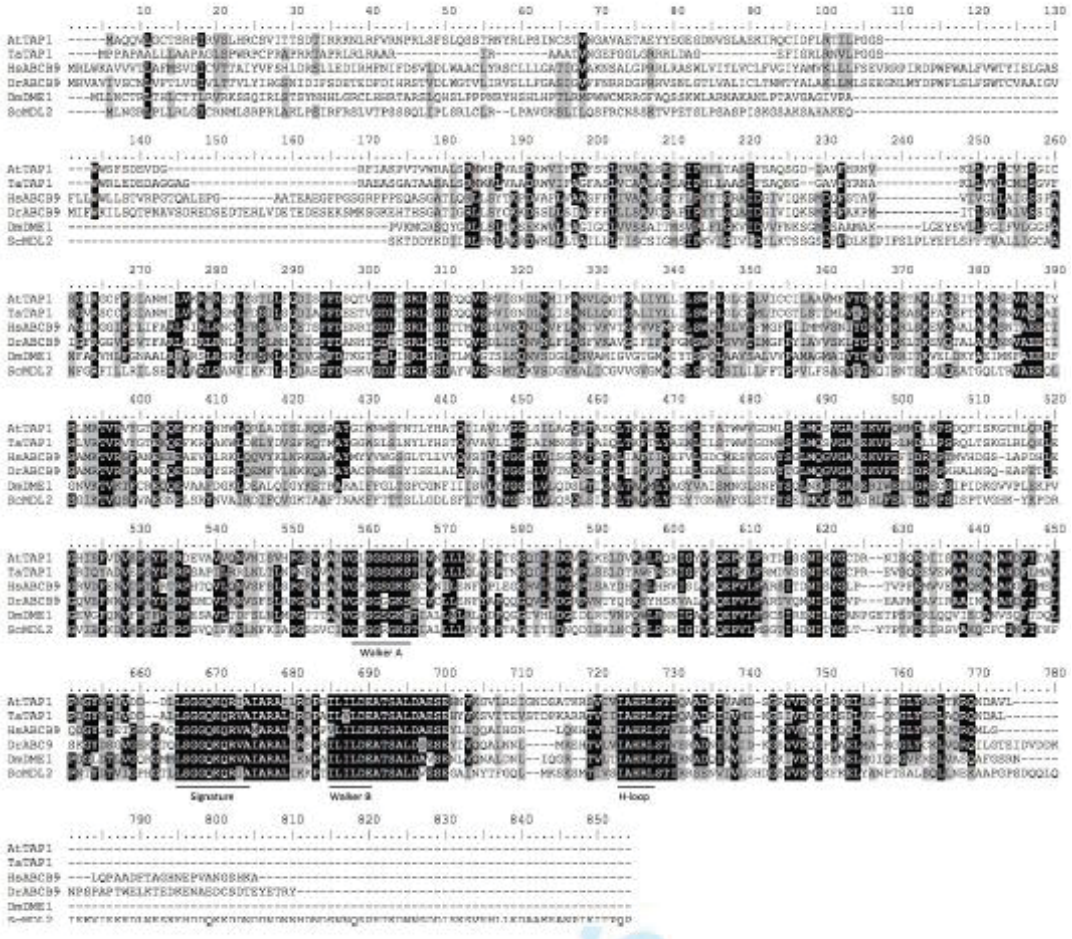

**Journal of Plant Research**

Figure 2

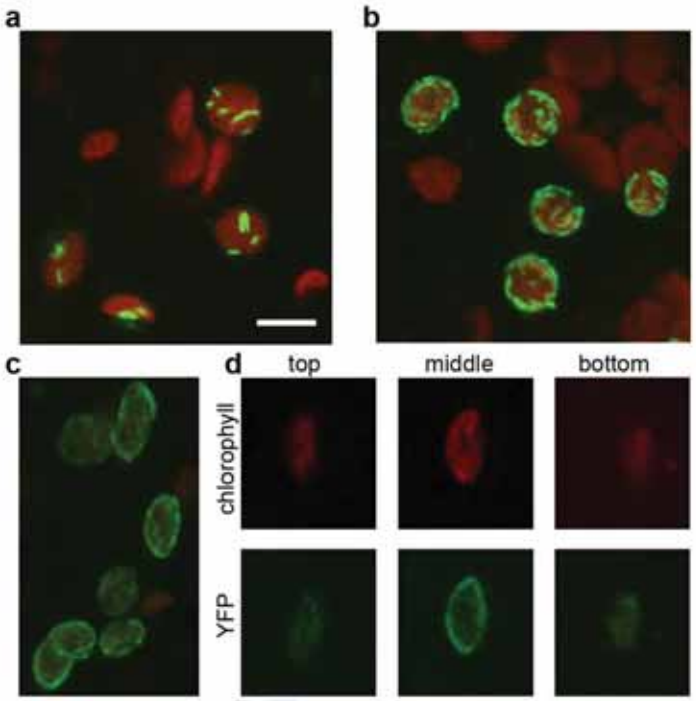

**Journal of Plant Research**

Figure 3

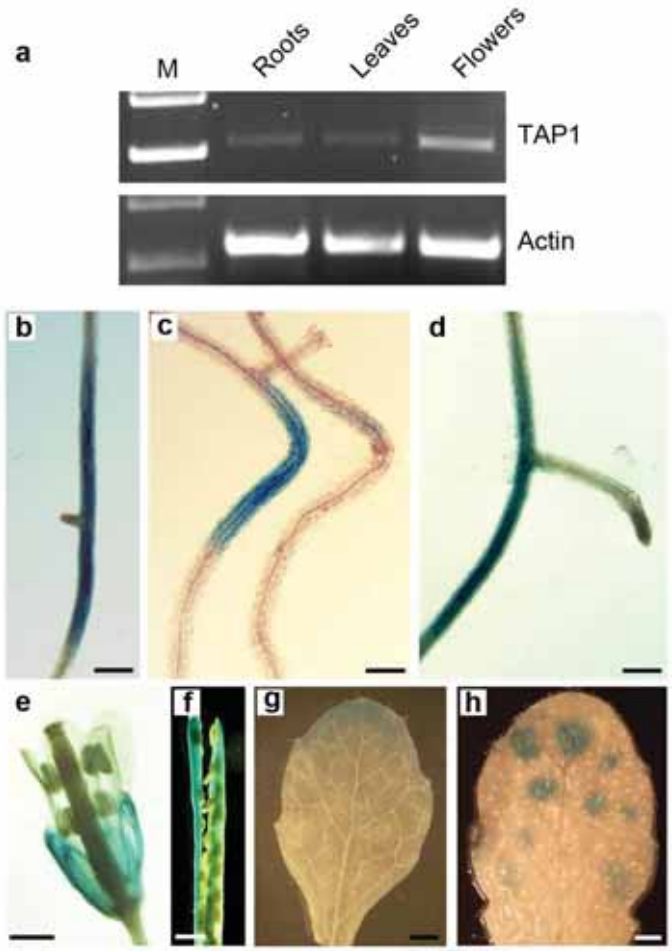

**Journal of Plant Research**

Figure 4

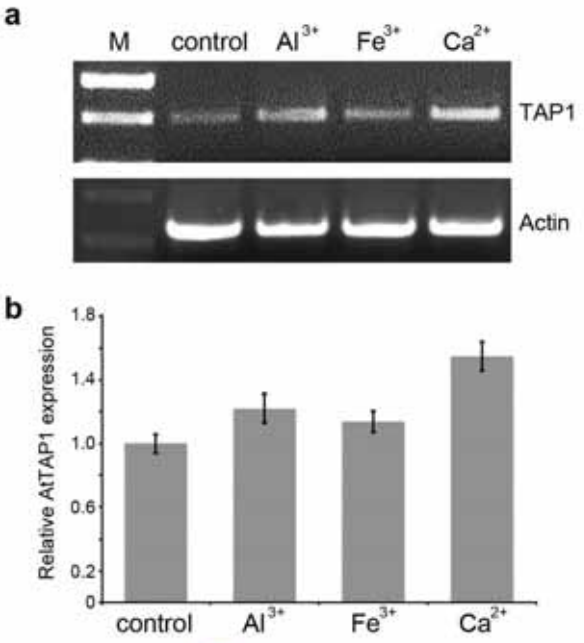

**Journal of Plant Research**

Figure 5

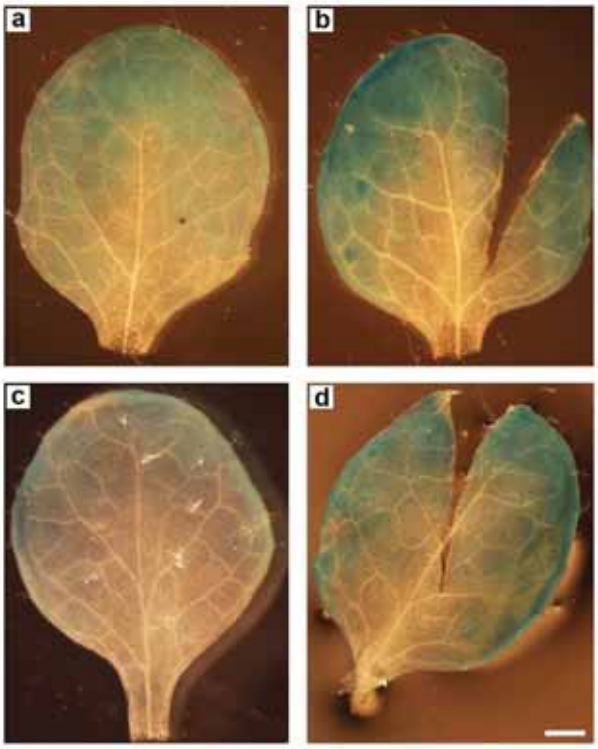

**Journal of Plant Research**

Figure 6